

Characterization of the *ZmUXT2* and *ZmLRR-RLK*

Candidate Tar Spot Resistance Genes in Maize

Emily Marion

A thesis submitted to the University of Ottawa

in partial fulfillment of the requirements for the degree of:

Master of Science in Biology

Department of Biology

Faculty of Science

University of Ottawa

Abstract

Tar spot is an emerging fungal disease that threatens maize production across North America due to a lack of genetic resistance in cultivated varieties. A major quantitative trait locus (*qRtsc8-1*) is associated with tar spot resistance in maize and putatively contains four candidate genes. We found that two of these genes, *ZmUXT2* and *ZmLRR-RLK*, are induced by microbe-associated molecular patterns (MAMPs). *ZmUXT2* is a predicted UDP-xylose transporter and has higher expression in a tar spot resistant genotype compared to a susceptible genotype. *ZmLRR-RLK* has similar expression between tar spot resistant and susceptible genotypes. The resistant maize genotype had higher MAMP-induced ROS accumulation and gene expression relative to the susceptible maize genotype. The coding sequences of *ZmUXT2* and *ZmLRR-RLK* genes were similar between resistant and susceptible maize genotypes with between 1-16 amino acid changes. Fluorescently tagged *ZmUXT2* localized to the endoplasmic reticulum, while *ZmLRR-RLK* localized to both the endoplasmic reticulum and plasma membrane during transient expression in *Nicotiana benthamiana*. No differences in subcellular localization were observed between resistant and susceptible alleles. Together, this suggests that inducible immunity influences expression of *ZmUXT2* and *ZmLRR-RLK* genes and that a tar spot resistant maize genotypes supports higher expression of *ZmUXT2* compared to a susceptible genotype even in the absence of stress.

Résumé

La tache goudronneuse est une maladie fongique émergente qui menace la production du maïs en Amérique du Nord en raison du manque de résistance génétique chez les variétés cultivées. Un locus majeur de caractère quantitatif (qRtsc8-1) est associé à la résistance à la tache goudronneuse chez le maïs et contiendrait quatre gènes candidats. Nous avons montré que deux de ces gènes, *ZmUXT2* et *ZmLRR-RLK*, sont induits par des motifs moléculaires associés aux microorganismes (MAMPs). *ZmUXT2* est un transporteur d'UDP-xylose prédit et présente une expression plus élevée chez un génotype de maïs résistant à la tache goudronneuse que chez un génotype sensible. L'expression de *ZmLRR-RLK* est similaire entre les génotypes résistants et sensibles. Le génotype résistant a présenté une accumulation plus importante d'espèces réactives de l'oxygène (ROS) et une expression génique induites par les MAMPs comparativement au génotype sensible. Les séquences codantes des gènes *ZmUXT2* et *ZmLRR-RLK* étaient semblables entre les génotypes résistants et sensibles, avec de 1 à 16 substitutions d'acides aminés. Lors d'une expression transitoire dans *N. benthamiana*, la protéine *ZmUXT2* marquée par fluorescence s'est localisée au réticulum endoplasmique, tandis que *ZmLRR-RLK* s'est localisée à la fois au réticulum endoplasmique et à la membrane plasmique. Aucune différence de localisation subcellulaire n'a été observée entre les allèles résistants et sensibles. Ensemble, ces résultats suggèrent que l'immunité inductible influence l'expression des gènes *ZmUXT2* et *ZmLRR-RLK*, et qu'un génotype de maïs résistant à la tache goudronneuse présente une expression plus élevée de *ZmUXT2* qu'un génotype sensible, même en l'absence de stress.

Acknowledgements

Firstly, I would like to thank my supervisor, Dr. Elizabeth Brauer, for the opportunity to research pathogen resistance in maize and for her guidance and support over the past two years. I am also grateful to my committee members, Dr. Yaseen Mottiar and Dr. Marina Cvetkovska, for their valuable feedback throughout this process.

I sincerely thank the staff at the Ottawa Research and Development Centre for their support. I am grateful to Whynn Bosnich and Sarita Khanal for their technical expertise, Dat Cotter-Buajitti for greenhouse support, Matthew Linsdell for fostering a sense of community, and Dr. Gopal Subramaniam and his lab members, especially Chris Blackman, for their help with troubleshooting and reagents. Thank you as well to Aida Kebede for your continued support.

I am deeply grateful for the encouragement, patience and love from my family and friends throughout this degree, including my sisters, Roxanne and Vanessa; my dear friends Hollie and Mady; my husband, Benjamin; and many others. Thank you for celebrating every success with me no matter how big and small, and for supporting me through every challenging moment.

Finally, thank you to my fellow graduate students, Marielle Zouein and Siddharthan Lakshmanan. I will always remember our trio, the support we gave one another, and the memories we shared along the way.

Table of Contents

Abstract	ii
Résumé.....	iii
Acknowledgements.....	iv
List of Tables	vii
List of Figures	viii
1. Introduction.....	1
1.1. Tar Spot.....	1
1.2. Plant Resistance to Tar Spot	8
1.2.1. Constitutive Defences	8
1.2.2. Inducible Defences.....	12
1.2.3. Pathogen Invasion.....	13
1.2.4. Host Transcriptional Responses to <i>P. maydis</i>	15
1.2.5. Genetic Resistance to Tar Spot	16
1.3. Research Objectives.....	19
2. Materials and Methods.....	19
2.1. Plant Material and Growth Conditions	19
2.2. RNA Extraction and qPCR	20
2.3. Phylogenetic Tree Construction.....	21
2.4. DNA Extraction and Sequencing.....	22
2.5. Transient Expression and Subcellular Localization in <i>N. benthamiana</i>	23
2.6. Reactive Oxygen Species Assay	25
3. Results.....	26
3.1. Expression patterns of putative resistance genes	26
3.2. Characterization of <i>ZmUXT2</i>	29
3.3. Characterization of <i>ZmLRR-RLK</i>	35
3.4. Inducible Defence Responses in a Resistant and Susceptible Genotypes	42
4. Discussion	46
4.1. UDP-Xylose Transporters.....	47
4.2. LRR-RLKs	52

4.3. Genotypic Variations in MAMP-Triggered Responses	54
5. Conclusion & Future Directions	55
6. References	58
Supplemental Tables	91

List of Tables

Table S1: List of qPCR primers used in this study

Table S2: List of sequencing primers used in this study

List of Figures

Figure 1. Disease cycle of tar spot of maize.

Figure 2. General schematic of the grass secondary cell wall matrix.

Figure 3. Expression of candidate genes in resistant and susceptible maize following MAMP treatment.

Figure 4. Phylogenetic analysis of *ZmUXT2* across plant species.

Figure 5. The UDP-xylose transporter contains a single amino acid polymorphism unique to the tar spot resistant maize line CML495.

Figure 6. Structural localization of CML495-specific amino acid substitutions in *ZmUXT2*.

Figure 7. *ZmUXT2* localizes to the endoplasmic reticulum in *N. benthamiana*.

Figure 8. Phylogenetic analysis of *ZmLRR-RLK* across plant species.

Figure 9. *ZmLRR-RLK* exhibits multiple CML495-specific amino acid polymorphisms distributed across the protein.

Figure 10. Structural localization of CML495-specific amino acid substitutions in *ZmLRR-RLK*.

Figure 11. *ZmLRR-RLK* localizes to the plasma membrane and endoplasmic reticulum in *N. benthamiana*.

Figure 12. Resistant maize line CML495 exhibits enhanced inducible immune responses.

Figure 13. Resistant and susceptible alleles of *ZmUXT2* and *ZmLRR-RLK* produce similar inducible immune responses during transient expression in *N. benthamiana*.

List of Abbreviations

AX: Arabinoxylans

An2: Anthocyanin regulatory factor 2

cDNA: Complementary deoxyribonucleic acid

CIMMYT: The International Maize and Wheat Improvement Center

DEG: Differentially expressed genes

DNA: Deoxyribonucleic acid

DTMA: Drought Tolerant Maize for Africa

EFR: EF-Tu receptor

ER: Endoplasmic reticulum

ETI: Effector triggered immunity

FLS2: Flagellin sensing 2

flg22: Flagellin 22

GAX: Glucuronoarabinoxylans

GFP: Green fluorescence protein

GWAS: Genome-wide association studies

IMAS: Improved Maize for African Soils

LRR: Leucine-rich repeat

LRR-RLK: Leucine-rich repeat receptor-like kinase

MAMP: Microbe-associated molecular pattern

MAPK: Mitogen-activated protein kinases

MTI: Microbe-associated molecular pattern-triggered immunity

MLG: Mixed-linkage glucans

NSTs: Nucleotide sugar transporters

PAMP: Pathogen-associated molecular pattern

PM: Plasma membrane

PR5: Pathogenesis-Related protein 5

PRR: Pathogen recognition receptor

PTI: Pattern triggered immunity

QTL: Quantitative trait locus

RBOH: Respiratory burst oxidase homologues

RLCK: Receptor like cytosolic kinases

RLK: Receptor like kinase

ROS: Reactive oxygen species

qPCR: Quantitative polymerase chain reaction

SA: Salicylic acid

SD: Standard deviation

SERK: Somatic embryogenesis receptor kinase

SNPs: Single nucleotide polymorphisms

TPT: Triose phosphate translocator

TS: Tar spot

UXT: UDP-xylose transporter

1. Introduction

1.1. Tar Spot

Tar spot (TS) is a major fungal disease of maize (*Zea mays* L.) native to several countries in Central and South America and capable of causing significant grain yield losses (Hock et al., 1995). First reported in Mexico in 1904, the disease causes grain yield reductions ranging from approximately 11% to over 50%, in addition to reducing the quality of silage, stover, and husks used for livestock feed (Maublanc, 1904; Hock et al., 1989; Pereyda-Hernandez et al., 2009; Loladze et al., 2019; Mottaleb et al., 2019; Ren et al., 2022). For over 100 years, TS was restricted to Central and South America, and the Caribbean, however, over the past decade, TS has been moving northward, reaching the Midwestern United States in 2015, followed by Southwestern Ontario, Canada in 2020 (Hock et al., 1995; Ruhl et al., 2016; Pearce, 2021). This range expansion may be driven by increasingly favourable environmental conditions for the pathogen, along with the presence of susceptible host genotypes (Ruhl et al., 2016; Camiletti, 2025). Large-scale epidemics can have substantial economic consequences; for example, the 2018 tar spot epidemic in the United States resulted in an estimated \$680 million USD in crop losses (Mueller et al., 2020). More recently, tar spot has become a major cause of yield losses across the U.S. Midwest and Canada, contributing to an estimated loss of 22.4 billion kilograms (637 million bushels) of maize and approximately \$3.1 billion in economic damages over a six-year period (Mueller et al., 2024; Mueller et al., 2023; Ferreira et al., 2025). Infection of susceptible maize genotypes occurs under favourable environmental conditions including high elevations, cool temperatures (15–21°C), high relative humidity (approximately 85%), and extended periods of leaf wetness exceeding seven hours (Hock et al., 1995). Severe infection may lead to rapid foliage destruction within 8–14 days, making TS one of the most destructive foliar diseases affecting maize (Bajet et al., 1994). Maize

can be infected at any stage of development; however, the most severe symptoms typically occur during the pollination (R1) stage and later developmental stages (Bajet et al., 1994; Hock et al., 1995).

Previous field studies conducted between 1986 and 1988 demonstrated that symptoms associated with *Phyllachora maydis* consistently appeared first, supporting its role as the primary causal agent of TS (Hock et al., 1995). Additional observations in Latin America indicated that in addition to *P. maydis*, *Monographella maydis* and *Coniothyrium phyllachorae* were present within the same infected tissue, suggesting that these fungi may act as opportunistic pathogens, which establish infection by exploiting conditions created by a primary pathogen (Hock et al., 1995; Mahuku et al., 2016). Recent work has suggested that *P. maydis* may employ effector proteins to suppress host immune responses, although whether such mechanisms influence interactions with secondary fungi remains unknown (Rogers et al., 2024). *P. maydis* is an ascomycete fungus that produces both sexual spores (ascospores) and asexual spores (conidia) (Valle-Torres, et al., 2020). Ascospores develop within single-walled asci that are contained in perithecia embedded in stromatic tissue on infected leaves, with each ascus typically producing eight ellipsoids to ovoid ascospores (Liu, 1973; Hock et al., 1992; Valle-Torres et al., 2020). These ascospores serve as the primary inoculum for infection under favourable environmental conditions (Valle-Torres et al., 2020). It is presumed that following the deposition of ascospores on leaf tissue, they germinate and differentiate into specialized infection structures, known as appressoria, which breach the surface of the leaf (Rogers et al., 2026). Following penetration, vegetative hyphae initiate colonization by forming a dense, melanized network within maize epidermal cells, ultimately leading to the characteristic tar spot lesions, referred to as stromata (Rogers et al., 2026). A pycnidial stage may also occur, producing filiform spermatia that are often found alongside

perithecia within stromata and are believed produce conidia in the life cycle of the pathogen (Parbery, 1967; Muller & Samuels, 1984; Valle-Torres et al., 2020). Although *P. maydis* has traditionally been classified as an obligate biotroph requiring living host tissue to grow and reproduce, similar to other species within the genus (Cannon, 1991), the fungus is capable of overwintering in infected crop debris as stromata, allowing survival between growing seasons in North American production systems (Kleczewski et al., 2019; Telenko et al., 2021; Solórzano et al., 2023). Its ability to overwinter in infected crop debris suggests that it may also survive saprophytically (Helm et al., 2022). This observation has led some authors to propose that *P. maydis* exhibits a hemibiotrophic lifestyle, alternating between biotrophic infection and saprophytic survival phases (Helm et al., 2022). Upon infection, *P. maydis* produces brown to black, glossy, raised circular stromata on the leaves and stems of maize plants that are typically 0.5–2.5 mm in diameter (Singh et al., 2023).

M. maydis is commonly described as a benign saprophyte on leaf surfaces, becoming pathogenic only in the presence of *P. maydis* (Mahuku et al., 2016). In 1989, Hock et al. identified *M. maydis* as the causal agent of the brown necrotic halo surrounding the black stromata produced by *P. maydis*, a symptom known as the “fisheye” lesion associated with tar spot disease (Hock et al., 1989; Hock et al., 1992; Bajet et al., 1994). This identification supported earlier observations by Müller and Samuels that *M. maydis* was associated with fisheye lesions; however, the identification was based solely on morphological characteristics (Mueller & Samuel, 1984; Valle-Torres et al., 2020). Subsequent research has failed to provide evidence confirming the presence or correct identification of this pathogen, and no voucher specimens were deposited to verify the original reports (Valle-Torres et al., 2020). While *C. phyllachorae* may be a hyperparasite of both *P. maydis* and *M. maydis*, its role in tar spot infection is not yet fully understood (Bajet et al., 1994;

Ceballos & Deutsch, 1992; Mahuku et al., 2016). Despite these findings, only *P. maydis* has been documented in association with tar spot of maize in the United States to date (McCoy et al., 2019; Valle-Torres et al., 2020). The host range of *P. maydis* appears to be largely restricted to *Zea mays*, although other *Phyllachora* species are known to cause tar spot on a wide range of grass species and other hosts (Parbery, 1967, 1971; Cline, 2019; Valle-Torres et al., 2020). Although *P. maydis* is considered the primary causal agent of tar spot, several additional fungal species have been associated with the disease (Hock et al., 1995; Mottaleb et al., 2019; Luis et al., 2023). In North America, *P. maydis* stromata have been shown to harbour members of the *Paraphaeosphaeria* and *Fusarium* genera, with *Fusarium sporotrichioides* positively correlated with the development of *P. maydis* “fisheye” lesions (McCoy et al., 2019; Caldwell et al., 2024; Rogers et al., 2026). The introduction of additional pathogens associated with tar spot, such as *M. maydis*, into North American production systems could potentially exacerbate disease severity and increase economic losses to the maize industry (Mottaleb et al., 2019; Yan et al., 2022).

The level of tar spot infection is influenced by the timing of disease onset, environmental conditions, and the susceptibility of the maize hybrid (Telenko et al., 2020). TS typically spreads from the lowest leaves to the upper leaves, leaf sheaths, and eventually the husks of developing ears (Sharpe et al., 2021). Severely infected leaves can limit photosynthetic activity and sugar availability, resulting in incomplete kernel filling and overall reductions in kernel weight and yield (Bayer, 2020). Disease severity can range from minor infections affecting 1–15% of leaf tissue to severe outbreaks exceeding 40–50% leaf area infection, with each 1% increase in tar spot severity corresponding to estimated yield losses of approximately 21.5–91.5 kg ha⁻¹ (Telenko et al., 2019). Species within the genus *Phyllachora* infect grasses and produce raised, melanized structures called stromata on their plant hosts (Broders et al., 2022). Ascospores are considered the primary

infectious propagules responsible for initiating disease, as maize inoculation with conidia did not produce tar spot symptoms on susceptible leaves (Solórzano et al., 2023). The ascospores develop within asci contained in perithecia, which rupture to release ascospores to the leaf surface where they can be dispersed by wind or rain splash (Caldwell et al., 2024; Telenko et al., 2021). Infected plant residues are therefore believed to represent the primary source of inoculum for subsequent epidemics. Ascospores are dispersed during periods of high humidity and have been shown to travel distances of up to 800 feet via wind or rain splash (Sharpe et al., 2021). Because tar spot is a polycyclic disease, multiple infection cycles may occur within a single growing season as newly produced ascospores reinfect maize foliage under favourable environmental conditions (Telenko et al., 2019, 2022). Following infection, symptoms typically appear within 14–21 days as stromata develop on the leaf surface and begin producing additional spores that can initiate secondary infections (Telenko et al., 2021). As the growing season progresses, infected tissue senesces and dries, returning fungal structures to the soil as crop residue where the pathogen persists as stromata (Figure 1) (Telenko et al., 2021). Once maize is replanted the following season and crops reach susceptible growth stages such as the R1 reproductive phase, overwintering stromata release ascospores that infect maize foliage under favourable environmental conditions (Bajet et al., 1994; Hock et al., 1995; Telenko et al., 2021).

Methods for mitigating yield losses caused by fungal pathogens such as *P. maydis* include cultural practices, agrochemical applications, and partial host genetic resistance (Roggenkamp et al., 2025). Current management strategies emphasize an integrated approach, including fungicide applications, residue management to reduce overwintering inoculum, and the use of resistant maize genotypes (Kleczewski, 2020; Bayer, 2020). Among these, the use of hybrids with partial resistance is considered a cornerstone of disease management, as it can significantly slow disease

development and, in some cases, reduce the need for fungicide application (Chilvers, 2025). Fungicide application remains an important component of management; however, no single product or application strategy has been consistently identified as most effective. Current recommendations favour fungicides with mixed modes of action, which generally provide improved disease suppression compared to single-mode products and may help delay the development of fungicide resistance in *P. maydis* populations (Chilvers, 2025). Increasing average temperatures associated with climate change may further drive the northward spread of *P. maydis* across the United States and Canada, particularly given the susceptibility of many cultivated maize varieties. These findings emphasize the complexity of *P. maydis* biology and tar spot epidemiology, underscoring the need for continued research to inform more effective and sustainable disease management approaches.

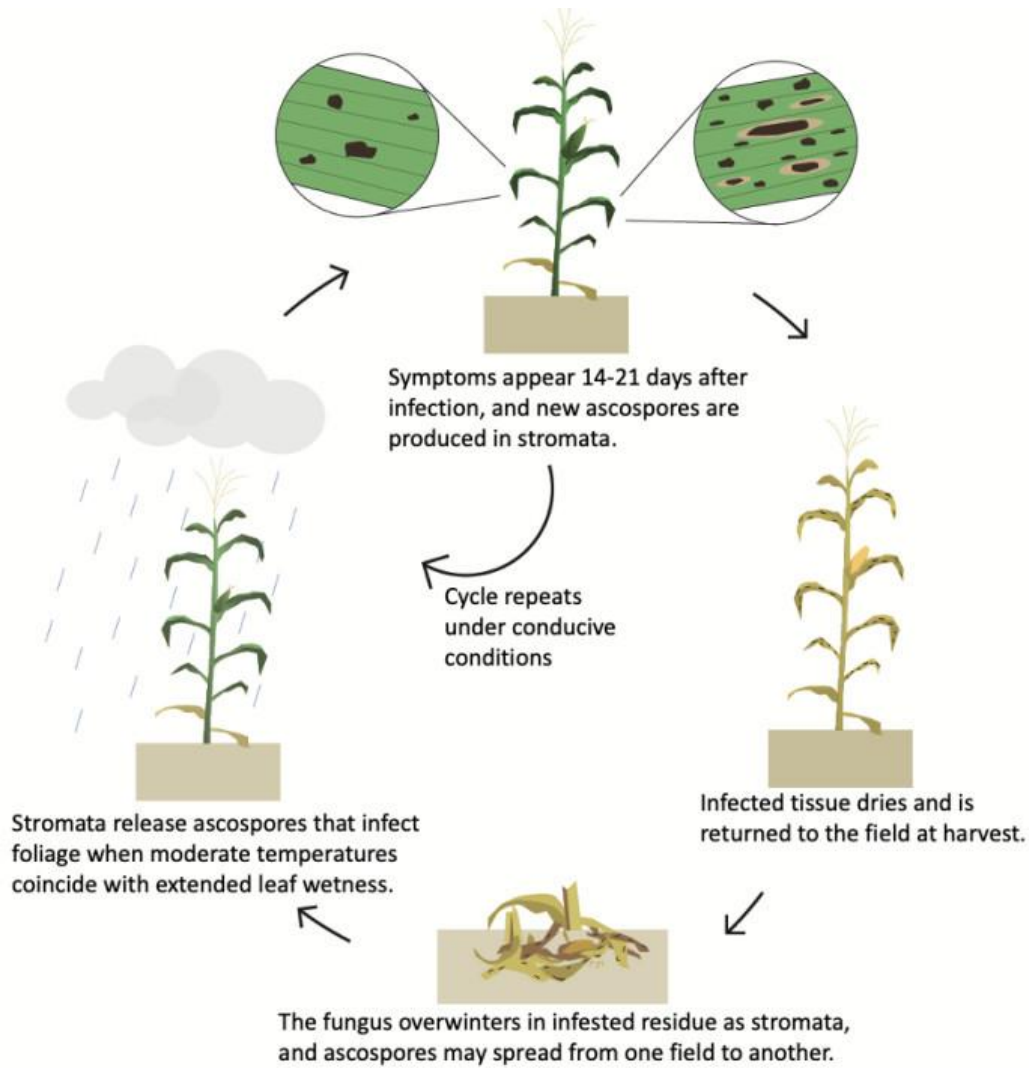


Figure 1. Disease cycle of tar spot of maize. *P. maydis* overwinter in infested crop debris as stromata. Stromata release ascospores that infect foliage under favourable conditions and spread via wind and rain. Reproduced from Telenko et al. (2021) and Iowa State University Integrated Pest Management, without modification.

1.2. Plant Resistance to Tar Spot

Plants possess both constitutive and inducible defence mechanisms that allow them to detect and respond to invading pathogens. Constitutive defences include preformed structural barriers that limit pathogen entry into plant tissues (Freeman & Beattie, 2008; Boots & Best, 2018). In contrast, inducible defences are mediated primarily through two interconnected layers of immunity, pattern-triggered immunity (PTI) and effector-triggered immunity (ETI) (Yu et al., 2017). Understanding which of these defence mechanisms contribute to tar spot resistance may provide insight into the molecular basis of disease resistance in maize.

1.2.1. Constitutive Defences

Constitutive defenses include protective barriers which limit pathogen entry into plant tissues or cells. The plant cuticle covers the aerial surfaces of plants is primarily composed of cutin and epicuticular and intracuticular waxes (Serrano et al., 2014; Zuch et al., 2022). Beneath the cuticle, the plant cell wall acts as a second physical barrier against pathogen invasion (Malinovsky et al., 2014; Narváez-Barragán et al., 2022). The plant cell wall is a complex extracellular matrix that provides structural support and protection against environmental stresses. Primary cell walls are composed of cellulose, hemicelluloses, pectin, meanwhile secondary cell walls contain lignin with little to no pectin (Zhong et al., 2019; Delmer et al., 2024). Primary cell walls are synthesized during cell growth and are relatively thin, pliant, and highly hydrated structures that allow for cell expansion (Cosgrove & Jarvis, 2012). The primary cell wall forms following cytokinesis of the cell plate and provides strength, elasticity, and plasticity as the cell grows and expands. In angiosperms, primary cell walls are broadly classified into two types (Carpita & Gibeau, 1993). Cereals, such as maize, possess a type II primary cell wall, which differs from dicot type I cell

walls in both composition and organization (Kozlova et al., 2020). These walls are built from a skeleton of cellulosic microfibrils embedded in a matrix of hemicelluloses, particularly glucuronoarabinoxylans (GAX) and mixed-linkage glucans (MLG), while containing relatively lower amounts of pectin (homogalacturonan, rhamnogalacturonan I, and rhamnogalacturonan II), xyloglucan, and glycoproteins (Santiago et al., 2013; Okekeogbu et al., 2019; Penning et al., 2019).

While primary cell walls are formed by all plant cells, secondary cell walls are produced only by some specialized cell types, such as xylem, that form after cell expansion has ceased and provide increased rigidity and mechanical strength to plant tissues (Cosgrove & Jarvis, 2012; Kumar et al., 2016). These walls are enriched in cellulose, hemicelluloses, and lignin, with cellulose comprising approximately 40–80% of the wall depending on tissue type (Brown et al., 2005; Zhong & Ye, 2015; Kumar et al., 2016; Zhang et al., 2025). Cellulose is synthesized at the plasma membrane (PM) by a large rosette-shaped protein complex known as the cellulose synthase complex (CSC). As the CSC moves within the plane of the PM, it extrudes cellulose chains that associate to form cellulose microfibrils, creating a stiff and rigid framework that supports the cell (Nishiyama, 2009; Kumar et al., 2016). Hemicelluloses are synthesized within the Golgi apparatus and transported to the PM, where they are integrated into the growing cell wall (Rennie & Scheller, 2014). They function as a flexible matrix that links the cellulose framework, providing the cell wall with flexibility and adaptability. Hemicelluloses are particularly abundant in grasses, where they can account for approximately 55% of the cell wall composition (Cosgrove et al., 1997; Santiago et al., 2013). Among these, xylan is the predominant hemicellulose. In grasses, ferulation of xylan facilitates covalent cross-linking between xylan chains, contributing to the structural integrity of the wall matrix (Figure 2) (Tan et al., 2013; Rennie & Scheller, 2014; Tryfona et al., 2023). Arabinoxylans (AX) can also form cross-linked networks through ferulate bridges, further

strengthening the cell wall structure. Both primary and secondary cell walls therefore play a crucial role in determining plant mechanical strength (Zhang et al., 2025).

Beyond their structural role, plant cell walls are increasingly recognized as an important component of plant defence. Numerous studies have demonstrated that alterations in cell wall composition or architecture can influence susceptibility to pathogens (Molina et al., 2021; Wang et al., 2023). For example, Molina et al. (2021) examined a collection of *Arabidopsis* cell wall mutants with different parasitic styles, a vascular bacterium (*Ralstonia pseudosolanacearum*), a necrotrophic fungus (*Plectosphaerella cucumerina*), and a biotrophic oomycete (*Hyaloperonospora arabidopsidis*) and found that over 85% displayed altered resistance phenotypes to at least one pathogen, highlighting the importance of wall composition in determining disease resistance (Molina et al., 2021). Similarly, studies in maize have shown that increased cell wall thickness and higher levels of structural polymers such as lignin and xylan are associated with resistance to insect pests such as the European and Mediterranean corn borers (Barros-Rios et al., 2011; Santiago et al., 2013). These findings suggest that differences in cell wall composition and structure may serve as an important constitutive barrier limiting pathogen entry or spread.

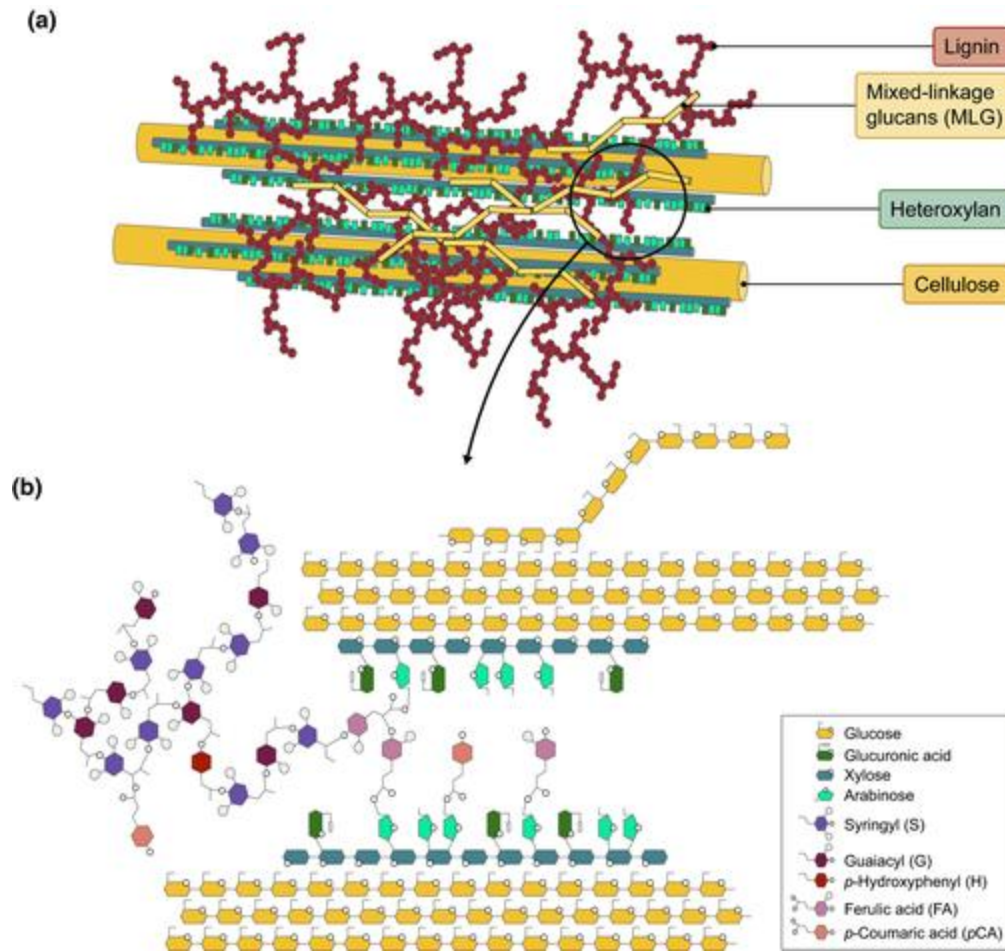


Figure 2. General schematic of the grass secondary cell wall matrix. The grass secondary cell wall matrix is composed of cellulose microfibrils, mixed-linkage glucans, heteroxylans, and lignins. (a) Generalised cartoon of grass secondary wall polymer interactions. (b) Schematic fine structure of the circled region in (a). Cellulose microfibrils consist of multiple, organised, $\beta(1,4)$ -linked glucose chains. Mixed-linkage glucans are also glucose chains but include $\beta(1,3)$ linkages. Heteroxylan has a xylose backbone decorated with sugar and phenolic side chains of xylose, arabinose, glucuronic acid, and hydroxycinnamates (FA and pCA). These polysaccharides can be interwoven with lignins, branched phenolic polymers composed of three main lignin units: syringyl (S), guaiacyl (G), and *p*-hydroxyphenyl (H). Lignins can also contain ferulic and *p*-coumaric acids. The figure reproduced without modification from Coomey et al. (2020).

1.2.2. Inducible Defences

In addition to constitutive structural barriers, plants possess inducible immune responses that are activated upon detection of pathogen-derived molecules (Yu et al., 2017). PTI is initiated through the recognition of conserved microbial molecules, known as microbe-associated molecular patterns (MAMPs), by pattern-recognition receptors (PRRs) located at the plant cell surface (Jones & Dangl, 2006; Boller & Felix, 2009; Yu et al., 2017). MAMPs represent conserved molecular features shared among groups of microbes that plants have evolved to recognize (Newman et al., 2013). For example, chitin, a major structural component of fungal cell walls, and flg22, a highly conserved 22-amino acid peptide derived from bacterial flagellin, are well-characterized fungal and bacterial MAMPs, respectively (Felix et al., 1999; Chinchilla et al., 2006; Sánchez-Vallet et al., 2015). Upon recognition by PRR complexes at the plasma membrane (PM), PTI is rapidly activated through a series of intracellular signalling events, including receptor phosphorylation, calcium influx, ion flux across the PM, and transcriptional activation of defence-related genes (Yu et al., 2017; Brauer et al., 2025).

PRRs belong primarily to the receptor-like kinase (RLK) family, which represents one of the largest gene families in plants and includes more than 700 members in maize (Dievart et al., 2020; Zhu et al., 2024). PRR activation often requires interaction with co-receptors such as SOMATIC EMBRYOGENESIS RECEPTOR KINASE (SERK) proteins, including BAK1, which stabilize receptor complexes and amplify downstream immune signalling (Ramírez-Zavaleta et al., 2022). Among these, leucine-rich repeat receptor-like kinases (LRR-RLKs) are well-characterized immune receptors that detect extracellular signals associated with pathogen presence (Noman et al., 2019; Narváez-Barragán et al., 2022). Well-studied examples of PRRs include FLAGELLIN-SENSING 2 (*FLS2*), which recognizes bacterial flagellin, and EF-Tu RECEPTOR (*EFR*), which

detects the bacterial elongation factor Tu (Jones & Dangl, 2006). Activation of PRR complexes triggers downstream defence responses including reactive oxygen species (ROS) production, stomatal closure, callose deposition, and activation of mitogen-activated protein kinase (MAPK) signalling pathways (Noman et al., 2019; Yu et al., 2017). One of the earliest PTI responses is the production of ROS, which can occur within minutes of pathogen recognition (Yu et al., 2017; Fedoreyeva, 2024). MAMP-induced ROS bursts occur primarily in the apoplast and are generated by plasma membrane-localized NADPH oxidases and apoplastic class III peroxidases (Torres et al., 2002; Daudi et al., 2012). These enzymes produce superoxide (O_2^-) and hydrogen peroxide (H_2O_2), which function both as signalling molecules and as direct antimicrobial agents, promoting cell wall reinforcement through oxidative cross-linking of wall polymers and induction of callose deposition (O'Brien et al., 2012; Rivas et al., 2024).

1.2.3. Pathogen Invasion

Despite the extensive defence mechanisms present in plants, pathogens have evolved multiple strategies to evade or suppress host immune responses. During infection, many pathogens secrete cell wall degrading enzymes, including pectate lyases, cellulases, and xylanases, which degrade plant cell wall components and facilitate tissue colonization (Bellincampi et al., 2014; Mitsumasu et al., 2015). In addition to these enzymes, pathogens deploy specialized secreted proteins that can function as effectors, manipulating host cellular processes to promote infection (Mukhtar et al., 2011; Jayami et al., 2014; Ahmed et al., 2020). Effector proteins may function in the plant apoplast or be translocated directly into host cells, where they can localize to a variety of subcellular compartments, including the nucleus, cytosol, PM, and other organelles (Whisson et al., 2016; Lorrain et al., 2018; Helm et al., 2022). Once delivered, these proteins often interfere

with host immune signalling pathways, including those associated with PTI, thereby suppressing early defence responses and facilitating pathogen establishment (Leiva-Mora et al., 2024). For successful infection, the delivery of effector proteins is often as important as the molecular function. Many obligate biotrophic pathogens form specialized infection structures known as haustoria, which invaginate into host cells while remaining separated from the host cytoplasm by a modified plant membrane (Coffey et al., 1972; Giraldo et al., 2013). The formation of haustoria requires extensive remodelling of the host PM and creates an intimate interface through which effectors can be delivered and nutrients acquired (Chaudhari et al., 2014). Through these mechanisms, pathogens can disrupt host immune signalling and cellular functions, thereby suppressing defence responses (Todd et al., 2022; Zhang et al., 2022; Leiva-Mora et al., 2024).

Recent studies suggest that *P. maydis* produces a suite of candidate effector proteins that may contribute to virulence during tar spot infection. Sequencing of the *P. maydis* genome by Telenko et al. (2020) identified 462 putatively secreted proteins and predicted 59 candidate effector proteins using EffectorP. EffectorP predicts fungal and oomycete effectors using supervised machine learning trained on experimentally validated effectors and secreted non-effector proteins, achieving over 80% specificity (Sperschneider et al., 2015; Sperschneider & Dodds, 2022). These candidates were further refined through a bioinformatic pipeline incorporating signal peptide prediction (SignalP v6.0), transmembrane domain filtering (TMHMM v2.0) and protein size constraints (<300 amino acids) to generate 40 putative effectors (Helm et al., 2022). In 2023, MacCready et al. reported an updated high-quality *P. maydis* genome, identifying 492 predicted secreted proteins, 163 of which encoded effector-like sequences based on EffectorP software. Building on this, Rogers et al. (2024) selected 18 candidate genes that met similar expression criteria to those described by Helm et al. (2022), while also selecting genes that

have expression during early disease development. Building on these predictions, Rogers et al. (2024) investigated whether candidate effectors could suppress early plant immune responses. Eighteen candidate genes with strong expression during early disease development were transiently expressed in *N. benthamiana*, and their effects on chitin-triggered ROS production, one of the earliest apoplastic defence responses associated with MAMP-triggered immunity, were evaluated using a luminol-based assay (Rogers et al., 2024). This oxidative burst consists primarily of O_2^- and H_2O_2 , which are generated in the apoplast following MAMP perception (Torres et al., 2002; O'Brien et al., 2012). Three candidate effectors consistently attenuated ROS accumulation, suggesting a role in suppressing MAMP-triggered immunity (Rogers et al., 2024). Consequently, suppression of this ROS burst suggests that these effectors may interfere with early chitin perception, downstream signaling pathways, or activation of ROS-producing enzymes during the initial stages of MAMP-triggered immunity. Transient expression assays in *N. benthamiana* revealed that these candidate proteins localize to diverse subcellular compartments within plant cells, including the nucleus, cytosol, PM, and chloroplasts (Helm et al., 2022). While the presence of signal peptides supports their secretion, there is currently no direct evidence demonstrating that the putative effectors translocate into host cells or that they have a role in manipulating host processes during infection. Establishing effector function requires further validation, including confirmation of expression during infection, host cell delivery, and the ability to modulate host immune responses or contribute to virulence (Sonah et al., 2016).

1.2.4. Host Transcriptional Responses to *P. maydis*

Complementary to the characterization of pathogen-derived secreted proteins, investigation of host transcriptional responses provides key insight into the molecular basis of

maize defence and resistance to *P. maydis*. Evidence that maize mounts a defence response to *P. maydis* infection has also been demonstrated through transcriptomic studies. Roggenkamp et al. (2025) compared gene expression in B73 maize following exposure to *P. maydis* and identified 3,160 differentially expressed genes (DEGs). These DEGs were enriched in genes associated with metabolism and defence responses including, mildew locus O proteins, calcium-dependent lipid-binding proteins, terpenoid biosynthetic enzymes, pathogenesis-related proteins, and osmotin-like proteins (Roggenkamp et al., 2025).

1.2.5. Genetic Resistance to Tar Spot

In addition to transcriptional responses, significant effort has been directed toward identifying genetic sources of resistance to tar spot in tropical and subtropical maize germplasm, which represents a major reservoir of genetic diversity for disease resistance. Tropical and temperate germplasm are distinguished primarily by their adaptation to photoperiod and flowering time. Tropical maize is generally more sensitive to day length and flowers later, whereas temperate germplasm has been selected for reduced photoperiod sensitivity and earlier maturity to suit shorter growing seasons at higher latitudes (Choquette et al., 2023). Compared with temperate germplasm, tropical germplasm also retains greater allelic diversity owing to its origin near the center of maize domestication and its adaptation to diverse environmental conditions and pathogen pressures, whereas temperate germplasm has experienced successive bottlenecks during adaptation and modern breeding (Hufford et al., 2012; Romay et al., 2013). A screen of 890 maize inbred genotypes derived from CIMMYT breeding programs, identified multiple loci and genotypes associated with tar spot resistance (Semagn et al., 2012; Wen et al., 2011; Mahuku et al., 2016). Among these, the tropical white maize inbred line CML495 was identified as highly resistant to

tar spot (Mahuku et al., 2016; Kushalappa et al., 2016; Lipps et al., 2022). CML495 is a CIMMYT-derived tropical lowland line originally developed through recurrent selection for drought tolerance under tropical growing conditions (CIMMYT, 2005). Its pedigree reflects contributions from multiple breeding populations that underwent successive cycles of crossing and selection, rather than a single biparental cross. Subsequent repeated selfing generations produced a genetically stable inbred line with a high degree of homozygosity across the genome (CIMMYT, 2005).

Through GWAS and quantitative trait locus (QTL) mapping, three tar spot resistance-associated loci were detected on chromosomes 2, 7, and 8, with a major QTL, designated *qRtsc8-1*, located on chromosome bin 8.03 (Mahuku et al., 2016; Cao et al., 2017). This locus was validated across multiple independent bi-parental populations and was estimated to explain between 18–43% of the phenotypic variation in tar spot resistance. Subsequent fine-mapping further confirmed its contribution, with more refined estimates suggesting it accounts for approximately 14–15% of phenotypic variance for tar spot resistance (Ren et al., 2022). The consistent identification of *qRtsc8-1* across diverse tropical populations underscores its importance as a major contributor to resistance. Interestingly, the genomic region encompassing bin 8.03 has also been associated with resistance to a wide range of other maize diseases, including rough dwarf disease, grey leaf spot, common rust, northern and southern leaf blight, smut diseases, and *Aspergillus flavus* infection (Di Renzo et al., 2004; Liu et al., 2014; Benson et al., 2015; Mammadov et al., 2015; Shi et al., 2014; Olukolu et al., 2016; Zheng et al., 2018; Balint-Kurti & Carson, 2007; Chung et al., 2011; Ding et al., 2008; Mideros et al., 2014; Wang et al., 2012; Yin et al., 2014; Yan et al., 2022). This repeated association suggests that this region may represent a

genomic hotspot for disease resistance, potentially harbouring genes involved in conserved or broad-spectrum defence mechanisms.

Fine-mapping of the *qRtsc8-1* region identified approximately 203 gene loci, including 104 putative uncharacterized proteins and 99 genes with predicted functional annotations (Mahuku et al., 2016; Ren et al., 2022). Subsequent analyses further refined this region through the identification of significant single nucleotide polymorphisms (SNPs) and candidate resistance genes. Among these, four genes have been proposed as potential contributors to resistance, including a UDP-xylose transporter (UXT), *GRMZM2G063511* (*ZmUXT2*), an LRR-RLK, *GRMZM2G073884* (*ZmLRR-RLK*), and two additional uncharacterized genes (*GRMZM2G071228* and *GRMZM5G869967*) (Mahuku et al., 2016; Ren et al., 2022; Yan et al., 2022). Importantly, evidence suggests that tar spot resistance may differ between tropical and temperate maize germplasm. Trygestad (2021) performed a GWAS using a temperate maize diversity panel and identified SNPs associated with resistance to *P. maydis*; however, these loci did not overlap with the previously identified *qRtsc8-1* region. This lack of overlap indicates that resistance mechanisms may be population-specific, with distinct genetic pathways underlying resistance in temperate versus tropical maize (Trygestad, 2021; Roggenkamp et al., 2025). To date, the functional roles of these temperate-associated loci remain largely uncharacterized. These findings highlight both the progress made and the remaining gaps in understanding tar spot resistance. While major loci such as *qRtsc8-1* have been identified, particularly in tropical germplasm, their underlying molecular mechanisms remain unresolved. Integrating transcriptomic, genetic, and functional approaches will be essential to define how these loci mediate defence against *P. maydis* and to support the development of resistant maize varieties.

1.3. Research Objectives

To improve understanding of putative candidate genes within the major *qRtsc8-1* resistance locus, this study compared candidate gene variation and inducible defence responses between resistant and susceptible maize genotypes.

Specifically, the objectives were to:

1. To evaluate the induced expression of four candidate genes identified within the resistance QTL *qRtsc8-1* under MAMP treatment.
2. To genetically characterize two candidate genes, *ZmUXT2* and *ZmLRR-RLK*, across susceptible and resistant maize alleles.
3. To compare inducible defence responses in resistant and susceptible genotypes of maize.

2. Materials and Methods

2.1. Plant Material and Growth Conditions

Seeds of maize (*Zea mays*) line CO428 were obtained from Aida Kebede at Agriculture and Agri-Food Canada's Ottawa Research and Development Centre (ORDC). Seeds of the resistant line CML495 were purchased from the CIMMYT gene bank in Mexico. Plants were grown in a Enconair AC-40T model growth chamber (Ecological Chambers Inc.) under a 16 h light (25°C) and 8 h dark (18°C) photoperiod at ambient humidity of approximately 50%. Within an experiment, five plants per line were sown individually in 24-cell trays, with one seed per cell at a depth of approximately 2 cm in a soil mixture of 75% PRO-MIX BX, 24% black earth, and 1% lime. Plants were watered twice daily, and no fertilizer was used.

N. benthamiana seeds were germinated in an in-house prepared Cornell soil mix consisting of peat moss, vermiculite, slow-release fertilizer, and lime (300:630:1:4.2). Seedlings were grown in 5-inch fibre-based paper pots in a Conviron E15 Model growth chamber (Controlled Environments Ltd.) under a long-day photoperiod (20 h light and 4 h dark) at a constant temperature of 25°C at ambient humidity of approximately 50%. After one week, seedlings were transplanted into individual 2-inch pots, and excess seedlings were removed to maintain one plant per pot. Plants were watered weekly during early growth and twice weekly following maturation. Fertilization was performed once weekly using 50 mL of Miracle-Gro 20-8-20 solution (2 g L⁻¹). Mature plants were dried for five weeks prior to seed collection for future experiments.

2.2. RNA Extraction and qPCR

To assess differences in gene expression, fully expanded leaves from approximately three-week-old plants were syringe-infiltrated with 500 µg/mL chitin, 5 µM flg22 peptide, or sterile water (control) by applying pressure with a needleless syringe to the abaxial leaf surface until infiltration occurred. Infiltrated regions were marked with permanent marker and after 4 hours, the infiltrated leaf tissue was excised, flash-frozen in liquid nitrogen, and stored at -80°C until RNA extraction. Frozen tissue was ground in liquid nitrogen prior to total RNA extraction using the RNeasy Plant Mini Kit (Qiagen, Germany) according to the manufacturer's instructions, including on-column DNase I digestion (Qiagen, Mississauga, Canada) to remove genomic DNA. RNA quantity and purity were assessed spectrophotometrically prior to cDNA synthesis using the High-Capacity cDNA Reverse Transcription Kit with random primers (Applied Biosystems, Thermo Fisher Scientific). Primer efficiencies and melt-curve analyses were performed to confirm primer specificity and amplification quality prior to gene expression analysis. qPCR reactions were

performed using four biological replicates per treatment in 10 μ L reaction volumes containing 1 \times Power SYBR Green Master Mix (Applied Biosystems, Thermo Fisher Scientific), 0.5 μ M of each gene-specific primer, and 1 μ L diluted cDNA template (900 ng total cDNA). Reactions were run on a QuantStudio 5 Real-Time PCR System (Applied Biosystems) under the following cycling conditions: 95°C for 2 min, followed by 40 cycles of 95°C for 15 s and 60°C for 1 min. The expression levels of the defense genes *anther ear 2* (*An2*) and *pathogenesis-related 5* (*PR5*) were normalized using two reference genes, *Domains of Unknown Function* (*DUF*) and *Cyclophilin* (*CYP*), which have previously been identified as constitutively expressed genes in maize (Lin, F. et al., 2014; Lin, Y. et al., 2014; Brauer et al., 2024). The expression values of *DUF* and *CYP* were averaged prior to normalization (Supplemental Table S1). Relative expression levels were subsequently calculated using the Pfaffl method (Pfaffl, 2001). For each genotype and treatment combination, four to five biological replicates (individual plants) were analyzed, with one infiltrated leaf sampled per plant. Statistical significance was determined using one-way ANOVA ($p < 0.05$).

2.3. Phylogenetic Tree Construction

Amino acid sequences for *ZmUXT2* and *ZmLRR-RLK* were retrieved from the NCBI Gene database using the B73 reference genome *Zm-B73-REFERENCE-NAM-5.0* (taxid: 4577) (Sayers et al., 2023). Full-length protein sequences of each candidate gene were used as BLASTP queries against the NCBI protein database. Crop species with the closest putative orthologs were selected for comparison, and representative dicot species were included as comparative outgroups. BLAST results were cross-referenced with Phytozome to confirm gene annotations and orthologue

assignments (Goodstein et al., 2012). Selected full-length amino acid sequences were aligned using MUSCLE and phylogenetic trees were constructed in MEGA12 using the neighbour-joining method with 1,000 bootstrap replicates to assess branch support (Kumar et al., 2024; Madeira et al.). The original tree topology generated by MEGA12 was used for figure presentation.

2.4. DNA Extraction and Sequencing

To extract DNA for gene sequencing, leaf tissue was collected from approximately three-week-old plants, flash-frozen in liquid nitrogen, and ground using a mortar and pestle. Approximately 100 mg of tissue was used for DNA extraction with the Phytopure Plant DNA Extraction Kit (GE Healthcare, RPN8511) according to the manufacturer's instructions. DNA concentration and purity were determined spectrophotometrically, and samples were stored at -20°C until use. Touchdown polymerase chain reaction (PCR) was performed using 25 μL reaction volumes containing approximately 100 ng genomic DNA, TaKaRa Ex Premier DNA Polymerase (Takara Bio Inc.), and gene-specific primers. Primers were designed from B73 genomic sequences using NCBI Primer-BLAST and Geneious Prime software with the following parameters: primer lengths of 18–24 bp, melting temperatures between 50 – 65°C , GC contents of 40–60%, and target amplicon lengths of 500–800 bp (Supplemental Table S2) (Ye et al., 2012; Geneious Prime, 2025). The touchdown PCR program consisted of an initial denaturation at 94°C for 1 min; 10 cycles of 98°C for 10 s, 68°C for 15 s, and 68°C for 1 minute; followed by 31 cycles of 98°C for 10 s, 58°C for 15s, and 68°C for 1 min; with a final extension at 68°C for 5 min and a hold at 10°C . Amplified fragments (500–800 bp) were verified by electrophoresis on 1% agarose gels alongside the GeneRuler 1 kb Plus DNA Ladder (Thermo Scientific), visualized under UV illumination. Verified

PCR products were excised and purified using the GenepHlow Gel/PCR kit (Geneaid, DFH100) and submitted to the Molecular Technology Laboratory (MTL, Agriculture and Agri-Food Canada) for Sanger sequencing. A second round of touchdown PCR was performed to amplify larger genomic fragments (1,000–2,000 bp) using the same cycling conditions and KOD Xtreme Hot Start DNA polymerase (Sigma Aldrich). Amplified products were purified using a PureLink PCR Purification Kit (Thermo Fisher Scientific, K310001) and were subsequently submitted to Eurofins Genomics for long-read Nanopore sequencing. Raw sequence reads were obtained in FASTA format and analyzed using Geneious Prime version 2025.1.3 (Biomatters Ltd.) (Geneious Prime, 2025). The sequences were aligned using the Geneious Pairwise Alignment tool and further refined with MUSCLE multiple sequence alignment to identify polymorphisms.

2.5. Transient Expression and Subcellular Localization in *N. benthamiana*

Subcellular localization of candidate resistance proteins was determined using *Agrobacterium*-mediated transient expression in *N. benthamiana* leaves. Coding sequences of *ZmUXT2* and *ZmLRR-RLK* from both CML495 and CO428 genotypes were synthesized (Gene Universal, Newark, DE, USA) into the donor vector pDONRzeo. Gateway LR Clonase II reactions (Thermo Fisher Scientific) were used to recombine inserts into the pEarleyGate103 expression vector, which drives expression under the cauliflower mosaic virus (CaMV) 35S promoter and generates C-terminal GFP–His fusion proteins (Earley et al., 2006; Brauer et al., 2016). Expression constructs were introduced into *Agrobacterium tumefaciens* strain GV3101 using a freeze–thaw transformation method. Briefly, 1 μL plasmid DNA (100–500 ng μL^{-1}) was added to 50 μL competent *A. tumefaciens* GV3101 cells and incubated on ice for 30 min. Cells were then frozen

in liquid nitrogen for 1 min and thawed at 37°C for 2 min. Following the addition of SOC medium, cultures were incubated for 2–3 h with shaking before plating on selective media. Successful transformation was confirmed by colony PCR and Sanger sequencing. PCR conditions consisted of an initial denaturation at 95°C for 2 min, followed by 30 cycles of 95°C for 30 s, 57°C for 45 s, and 72°C for 1 min, with a final extension at 72°C for 10 min (Supplemental Table S2).

A. tumefaciens strain GV3101 carrying the construct of interest was grown overnight in Luria–Bertani (LB) medium supplemented with appropriate antibiotics at 28°C with shaking at 220 rpm. Bacterial cells were collected by centrifugation and resuspended in infiltration buffer (10 mM MES, 10 mM MgCl₂, 150 μM acetosyringone, pH 5.6) to a final OD₆₀₀ of 0.4. *A. tumefaciens* strain GV2260 carrying the P19 silencing suppressor construct was prepared separately in infiltration buffer to an OD₆₀₀ of 0.8. Equal volumes of GV3101 cultures carrying the construct of interest and GV2260 cultures carrying P19 were mixed immediately prior to infiltration to enhance transient expression (Cao et al., 2017; Popescu et al., 2007). For co-localization experiments, the GV3101/P19 mixture was further mixed 1:1 with *A. tumefaciens* GV2260 cultures carrying the HDEL–mCherry endoplasmic reticulum (ER) marker construct at an OD₆₀₀ of 0.8 (Gomord et al., 1997; Brauer et al., 2016). *Agrobacterium* suspensions were infiltrated into the abaxial surface of the middle three leaves of four-week-old *N. benthamiana* plants using a 1 mL blunt-end syringe. Plants were maintained in a controlled growth chamber for 3–4 days post-infiltration.

Leaf disks (~3 mm diameter) were excised from infiltrated regions and examined for GFP fluorescence using a Zeiss confocal laser scanning microscope with an emission range of 500–535 nm. HDEL–mCherry fluorescence was visualized using an emission range of 600–650 nm. Plasma membrane staining was performed using FM4-64FX (Thermo Fisher Scientific) at a final

concentration of 15 μM . Leaf disks were incubated in the stain for 5 min prior to imaging using an emission range of 600–650 nm. All images were acquired using the 488 nm laser on the confocal microscope.

2.6. Reactive Oxygen Species Assay

Apoplastic ROS production was quantified using a luminol-based chemiluminescence assay as previously described (Brauer, 2024). In the presence of horseradish peroxidase, this assay detects extracellular hydrogen peroxide (H_2O_2) released into the apoplast following immune activation. Leaf disks (4-mm diameter) were collected from fully expanded leaves of approximately three-week-old plants using a cork borer. Three disks per well were floated adaxial side up in 200 μL sterile distilled water in white 96-well plates (Greiner Bio-One) and incubated overnight (~16 h) in the dark at room temperature. The following day, the water was carefully removed and replaced with 100 μL freshly prepared assay solution containing 20 μL of 4 mg/mL L-012 (FujiFilm, 120-04891), 4 μL of 10 mg/mL horseradish peroxidase (type VI-A, Sigma, P6782), and the appropriate elicitor to achieve final concentrations of 5 μM flg22 peptide, 500 $\mu\text{g}/\text{mL}$ chitin, or sterile water as a control. Luminescence was measured immediately using a Tecan Infinite F Plex 200 Pro Multi-Mode Microplate Reader (Life Sciences, Tecan) with readings recorded in relative light units (RLU) at 2-minute intervals over a 60-minute period. Each treatment consisted of 9–12 biological replicates (individual wells containing disks from different plants) per genotype. The experiment was repeated four independent times with consistent results. To assess the effect of candidate gene expression on ROS production, luminol-based assays were also performed using transiently transformed *N. benthamiana* leaves expressing constructs of

ZmUXT2 or *ZmLRR-RLK*, or empty vector controls. Leaf disks (4-mm diameter) were collected 4 days post-infiltration and incubated overnight in sterile distilled water as described above. Samples were treated with 1 μ M flg22 peptide, 100 μ g/mL chitin, or sterile water as a control. Four biological replicates per construct were analyzed, with four leaf disks collected per plant.

3. Results

3.1. Expression patterns of putative resistance genes

Tar spot resistance is associated with a region on chromosome 8 containing four putative genes, including a UXT, *GRMZM2G063511* (*ZmUXT2*), an LRR-RLK, *GRMZM2G073884* (*ZmLRR-RLK*), and two uncharacterized genes: *GRMZM2G071228* and *GRMZM5G869967* (Mahuku et al., 2016; Ren et al., 2022). Expression profiling revealed that *ZmUXT2* is expressed in floral tissues, leaves, and roots, whereas *ZmLRR-RLK* expression appears to be restricted to leaf tissue (Waese et al., 2017; Papatheodorou et al., 2020).

To determine if the genes were expressed in the main tissue involved in tar spot development, the leaves, we evaluated expression using quantitative PCR (qPCR) on 3-week-old leaf tissue. We were also interested in determining whether gene expression differed between resistant (CML495) and susceptible (CO428) maize genotypes or after inducing immunity. Since we could not induce immunity with *P. maydis* inoculation due a lack of functional methods, we used the MAMPs chitin and flg22 to activate plant immune responses. *ZmUXT2* was induced by the flg22 treatment in both genotypes and uniquely exhibited higher basal expression in the resistant genotype compared to the susceptible line following both chitin and flg22 treatments (Figure 3). *ZmLRR-RLK* expression was significantly induced by both chitin and flg22 relative to

water treatment in both genotypes; however, following flg22 treatment, expression was higher in CO428 than in CML495 (Figure 3). *GRMZM5G869967* and *GRMZM2G071228* were expressed in leaf tissue of both genotypes but were not induced by either MAMP treatment. *GRMZM5G869967* expression was higher in flg22-treated CO428 than in CML495 (Figure 3). The elevated basal and MAMP-induced expression of *ZmUXT2* and *ZmLRR-RLK* motivated further investigation into their potential roles in tar spot resistance.

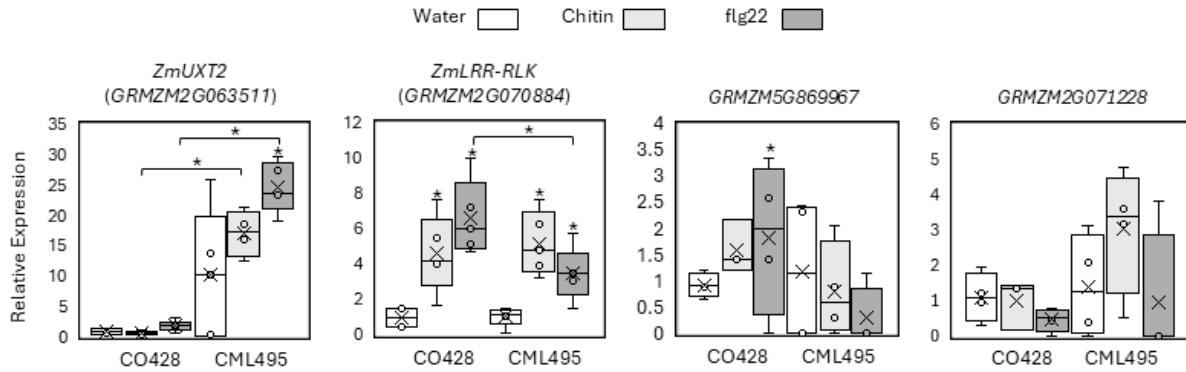


Figure 3. Expression of candidate genes in resistant and susceptible maize following MAMP treatment. Relative expression of the maize genes *ZmUXT2* (GRMZM2G063511), *ZmLRR-RLK* (GRMZM2G070884), *GRMZM5G869967*, and *GRMZM2G071228* was quantified in leaves of 3-week-old resistant (CML495) and susceptible (CO428) maize plants following infiltration with chitin (500 $\mu\text{g mL}^{-1}$), flg22 (5 μM), or water (control). Leaf tissue was harvested 4 h post-infiltration, and transcript abundance was normalized to the reference genes *DUF* and *CYP* (n = 4-5). Data shown are representative of one of three independent experiments, each producing comparable results. Box plots indicate the median (centre line), first and third quartiles (box), and range (whiskers), with means denoted by “×”. Asterisks placed above box plots indicate significant differences between MAMP treatments and the corresponding water control within each genotype (one-way ANOVA; $p < 0.05$). Hovering brackets denote significant differences between genotypes under the indicated treatment condition ($p < 0.05$).

3.2. Characterization of *ZmUXT2*

To further characterize *ZmUXT2*, the predicted domain, phylogenetic relationships, sequence variation, and subcellular localization patterns were investigated. *ZmUXT2* contains a conserved triose-phosphate transporter (TPT) family transmembrane domain involved in the transport of phosphorylated molecules across membranes (Figure 4) (Parker et al., 2019). Within the maize nucleotide-sugar transporters (NSTs), *ZmUXT2* is assigned to the UXT2b subgroup within Group I transporters (Penning et al., 2019). Group I NSTs form a phylogenetically related clade of TPT-domain-containing integral membrane proteins associated with endomembrane transport and cell wall biosynthesis, including the Arabidopsis genes *AT1G06890* (*UXT3*) and *AT2G30460* (*UXT2*) (Penning et al., 2019). *ZmUXT2* shares 98% amino acid identity with the closely related maize protein *ZmUXT2a* (*GRMZM2G063253*) and 89% identity with *ZmUXT3a* (*GRMZM2G081848*) (Figure 4) (Penning et al., 2019). Amino acid sequence comparisons further revealed 79% identity with Arabidopsis *UXT2*, 95% similarity to the wheat homologue *TraesCS1B03G0359900* and greater than 80% similarity to homologues from wild rice, potato, and *Magnolia*, indicating that *ZmUXT2* belongs to a conserved gene family across flowering plants (Figure 4). To characterize sequence variation in *ZmUXT2*, coding sequences from resistant and susceptible maize genotypes were compared. The coding sequence of *ZmUXT2* was sequenced from the resistant genotype CML495 and the susceptible genotype CO428 and aligned with publicly available sequences from the susceptible maize inbred genotypes B73, B84, and PH207. Sequence comparisons identified a single amino acid substitution unique to CML495 within the conserved TPT transmembrane domain (Figure 5). Mapping onto the AlphaFold-predicted structure showed that this substitution is in a surface-exposed region α -helix secondary structure of the protein fold (Figure 6).

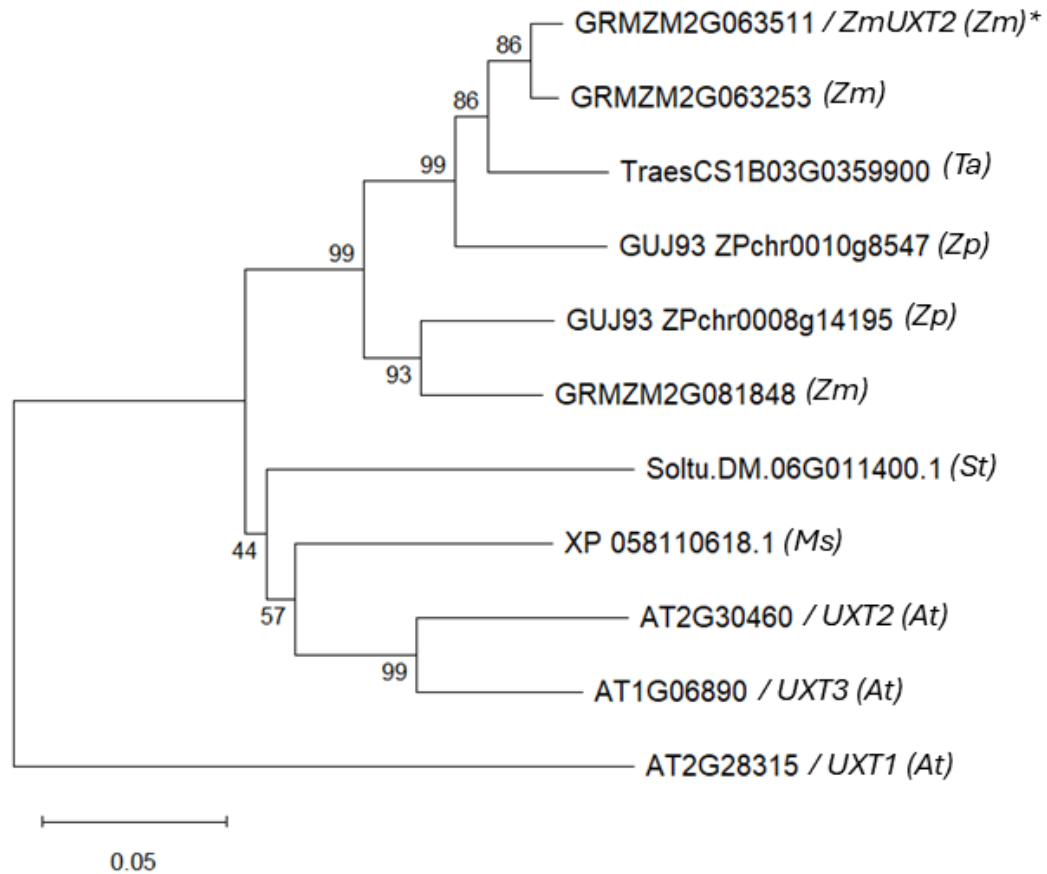


Figure 4. Phylogenetic analysis of *ZmUXT2* across plant species. Full-length amino acid sequence of the *ZmUXT2* (GRMZM2G063511) was aligned with homologous sequences from selected monocot and eudicot species using MUSCLE. Phylogenetic trees were constructed in MEGA12 (Kumar et al., 2024) using the neighbour-joining method. Bootstrap support values were calculated from 1,000 replicates, and bootstrap percentages are shown at the corresponding nodes. The scale bar represents 0.05 amino acid substitutions per site. Species abbreviations are *Zm* = *Zea mays*, *Ta* = *Triticum aestivum*, *Zp* = *Zizania palustris*, *St* = *Solanum tuberosum*, *Ms* = *Magnolia sinica*, *At* = *Arabidopsis thaliana*. The * indicates gene of interest.

Legend: Grey = mismatch across varieties, Red = unique to CML495, Orange = Triose-phosphate transporter domain

B84	MSSSLGFNFATTLTSWHLLVTFCSLHVALWMKFFEHPFDSRTVMGFGVLNGISIGLLNLS	60
C0428	--MYLSSAATTLTSWHLLVTFCSLHVALWMKFFEHPFDSRTVMGFGVLNGISIGLLNLS	58
B73	MSSSLGFNFATTLTSWHLLVTFCSLHVALWMKFFEHPFDSRTVMGFGVLNGISIGLLNLS	60
PH207	MSSSLGFNFATTLTSWHLLVTFCSLHVALWMKFFEHPFDSRTVMGFGVLNGISIGLLNLS	60
CML495	--MYLSSAATTLTSWHLLVTFCSLHVALWMKFFEHPFDSRTVMGFGVLNGISIGLLNLS	58
<hr/>		
B84	LGFN SVGFYQMTKLAIIPCTVILETLFFRKKFSRSIQMSLSVLLLGV-----GVA	110
C0428	LGFN SVGFYQMTKLAIIPCHCLRDTFLQEEVQRSIQMSLSVLLLGV-----GVA	108
B73	LGFN SVGFYQMTKLAIIPCTVILETLFFRKKFSRSIQMSLSVLLLGV-----GVA	110
PH207	LGFN SVGFYQMTKLAIIPCTVILETLFFRKKFSRSIQMSLSVLLLGVG VATVXLLGVGVA	120
CML495	LGFN SVGFYQMTKLAIIPCHCLRNTFLQEEVRSIQMSLSVLLLGV-----GVA	108
<hr/>		
B84	TVTDLQLNAVGSILSLLAIITTCIAQIMTNTIQKKFKVSS TQLLYQSCP YQSLTLFLIGP	170
C0428	TVTDLQLNAVGSILSLLAIITTCIAQIMTNTIQKKFKVSS TQLLYQSCP YQSLTLFLIGP	168
B73	TVTDLQLNAVGSILSLLAIITTCIAQIMTNTIQKKFKVSS TQLLYQSCP YQSLTLFLIGP	170
PH207	TVTDLQLNAVGSILSLLAIITTCIAQIMTNTIQKKFKVSS TQLLYQSCP YQSLTLFLIGP	180
CML495	TVTDLQLNAVGSILSLLAIITTCIAQIMTNTIQKKFKVSS TQLLYQSCP YQSLTLFLIGP	168
<hr/>		
B84	FLDGF LTNQNVFAFNYSQV VFFIVLSCLISVSVNFSTFLVIGKTS PVTYQVLGHLKTCL	230
C0428	FLDGF LTNQNVFAFNYSQV VFFIVLSCLISVSVNFSTFLVIGKTS PVTYQVLGHLKTCL	228
B73	FLDGF LTNQNVFAFNYSQV VFFIVLSCLISVSVNFSTFLVIGKTS PVTYQVLGHLKTCL	230
PH207	FLDGF LTNQNVFAFNYSQV VFFIVLSCLISVSVNFSTFLVIGKTS PVTYQVLGHLKTCL	240
CML495	FLDGF LTNQNVFAFNYSQV VFFIVLSCLISVSVNFSTFLVIGKTS PVTYQVLGHLKTCL	228
<hr/>		
B84	VLTFGYVLLHDPFSWRN ILGILIAVVGMLVLSYFCTVETQHKNTEVSPQQVKESEAAPLI	290
C0428	VLTFGYVLLHDPFSWRN ILGILIAVVGMLVLSYFCTVETQHKNTEVSPQQVKESEAAPLI	288
B73	VLTFGYVLLHDPFSWRN ILGILIAVVGMLVLSYFCTVETQHKNTEVSPQQVKESEAAPLI	290
PH207	VLTFGYVLLHDPFSWRN ILGILIAVVGMLVLSYFCTVETQHKNTEVSPQQVKESEAAPLI	300
CML495	VLTFGYVLLHDPFSWRN ILGILIAVVGMLVLSYFCTVETQHKNTEVSPQQVKESEAAPLI	288
<hr/>		
B84	SDSLSKVENG GGVV DDEPLKVP MWSSKYSRE*	321
C0428	SDSLSKVENG GGVV DDEPLKVP MWSSKYSRE*	319
B73	SDSLSKVENG GGVV DDEPLKVP MWSSKYSRE*	321
PH207	SDSLSKVENG GGVV DDEPLKVP MWSSKYSRE*	331
CML495	SDSLSKVENG GGVV DDEPLKVP MWSSKYSRE*	319

Figure 5. The UDP-xylose transporter contains a single amino acid polymorphism unique to the tar spot resistant maize line CML495. Amino acid sequences of the UDP-xylose transporter (*ZmUXT2*) from five maize genotypes B73, B84, PH207, and CO428 (susceptible) and CML495 (resistant) were aligned. The predicted triose-phosphate transporter (TPT) family transmembrane domain is highlighted in orange. The single amino acid substitution unique to CML495 is highlighted in red, while amino acid differences that are not CML495 specific are shown in grey. Protein sequences were retrieved from MaizeGDB (Portwood et al., 2019), the National Center for Biotechnology Information (NCBI; Sayers et al., 2023), and Phytozome v13 (Goodstein et al., 2012). Multiple sequence alignment was performed using MUSCLE alignment (Madeira et al., 2019), and the figure was generated using Canva Pro.

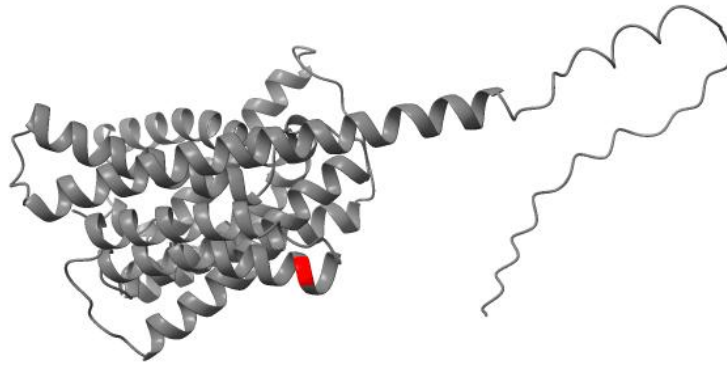


Figure 6. Structural localization of CML495-specific amino acid substitutions in ZmUXT2.

Predicted protein structures of ZmUXT2 and ZmLRR-RLK were generated using the AlphaFold Server from the CML495 amino acid sequences. The top-ranked structural models (model 0) were visualized and edited in ChimeraX. Protein backbones are shown in gray, while amino acid substitutions unique to the resistant CML495 genotype are highlighted in red to indicate their positions within the predicted protein folds. The ZmUXT2 substitution is located within the predicted TPT transmembrane domain.

To determine the subcellular localization of ZmUXT2, localization analyses were performed using LOCALIZER and TargetP 2.0, both of which predicted targeting to the secretory system (Armenteros et al., 2019; Sperschneider et al., 2017). A ZmUXT2–GFP fusion construct was generated and transiently expressed in *N. benthamiana* leaves using coding sequences from both the resistant (CML495) and susceptible (CO428) maize genotypes. Non-transformed leaf epidermal cells exhibited no detectable green fluorescence, and a weak chlorophyll autofluorescence (Figure 7). Confocal microscopy of ZmUXT2–GFP in both mesophyll and epidermal tissues revealed a reticulate pattern of green fluorescence characteristic of the ER network (Figure 7). Representative images shown in Figure 7 correspond to epidermal tissue for CML495 and mesophyll tissue for CO428. Red fluorescence from the ER marker HDEL–mCherry exhibited a similar reticulate pattern and overlapped with the ZmUXT2–GFP signal, confirming localization of ZmUXT2 to the ER (Figure 7). Similar localization patterns were observed for both the CML495 and CO428 alleles, with no obvious differences in subcellular distribution between alleles.

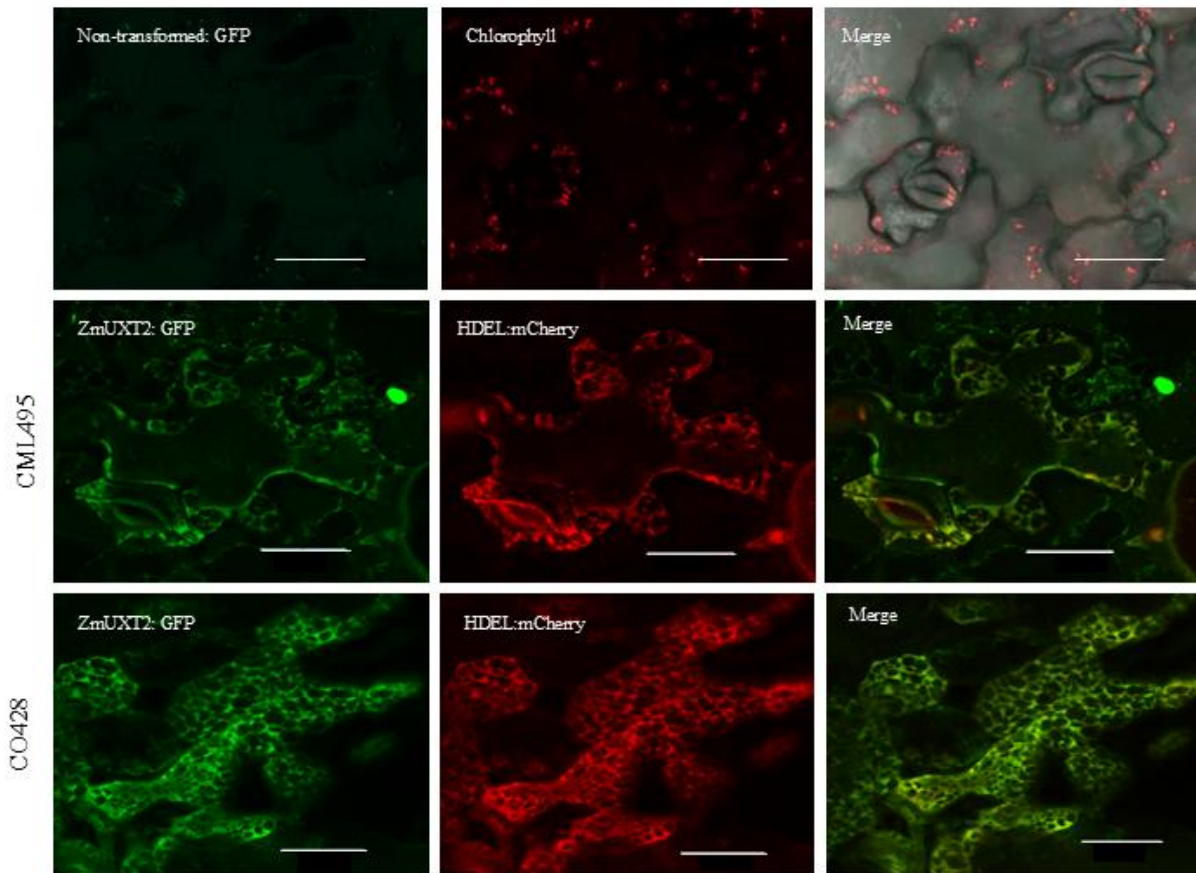


Figure 7. ZmUXT2 localizes to the endoplasmic reticulum in *N. benthamiana*. C-terminal ZmUXT2–GFP fusions from CML495 and CO428 were transiently co-expressed with the HDEL–mCherry ER marker in *N. benthamiana* leaves. Both alleles colocalize with the ER marker, and experiments were conducted twice with a minimum of 5 leaves at the epidermal (non-transformed leaf and CML495) and mesophyll cells (CO428). The white bar indicates 20 μ m.

3.3. Characterization of *ZmLRR-RLK*

To further characterize *ZmLRR-RLK*, the phylogenetic relationships, sequence variation, and subcellular localization patterns were investigated. *ZmLRR-RLK* belongs to the LRR-RLK subfamily XII, which represents one of the largest LRR-RLK clades in maize, comprising approximately 40 of the 205 annotated LRR-RLK genes (Sun et al., 2013; Gao et al., 2025). *ZmLRR-RLK* is a non-RD receptor-like kinase, which are commonly associated with immune signalling functions (Dardick et al., 2006). Arabidopsis orthologues include the PRRs *FLS2* and *EFR*, which share a modest 34% and 39% amino acid identity with *ZmLRR-RLK*, respectively (Figure 8) (Gómez-Gómez & Boller, 2000; Chinchilla et al., 2005). *ZmLRR-RLK* also shares 83% identity with the sorghum homologue *Sobic.009G058900* but only has 48% identity with the next closest maize LRR-RLK, *GRMZM2G171114* (Figure 8).

ZmLRR-RLK contains 20 predicted LRR domains, a transmembrane domain, and a cytoplasmic kinase domain (Figure 9) (Goodstein et al., 2012; Sayers et al., 2023). Amino acid comparisons between resistant and susceptible genotypes identified several CML495-specific substitutions distributed throughout the predicted protein structure, including within both the extracellular LRR region and intracellular kinase domain (Figures 9). In *ZmLRR-RLK*, there were sixteen total changes unique to CML495, four of those amino acid substitutions were identified within the LRR domains, with an additional six substitutions located within the kinase domain (Figure 8). None of these substitutions were in the conserved catalytic motifs required for kinase activity (Popescu et al., 2017; Brauer et al., 2022). The predicted protein fold was annotated to highlight CML495 substitutions in red and revealed of the twelve substitutions were located in β -sheet secondary structures, while four were in α -helix structures of the protein fold (Figure 10).

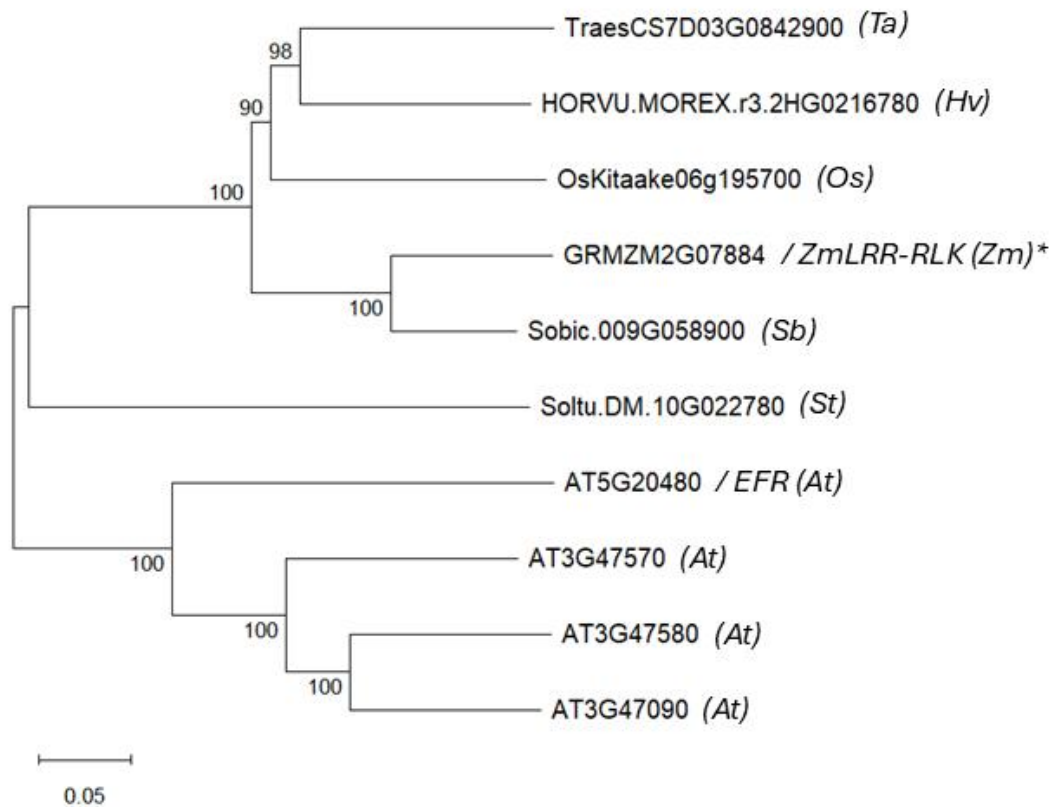


Figure 8. Phylogenetic analysis of *ZmLRR-RLK* across plant species. The full-length amino acid sequence of the *ZmLRR-RLK* (*GRMZM2G070884*) was aligned with homologous sequences from selected monocot and eudicot species using MUSCLE. Phylogenetic trees were constructed in MEGA12 (Kumar et al., 2024) using the neighbour-joining method. Bootstrap support values were calculated from 1,000 replicates, and bootstrap percentages are shown at the corresponding nodes. The scale bar represents 0.05 amino acid substitutions per site. Species abbreviations are *Ta* = *Triticum aestivum*, *Hv* = *Hordeum vulgare*, *Os* = *Oryza sativa*, *Zm* = *Zea mays*, *Sb* = *Sorghum bicolor*, *St* = *Solanum tuberosum*, *At* = *Arabidopsis thaliana*. The * indicates gene of interest.

Legend: Grey = mismatch across varieties, Red = unique to CML495, Purple = LRR, Green = Transmembrane domain, Blue = Kinase domain

B84	MSHTTMAPVGTLSSSLPLIILLASLSPLLLSTPSLAATPLGRSPNDDMEALLCLKHH	60
C0428	MSHTTMAPVGTLGFSPLIILLASISALLA-----TTPNDMEALLCLKHH	47
B73	MSQTTYMAPVGTLGFSPLIILLASLSALLA-----TTPNDMEALLCLKHH	47
PH207	MSHTTMAPVGTLGFSPLIILLASISALLA-----TTPNDMEALLCLKHH	47
CML495	MSHTTMAPVSTLGFSPLIILLASLSALLA-----TTPNDMEALLCLKHH	47
B84	LSASSDPTGTLPSWK-NDSTQFCSWSGVTCCKRHSSRVVALDLESLDLHGQIPPCIGNLT	119
C0428	LSASSDATGTLPSWKNNDSTQLCSWSGVTCCKRHSSRVVALDLESLDLHGQIPPCIGNLT	107
B73	LSASSDPTGTLPSWK-NDSTQFCSWSGVTCCKRHSSRVVALDLESLDLHGQIPPCIGNLT	106
PH207	LSASSDATGTLPSWKNNDSTQLCSWSGVTCCKRHSSRVVALDLESLDLHGQIPPCIGNLT	107
CML495	LSASSDPTGTLPSWK-NDSTQFCSWSGVTCCKRHSSRVVALDLESLDLHGQIPPCIGNLT	106
B84	FLTRIHMPNNQLQGQIPAEGLQNLRLRYINLSSNSFISGEIPETLSSCFALQAIDLSRNS	179
C0428	FLTRIHMPNNQLQGQIPAEGLQNLRLRYINLSSNSFISGEIPETLSSCLALQAIDLSRNS	167
B73	FLTRIHMPNNQLQGQIPAEGLQNLRLRYINLSSNSFISGEIPETVSSCLALQAIDLSRNS	166
PH207	FLTRIHMPNNQLQGQIPAEGLQNLRLRYINLSSNSFISGEIPETLSSCLALQAIDLSRNS	167
CML495	FLTRIHMPNNQLQGQIPAEGLQNLRLRYINLSSNSFISGEIPETLSSCLALQAIDLSRNS	166
B84	LSGSIPEGLGSLGNLSDLRLSGNYLTGSIPASLGSSSLVSVVNNNSLTGPIPSLLAN	239
C0428	LSGSIPEFGSLGNLSDLRLSGNYLTGSIPASLGRSSSLVSVVNNNSLTGPIPSLLAN	227
B73	LSGSIPEGLGSLGNLSDLRLSGNHLTGSIPASLGSSSLVSVVNNNSLTGPIPSLLAN	226
PH207	LSGSIPEFGSLGNLSDLRLSGNYLTGSIPASLGRSSSLVSVVNNNSLTGPIPSLLAN	227
CML495	LSGSIPEGLGSLGNLSDLRLSGNYLTGSIPASLGSSSLVSVVNNNSLTGPIPSLLAN	226
B84	SSSLQRLGLRNNHLSGLIPQSLCNSTSLLEMLVLAGNSFAGSIPVVSNTVVDSP-PPPLQY	298
C0428	SSSLQRLGLRNNHLSGLIPQSLFNSTSLLEMLVLAGNSFAGSIPVVSNTVVDSPSPPLQY	287
B73	SSSLQRLGLRNNRSLGLIPQSLFNSTSLLEMLVLAGNSFAGIPAVSNTVVDSP-PPPLQY	285
PH207	SSSLQRLGLRNNHLSGLIPQSLFNSTSLLEMLVLAGNSFAGSIPVVSNTVVDSPSPPLQY	287
CML495	SSSLQRLGLRNNHLSGLIPQSLFNSTSLLEMLVLAGNSFAGIPAVSNTVVDSP-PPPLQY	284
B84	LILDSNDLTGPLPSTLGNLTSLLWLTGGNGFHGSIPTSLGALANLQVLDMTNNALSGTV	358
C0428	LILDSNDLTGPLPSTLGNLTSLLWLTGGNGFHGSIPTSLGALANLQVLDMTNNALSGTV	347
B73	LILDSNDLTGPLPSTLGNLTSLLWLTGGNGFHGSIPTSLGALVNLQVLDMTNNALSGTV	345
PH207	LILDSNDLTGPLPSTLGNLTSLLWLTGGNGFHGSIPTSLGALANLQVLDMTNNALSGTV	347
CML495	LLILDSNDLTGPLPSTLGNLTSLLWLTGGNGFHGSIPTSLGALANLQVLDMTNNALSGTV	344
B84	PASIYNMSALTHLGMGINNLTGEIPANVGYSLPRIVNLIMARNKFTGQIPVSLTKATNLQ	418
C0428	PASIYNMSALTHLGMGINNLTGEIPANVGYSLPRIVNLIMARNKFTGQIPVSLTKATNLQ	407
B73	PASIYNMSALTHLGMGMNLTGEIPANVGYSLPRIVNLIMARNKFTGQIPVSLTKATNLQ	405
PH207	PASIYNMSALTHLGMGINNLTGEIPANVGYSLPRIVNLIMARNKFTGQIPVSLTKATNLQ	407
CML495	PASIYNMSALTHLGMGINNLTGEIPANVGYSLPRIVNLIMARNKFTGQIPVSLTKATNLQ	404
B84	IINLWDNALTGTVPLFGALPNLVELDLTKNQLEAGGDWSFLTSLTNCKQLVTLYDRNTL	478
C0428	IINLWDNALTGTVPLFGALPNLVELDLTKNQLEAGGDWSFLTSLTNCTQLVTLYDRNTL	467
B73	IINLWDNALTGTVPLFGALPNLVELDLTKNQLEAGRDWSFLTSLTNCTQLVTLYDRNTL	465
PH207	IINLWDNALTGTVPLFGALPNLVELDLTKNQLEAGGDWSFLTSLTNCTQLVTLYDRNTL	467
CML495	IINLWDNALTGTVPLFGALPNLVELDLTKNQLEAGRDWSFLTSLTNCKQLVTLYDRNTL	464
B84	GGVLPKSIQDLPISGLEVLFLSANGISGTIPNEIGRLKNLKLLYLDRNLLAGSIPYSLGHL	538
C0428	GGVLPKSIQDLPISGLEVLFLSANGISGTIPNEIGRLKNLKLLYLDRNLLAGSIPYSLGHL	527
B73	GGVLPKSIQDLPISGLEVLFLSANGISGTIPNEIGRLKNLKLLYLDRNLLAGSIPYSLGHL	525
PH207	GGVLPKSIQDLPISGLEVLFLSANGISGTIPNEIGRLKNLKLLYLDRNLLAGSIPYSLGHL	527
CML495	GGVLPKSIQDLPISGLEVLFLSANGISGTIPNEIGRLKNLKLLYLDRNLLAGSIPYSLGHL	524
B84	PNMFALSLAQNKLSGQVPASLGNLSQLSELYLQENNLSGIPGALGRCKNLDKLNLSCNS	598
C0428	PNMFALSLAQNKLSGQVPASLGNLSQLSELYLQENNLSGIPGALGRCKNLDKLNLSCNS	587
B73	PNMFALSLAQNKLSGQVPASLGNLSQLSELYLQENHLSGIPGALGRCKNLDKLNLSCNS	585
PH207	PNMFALSLAQNKLSGQVPASLGNLSQLSELYLQENNLSGIPGALGRCKNLDKLNLSCNS	587
CML495	PNMFALSLAQNKLSGQVPASLGNLSQLSELYLQENNLSGIPGALGRCKNLDKLNLSCNS	584

B84	FGGGIPEELFTLSSLSNELDSLHNQLSGEIPLEIGSFVNLGLLNISNNMLAGRIPSTLGQ	658
C0428	FGGGIPEELFTLSSLSNELDSLHNQLSGEIPLEIGSFVNLGLLNISNNMLAGRIPSTLGQ	647
B73	FGGGIPEELFTLSSLSNELDSLHNQLSGEIPLEIGSFVNLGLLNISNNMLAGRIPSTLGQ	645
PH207	FGGGIPEELFTLSSLSNELDSLHNQLSGEIPLEIGSFVNLGLLNISNNMLAGRIPSTLGQ	647
CML495	FGGGIPEELFTLSSLSNELDSLHNQLSGEIPLEIGSFVNLGLLNISNNMLAGRIPSTLGQ	644
B84	CVHLESLHMEGNLLDGRIPQSLQGLRGLVEMDMSRNLSGEIPEFFETFSSMKLLNLSFN	718
C0428	CVHLESLHMEGNLLDGRIPQSLQGLRGLVEMDMSRNLSGEIPEFFETFSSMKLLNLSFN	707
B73	CVHLESLHMEGNLLDGRIPQSLQGLRGLVEMDMSRNLSGEIPEFFETFSSMKLLNLSFN	705
PH207	CVHLESLHMEGNLLDGRIPQSLQGLRGLVEMDMSRNLSGEIPEFFETFSSMKLLNLSFN	707
CML495	CVHLESLHMEGNLLDGRIPQSLQGLRGLVEMDMSRNLSGEIPEFFETFSSMKLLNLSFN	704
B84	DLEGPVPTGGIFQDARDVFVQGNKDLCCSSSAHLLQLPLCTTDTTSKRHRHTSSVYLKLV	778
C0428	DLEGPVPTGGIFQDARDVFVQGNKDLCCSS--TLLQLPLCSTDTTSKRHRHTSSVYLKLV	765
B73	DLEGPVPTGGIFQDARDVFVQGNKDLCCSS--TLLQLPLCTTDTTSKRHRHTSSVYLKLV	763
PH207	DLEGPVPTGGIFQDARDVFVQGNKDLCCSS--TLLQLPLCSTDTTSKRHRHTSSVYLKLV	765
CML495	DLEGPVPTGGIFQDARDVFVQGNKDLCCSS--TLLQLPLCNDTTSKRHRHTSSVYLKLV	761
B84	GFTALSLVLLLCFAVVLKRRKKFQQVDHPSSMDLKKFTYAGLVKATNSFSSDNLVGS GK	838
C0428	GFTALSLVLLLCFAVVLKRRKKFQQVDHPSSMDLKKFTYAGLVKATNSFSSDNLVGS GK	825
B73	GFTALSLVLLLCFAVVLKRRKKVQQVDHPSSMDLKKFTYAGLVKATNSFSSDNLVGS GK	823
PH207	GFTALSLVLLLCFAVVLKRRKKFQQVDHPSSMDLKKFTYAGLVKATNSFSSDNLVGS GK	825
CML495	GFTALSLVLLLCFAVVLKRRKKVQQVDHPSSMDLKKFTYAGLVKATNSFSSDNLVGS GK	821
B84	CGLVYKGRFWDDEHVVAIKVFKLDQLGAPNSFLAECEALRNRHRNLVKVITACSTIDSE	898
C0428	CGLVYKGRFWDDEHVVAIKVFKLDQLGAPNSFLAECEALRNRHRNLVKVITACSTIDSE	885
B73	CGLVYKGRFWDDEHVVAIKVFKLDQLGAPNSFLAECEALRNRHRNLVKVITACSTIDSE	883
PH207	CGLVYKGRFWDDEHVVAIKVFKLDQLGAPNSFLAECEALRNRHRNLVKVITACSTIDSE	885
CML495	CGLVYKGRFWDDEHVVAIKVFKLDQLGAPNSFLAECEALRNRHRNLVKVITACSTIDSE	881
B84	GHDFKAVILEYMSNGSLDNWLYPKLNRYGIRKPLSLGSRKIAADIACALDYLHNHCVPA	958
C0428	GHDFKAVILEYMSNGSLDNWLYPKLNRYGIRKPLSLGSRKIAADIACALDYLHNHCVPA	945
B73	GHDFKAVILEYMSNGSLDNWLYPKLNRYGIRKPLSLGSRKIEADIACALDYLHNHCVPA	943
PH207	GHDFKAVILEYMSNGSLDNWLYPKLNRYGIRKPLSLGSRKIAADIACALDYLHNHCVPA	945
CML495	GHDFKAVILEYMSNGSLDNWLYPKLNRYGIRKPLSLGSRKIEADIACALDYLHNHCVPA	941
B84	IVHCDLKPSNVLLDDAMVAHLGDFGLAKLLHTCSYSIITHSSSTSLIGPRGSIYIAPEYG	1018
C0428	IVHCDLKPSNVLLDDAMVAHLGDFGLAKLLHTCSYSIITHSSSTSLIGPRGSIYIAPEYG	1005
B73	IVHCDLKPSNVLLDDAMVAHLGDFGLAKLLHTCSYSIITHSSSTSLIGPRGSIYIAPEYG	1003
PH207	IVHCDLKPSNVLLDDAMVAHLGDFGLAKLLHTCSYSIITHSSSTSLIGPRGSIYIAPEYG	1005
CML495	IVHCDLKPSNVLLDDAMVAHLGDFGLAKLLHTCSYSIITHSSSTSLIGPRGSIYIAPEYG	1000
B84	FGSKLSTQGDVYSYGITVLEMLTGKRPTDEMFSKGLTLHKLVKEAFPQKTHEILDPSIFP	1078
C0428	FGSKLSTQGDVYSYGITVLEMLTGKRPTDEMFSKGLTLHKLVKEAFPQKTHEILDPSIFP	1065
B73	FGSKLSTQGDVYSYGITVLEMLTGKRPTDEMFSKGLTLHKLVKEAFPQKTHEILDPSIFP	1063
PH207	FGSKLSTQGDVYSYGITVLEMLTGKRPTDEMFSKGLTLHKLVKEAFPQKTHEILDPSIFP	1065
CML495	FGSKLSTQGDVYSYGITVLEMLTGKRPTDEMFSKGLTLHKLVKEAFPQKTHEILDPSIFP	1060
B84	VTR=DGDNHTTDEITRSIMNLLKIGISCSADAPTRPTIDDVYAKVITIKETFLDLC*	1135
C0428	VTR=DDGDNHTTDEITRSIMNLLKIGISCSADAPTRPTIDDVYAKVITIKETFLDLC*	1123
B73	VTR=DGDNHTTDEITRSIMNLLKIGISCSADAPTRPTIDDVYAKVITIKETFLDLC*	1120
PH207	VTR=DDGDNHTTDEITRSIMNLLKIGISCSADAPTRPTIDDVYAKVITIKETFLDLC*	1123
CML495	VTR=DGDNHTTDEITRSIMNLLKIGISCSADAPTRPTIDDVYAKVITIKETFLDLC*	1117

Figure 9. *ZmLRR-RLK* exhibits multiple CML495-specific amino acid polymorphisms distributed across the protein. Amino acid sequences of the *ZmLRR-RLK* from five maize genotypes B73, B84, PH207, and C0428 (susceptible) and CML495 (resistant) were aligned. Leucine-rich repeat domains are highlighted in purple, the transmembrane domain in green, and the kinase domain in blue. Amino acid substitutions unique to CML495 are highlighted in red, while amino acid differences that are not unique to CML495 are shown in grey. Amino acid sequences were obtained from MaizeGDB, NCBI, and Phytozome. Multiple sequence alignment was performed using MUSCLE alignment, and the figure was generated using Canva Pro.

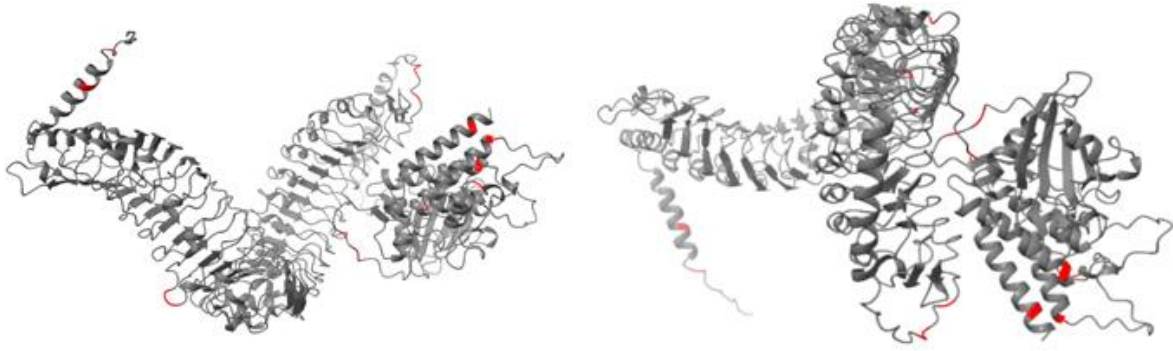


Figure 10. Structural localization of CML495-specific amino acid substitutions in ZmLRR-RLK. Predicted protein structures of ZmLRR-RLK were generated using the AlphaFold Server from the CML495 amino acid sequences. The top-ranked structural models (model 0) were visualized and edited in ChimeraX. Protein backbones are shown in gray, while amino acid substitutions unique to the resistant CML495 genotype are highlighted in red to indicate their positions within the predicted protein folds. Substitutions in ZmLRR-RLK are distributed throughout the extracellular LRR region and intracellular kinase domain.

The predicted subcellular localization of ZmLRR-RLK from LOCALIZER and TargetP 2.0 suggested targeting to the secretory system (Armenteros et al., 2019; Sperschneider et al., 2017). To validate this prediction, ZmLRR-RLK–GFP fusion proteins derived from the resistant (CML495) and susceptible (CO428) alleles were transiently expressed in *N. benthamiana* leaves. Non-transformed epidermal leaf cells showed little or no green and red fluorescence (Figure 11). Confocal microscopy of the ZmLRR-RLK constructs revealed green fluorescence at the cell periphery and within internal membrane structures (Figure 11). The green fluorescence signal overlapped with the red fluorescence of FM4-64, indicating plasma membrane localization, and co-localized with the red fluorescence of the ER marker HDEL–mCherry, consistent with localization to both the PM and ER (Figure 11). As observed for ZmUXT2, the CML495 and CO428 alleles displayed similar localization patterns, with no obvious differences in subcellular distribution between alleles.

Collectively, these analyses indicate that both *ZmUXT2* and *ZmLRR-RLK* are responsive to immune induction. *ZmLRR-RLK* localized to both the ER and PM and exhibited similar transcript abundance and subcellular localization between resistant and susceptible genotypes despite minor sequence variation. In contrast, *ZmUXT2* localized exclusively to the ER and showed elevated expression in the resistant genotype relative to the susceptible genotype.

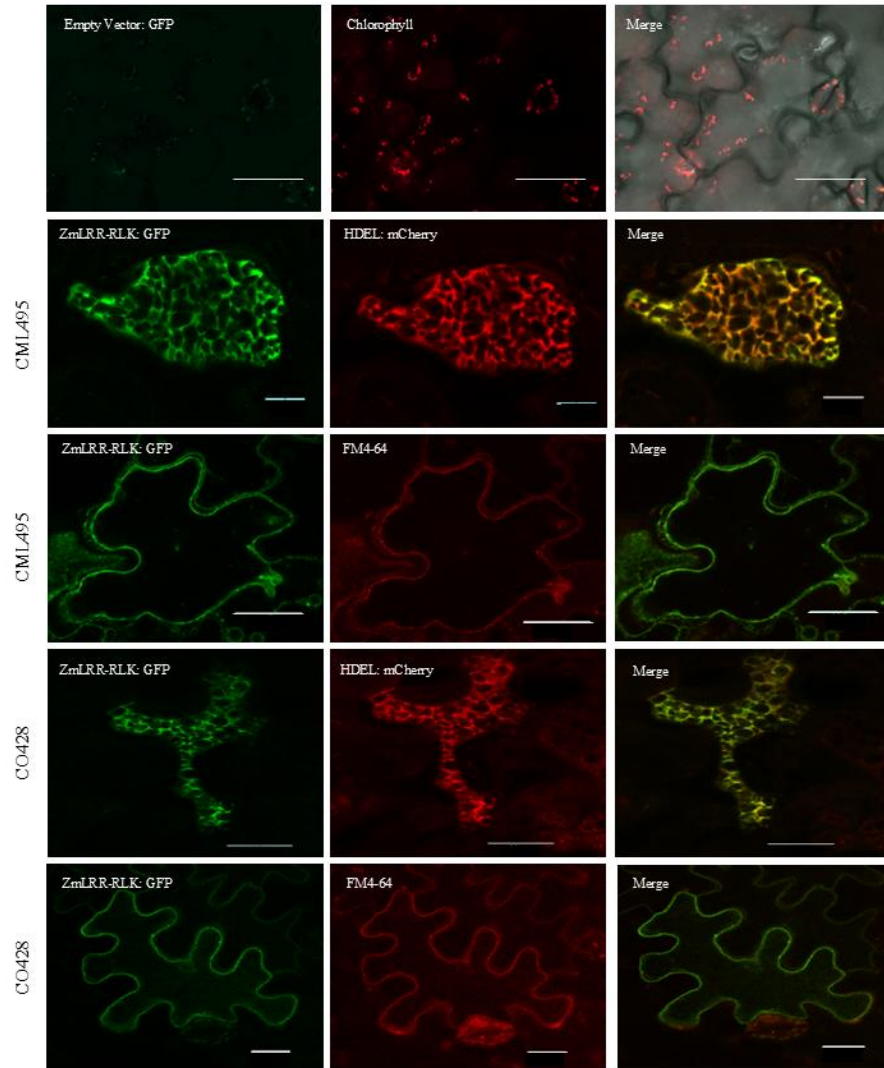


Figure 11. ZmLRR-RLK localizes to the plasma membrane and endoplasmic reticulum in *N. benthamiana*. C-terminal ZmLRR-RLK–GFP fusions from CML495 and CO428 were transiently coexpressed with the HDEL–mCherry ER marker in *N. benthamiana* mesophyll leaf cells. Alternatively, infiltrated leaves were stained with the lipid dye FM4-64, which shows PM binding after 10 minutes of staining of epidermal leaf cells. Both alleles colocalize with the ER marker and with the dye FM4-64 experiments were conducted twice with a minimum of 5 leaves. The white bar indicates 20 μ m.

3.4. Inducible Defence Responses in a Resistant and Susceptible Genotypes

To determine whether inducible immune responses differed between the susceptible CO428 and resistant CML495 genotypes, chitin and flg22 MAMPs were used to activate immune responses in both lines. CML495 exhibited a significantly stronger ROS burst in response to both flg22 and chitin treatments than CO428 (Figure 12A). Gene expression analysis through qPCR showed that *An2*, a copalyl diphosphate synthase (CPS)-like protein previously reported to be strongly upregulated in response to *Fusarium graminearum* attack (Harris et al., 2005), was induced by flg22 in CO428 but not in CML495. Despite this differential response, no significant differences in *An2* expression were observed between the two genotypes (Figure 12B). This analysis further revealed that *PR5*, a defense-related gene previously shown to be induced during *Fusarium verticillioides* infection, was upregulated by both chitin and flg22 in CO428, whereas only flg22 significantly induced expression in CML495 (Figure 12B). Although *PR5* was induced in both genotypes, transcript abundance was significantly higher in flg22-treated CML495 plants than in CO428 (Figure 12B). Previous studies have shown that overexpression of *PR5* enhances antioxidant responses following pathogen inoculation, supporting its role in plant defense (Yang et al., 2025). To assess the contribution of the candidate resistance proteins to MAMP-induced immune responses, ROS production was measured in *N. benthamiana* leaves transiently expressing *ZmUXT2* or *ZmLRR-RLK* alleles from the resistant and susceptible genotypes (Figure 13). Preliminary results showed no detectable differences in ROS production between leaves expressing *ZmUXT2*, *ZmLRR-RLK*, or the empty vector control (Figure 13). Collectively, this suggests that the CML495 resistant genotype might have higher inducible immune responses than the susceptible genotype CO428.

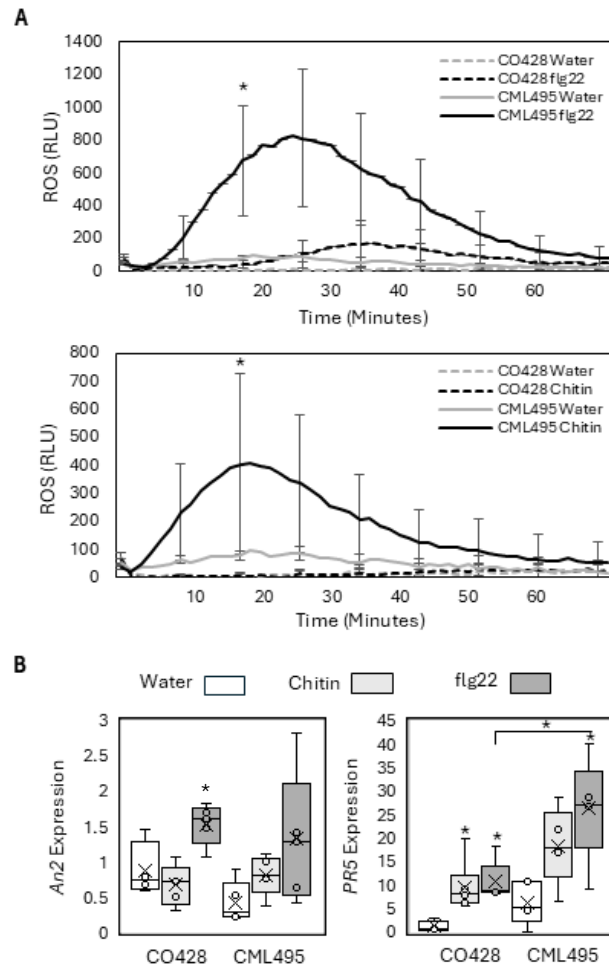


Figure 12. Resistant maize line CML495 exhibits enhanced inducible immune responses.

(A) ROS production was measured in leaf discs from 3-week-old resistant (CML495) and susceptible (CO428) maize plants following treatment with water (control), chitin ($500 \mu\text{g mL}^{-1}$), or flg22 ($5 \mu\text{M}$). ROS accumulation was measured using a luminol-based assay to detect extracellular H_2O_2 and monitored over a 60-minute time course presented as relative luminescence units (RLU; mean \pm SD, $n = 12$ plants). Data shown are representative of one of four independent experiments with similar results. Statistical significance was determined using unpaired, one-tailed t-tests ($p < 0.05$).

(B) Relative expression of the defence marker genes *PR5* and *An2* was measured by qPCR in 3-week-old maize leaves treated with water (control), chitin (500 $\mu\text{g mL}^{-1}$), or flg22 (5 μM), and harvested 4 h after infiltration. Gene expression was normalized to housekeeping genes *DUF* and *CYP* ($n = 5$). Data shown are from one of three independent experiments with comparable results. Box plots display the median (center line), first and third quartiles (box), and range (whiskers); means are indicated by “×”. Asterisks indicate significant differences between MAMP treatments and the corresponding water control within each genotype (one-way ANOVA; $p < 0.05$). Brackets denote significant differences between genotypes under the indicated treatment condition ($p < 0.05$).

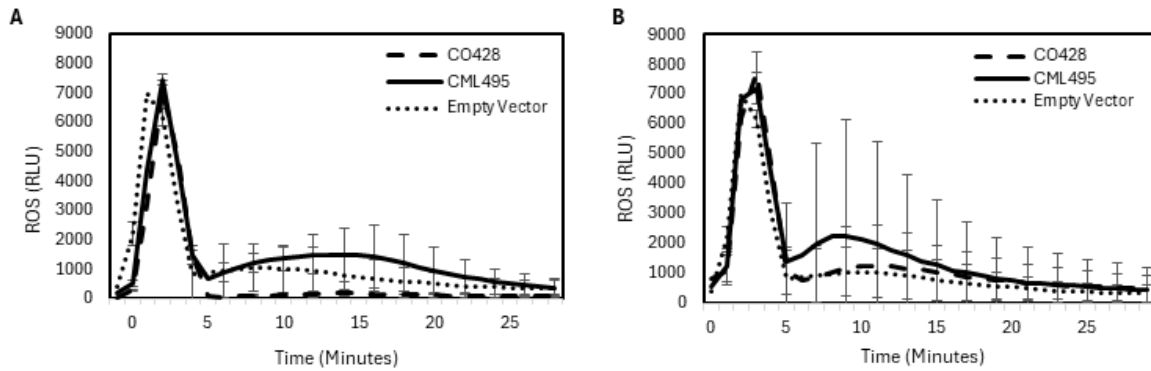


Figure 13. Resistant and susceptible alleles of *ZmUXT2* and *ZmLRR-RLK* produce similar flg22-induced ROS responses during transient expression in *N. benthamiana*.

(A) ROS production in relative light units (RLU) from leaf discs expressing *ZmUXT2* alleles from resistant (CML495) or susceptible (CO428) maize genotypes or an empty vector control. Leaf discs (n=4) were treated with 1 μ M flg22, and ROS was measured over 60-minutes using a luminol-based assay to detect extracellular H₂O₂. Data represent mean \pm SD from a single experiment and the experiment was repeated once. No significant differences were observed between alleles and the empty vector control using a one-way ANOVA.

(B) ROS production in relative light units (RLU) from leaf discs expressing *ZmLRR-RLK* alleles from resistant (CML495) or susceptible (CO428) maize genotypes or an empty vector control. Leaf discs (n=4) were treated with 1 μ M flg22, and ROS was measured over 60-minutes using a luminol-based assay to detect extracellular H₂O₂. Data represent mean \pm SD from a single experiment and the experiment was repeated once. No significant differences were observed between alleles and the empty vector control using a one-way ANOVA.

4. Discussion

Recent work has identified multiple QTLs associated with tar spot resistance, including the major QTL *qRtsc8-1*, which contains four candidate genes. In the present study, these genes were evaluated following MAMP treatment, revealing that *ZmUXT2* and *ZmLRR-RLK* displayed differential expression, whereas *GRMZM5G869967* and *GRMZM2G071228* did not. *ZmLRR-RLK* and *GRMZM5G869967* were more highly expressed in flg22-treated CO428 compared to CML495, while *ZmUXT2* showed elevated expression in the resistant genotype CML495. The higher basal and MAMP-induced expression of *ZmUXT2* and *ZmLRR-RLK* prompted further characterization of potential differences between resistant and susceptible alleles. *ZmUXT2* was identified as a member of the UXT family, with *Arabidopsis thaliana UXT2* representing its closest characterized homologue. The protein contained a single amino acid substitution unique to CML495 and localized to the ER in both the CO428 and CML495 alleles. In contrast, *ZmLRR-RLK* clustered within LRR-RLK subfamily XII, which includes immune receptors such as *FLS2* and *EFR*. *ZmLRR-RLK* contained 11 amino acid substitutions unique to CML495 and localized to both the ER and PM in both alleles. Additionally, the resistant maize genotype CML495 exhibited enhanced PTI-associated responses, including a stronger ROS burst and elevated expression of the defence-related gene *PR5*.

Overall, these findings demonstrate that *ZmUXT2* and *ZmLRR-RLK* differ in both expression and protein sequence between resistant and susceptible maize genotypes, while maintaining similar subcellular localization patterns. In addition, ROS accumulation and *PR5* expression differed between CO428 and CML495, with the resistant genotype exhibiting stronger inducible defence responses. Although all candidate genes within *qRtsc8-1* remain potential contributors to

tar spot resistance, many additional mechanisms and loci likely contribute to resistance and were not examined in this study. One limitation of GWAS is their reliance on statistical associations rather than direct causal relationships, which can complicate the interpretation and functional validation of candidate loci. Furthermore, GWAS often explain only a limited proportion of disease heritability (Witte, 2014). Despite these limitations, the elevated basal and MAMP-induced expression of *ZmUXT2* in the resistant genotype CML495 makes this gene a particularly compelling candidate for further investigation.

4.1. UDP-Xylose Transporters

Cell wall composition plays an important role in plant defence by functioning as both a physical barrier to pathogen invasion and a source of damage-associated molecular patterns that activate immune signalling pathways (Malinovsky et al., 2014). In grasses such as maize, the cell wall is highly enriched in hemicellulosic polysaccharides, particularly xylan, which contribute substantially to wall strength and structural integrity (Cosgrove et al., 1997; Santiago et al., 2013). Because these polysaccharides are synthesized primarily within the Golgi lumen, UDP-xylose (UDP-Xyl) must be transported from the cytosol into the endomembrane system by nucleotide-sugar transporters (NSTs). UXTs are specialized membrane proteins that mediate the transport of cytosolic UDP-Xyl into the Golgi and ER lumen, thereby supplying the activated sugar donors required for glycosylation and cell wall polysaccharide biosynthesis (Knappe et al., 2003; Scheible & Pauly, 2004; Liepman et al., 2010).

ZmUXT2, along with 3,159 other genes, was previously shown to exhibit increased expression 10 days following exposure to *P. maydis* relative to non-exposed controls, indicating responsiveness to pathogen challenge (Roggenkamp et al., 2025). Consistent with this finding, our

gene expression analysis demonstrated that *ZmUXT2* was significantly induced by both chitin and flg22 treatments, supporting its responsiveness to MAMP perception and downstream immune signalling pathways. Importantly, *ZmUXT2* also displayed higher expression in the resistant maize genotype CML495. Elevated expression of UXT transporters could increase the availability of UDP-xylose within the Golgi lumen, potentially enhancing xylan and xyloglucan biosynthesis by xylosyltransferases (Ebringerová & Heinze, 2000; Scheller & Ulvskov, 2010). Altered UDP-xylose availability is therefore expected to influence the abundance and structure of xylan polymers, including GAX and AX, which may affect cellulose–hemicellulose interactions and overall cell wall integrity (Ebert et al., 2015; Zhao et al., 2018; Curry et al., 2023; Kundu et al., 2025).

Modifications to cell wall xylose content have been shown to influence resistance to multiple pathogens in *Arabidopsis* (Hernández-Blanco et al., 2007; Delgado-Cerezo et al., 2012; Bacete et al., 2018; Xu et al., 2025). Early work by Hernández-Blanco et al. (2007) demonstrated that disruption of secondary cell wall biosynthesis enhanced resistance to both the vascular bacterium *Ralstonia solanacearum* and the necrotrophic fungus *Plectosphaerella cucumerina*, likely through activation of defence pathways triggered by altered cell wall integrity. Similarly, Delgado-Cerezo et al. (2012) investigated the role of heterotrimeric G-proteins in resistance to necrotrophic fungi using *Arabidopsis* G-protein mutants in combination with pathogen assays, transcriptomics, FTIR spectroscopy, and cell wall composition analyses. Mutants with increased fungal susceptibility also exhibited altered cell wall composition, including reduced xylose content, supporting the conclusion that cell wall integrity and polysaccharide composition contribute to plant immunity. Bacete et al. (2018) further demonstrated that variation in cell wall glycan composition, including xylan-associated epitopes, correlates with resistance phenotypes across multiple pathogens,

although these effects appear highly context dependent. In contrast, Xu et al. (2025) provided evidence for a more direct structural role of xylan in defence, showing that increased xylan biosynthesis enhanced resistance to the fungal pathogen *Fusarium verticillioides*, likely by reinforcing the cell wall and limiting pathogen penetration. Likewise, disruption of xylan modification, such as reduced *O*-acetylation in rice *tbl1 tbl2* mutants, decreased resistance to bacterial leaf blight disease (Gao et al., 2017). In maize, increased incorporation of UDP-xylose-derived residues into cell wall polysaccharides has also been associated with enhanced resistance to *F. verticillioides*, further supporting a role for cell wall reinforcement in limiting pathogen invasion (Xu et al., 2025).

In addition to hemicellulose, lignin deposition contributes substantially to cell wall strength and resistance to pathogen penetration. Xylan and lignin are closely associated within the secondary cell wall matrix, where covalent and non-covalent interactions enhance wall rigidity (Kang et al., 2019; Sapouna et al., 2023). Transcriptomic analyses of tar spot-infected maize have identified differential regulation of genes involved in lignin biosynthesis and degradation pathways following *P. maydis* infection (Roggenkamp et al., 2025). This is consistent with predictions that *P. maydis* secretes carbohydrate-active enzymes and other cell wall-degrading enzymes to facilitate host colonization (MacCready et al., 2023; Rogers et al., 2024). Collectively, these studies support the hypothesis that altered UDP-xylose transport and downstream cell wall composition may contribute to tar spot resistance, although further work is required to determine the direct impact of *ZmUXT2* on cell wall architecture and defence.

In *Arabidopsis*, UXT1, UXT2 and UXT3 localized in the Golgi apparatus, meanwhile UXT1 was also observed in the ER (Ebert et al., 2015). In this study, *ZmUXT2* localized predominantly

to the ER, consistent with some UXT family members that function within the early secretory pathway. Cell wall biosynthesis relies on coordinated activity across multiple compartments of the endomembrane system, including the ER, Golgi apparatus, trans-Golgi network, and secretory vesicles (Aniento et al., 2022; Hoffmann, 2024). Protein synthesis is initiated in the ER before cargos are trafficked through the Golgi apparatus for further modification and sorting (Alberts et al., 2002). Members of the SLC35 (solute carrier 35) family, which includes NSTs, are commonly localized to the ER and/or Golgi apparatus and function to transport activated sugars from the cytosol into the lumen of these organelles for glycosylation reactions (Hadley et al., 2014; Hadley et al., 2019; Van den Bossche et al., 2024). Because glycosyltransferases responsible for polysaccharide biosynthesis reside within the endomembrane lumen, NSTs are essential for linking cytosolic nucleotide-sugar synthesis with glycosylation processes required for cell wall assembly. Although ER localization is consistent with the general distribution of NSTs and with the initiation of *N*-glycosylation in this compartment, UXT proteins are more commonly associated with xylosylation processes occurring in the Golgi apparatus (Fitchette-Lainé et al., 1994; Egelund et al., 2006; Ebert et al., 2015). Therefore, the ER localization of *ZmUXT2* was somewhat unexpected, and its biological significance remains unclear. This observation may indicate a previously uncharacterized role for *ZmUXT2* within the early secretory pathway; however, the current study was not designed to resolve this possibility fully. It is also possible that transient expression in *N. benthamiana* did not fully capture native localization patterns occurring in maize tissues.

Functional studies in *Arabidopsis* further support the importance of UXT transporters in cell wall biosynthesis. Ebert et al. (2015) demonstrated that although all three *Arabidopsis* UXT transporters can transport UDP-xylose, their contributions to cell wall composition differ. Loss-

of-function *uxt1* mutants exhibit reduced xylose content, whereas *uxt2* and *uxt3* single mutants display only minor phenotypic effects (Ebert et al., 2015). However, stronger phenotypes emerge in higher-order mutants. Both the *uxt1 uxt3* double mutant and the *uxt1 uxt2 uxt3* triple mutant exhibit delayed growth, darker leaf coloration, shorter stems, and severely collapsed vascular tissues (Zhao et al., 2018). The triple mutant additionally shows more severe developmental defects than the *uxt1 uxt3* double mutant, suggesting that *UXT2* contributes to plant growth and development in combination with other UXT family members. Furthermore, *uxt1 uxt2 uxt3* mutants exhibit a 20–40% reduction in cell wall thickness relative to wild type (Zhao et al., 2018). Together, these findings highlight the importance of UDP-xylose transport for proper cell wall biosynthesis and structural integrity. It is possible that *ZmUXT2* may have a role in maize xylan biosynthesis and cell wall-mediated defence, but further work is needed to confirm the function of *ZmUXT2*.

Future work should focus on further characterizing the function of *ZmUXT2* in maize and determining how its expression is differentially regulated between resistant and susceptible genotypes. Variation within the promoter region of *ZmUXT2* may influence transcription factor binding or regulatory element activity, thereby contributing to differences in gene expression between genotypes. Promoter–reporter assays could be used to test whether regulatory sequences from resistant genotypes confer stronger transcriptional activation following immune elicitation (Köhler et al., 1995). In addition, functional studies manipulating *ZmUXT2* expression, including overexpression and loss-of-function approaches, would help determine whether altered transcript abundance directly affects tar spot susceptibility. Together, these approaches would clarify whether regulatory variation at *ZmUXT2* contributes to resistance differences between maize genotypes.

4.2. LRR-RLKs

LRR-RLK proteins constitute a large and functionally diverse receptor family in plants, with more than 200 members encoded in the maize genome (Ng et al., 2011; Sun et al., 2017; Gao et al., 2025). These receptors are involved in a broad range of biological processes, including plant growth and development, immune signalling, and responses to biotic and abiotic stresses (Shi et al., 2023; Sun et al., 2023; Gao et al., 2025). Structurally, LRR-RLKs contain extracellular leucine-rich repeat (LRR) domains that perceive external ligands and activate intracellular kinase domains through phosphorylation and autophosphorylation, thereby initiating downstream signalling cascades (Lemmon, 2000; Hubbard et al., 2007; Gao et al., 2025).

Transcriptomic analyses of tar spot-infected maize identified three genes near the *qRtsc8-1* region that were differentially expressed following *P. maydis* infection, including *ZmLRR-RLK*, which was upregulated during pathogen challenge (Roggenkamp et al., 2025). Consistent with these findings, our gene expression analysis demonstrated that *ZmLRR-RLK* was strongly induced by both chitin and flg22 treatments, supporting a role in stress-responsive signalling pathways. In addition to immune elicitation, *ZmLRR-RLK* has also been reported to be induced under cold stress conditions (Hoopes et al., 2019), suggesting that its expression may be regulated by multiple environmental and stress-related cues.

Phylogenetic analysis placed *ZmLRR-RLK* within LRR-RLK subfamily XII, which includes well-characterized PRRs such as *FLS2* and *EFR* (Chinchilla et al., 2006; Zipfel et al., 2006; Kileeg & Mott, 2025). Consistent with previously reported localization patterns of LRR-RLK proteins, *ZmLRR-RLK* localized to both the ER and the PM. Gao et al. (2025) studied all 205 identified LRR-RLKs in maize from 15 subfamilies and found that all proteins localized to the cytoplasmic

membrane. In other LRR-RLK family members, the ER serves as an important site for protein folding, N-glycosylation, and quality-control processes mediated by ER chaperones prior to trafficking of mature receptors to the plasma membrane, where ligand perception and signal transduction occur (Li et al., 2009; Tintor & Saijo, 2014). Defects in ER quality control can impair receptor accumulation and signalling at the cell surface, highlighting the importance of ER processing for proper receptor function. Therefore, localization of *ZmLRR-RLK* to both the ER and PM is consistent with its predicted role as a membrane-associated receptor. Similar localization patterns were observed for both resistant and susceptible alleles, indicating that the identified amino acid substitutions do not substantially alter subcellular localization.

Despite strong induction by MAMP treatment, *ZmLRR-RLK* displayed relatively similar expression patterns between resistant and susceptible genotypes and contained only minor amino acid variation. This may suggest that *ZmLRR-RLK* does not function as a major determinant of resistance or that its contribution depends on protein activity rather than transcript abundance alone. Notably, some LRR-RLK family members act as negative regulators of immunity. For example, *CDGI* promotes degradation of immune receptors such as *FLS2* and *CERK1*, while downstream signalling regulators including *CPK28* and *PUB12/PUB13* attenuate immune responses (Yang et al., 2021). Therefore, the induction of *ZmLRR-RLK* during immune stimulation does not necessarily indicate a positive role in defence signalling. Further functional validation is required to clarify the role of *ZmLRR-RLK* in maize immunity. Generation of knockout genotypes in a resistant background, combined with overexpression or complementation studies in a susceptible background, would provide direct evidence of function. In addition, PTI-associated responses, including ROS production, MAPK activation, defence gene expression, and callose deposition, should be assessed following MAMP treatment in these genotypes. Protein interaction

and ligand-binding assays would further help determine whether *ZmLRR-RLK* functions as a receptor, co-receptor, or downstream signalling component (Du et al., 2016).

Overall, this study advances the characterization of two candidate genes within the tar spot resistance locus *qRtsc8-1*. *ZmUXT2* and *ZmLRR-RLK* belong to conserved gene families associated with cell wall biosynthesis and immune signalling, respectively, and both genes were responsive to MAMP treatment. *ZmUXT2* exhibited elevated expression in the resistant genotype CML495, contained a single amino acid substitution unique to CML495, and localized to the ER in both alleles. In contrast, *ZmLRR-RLK* showed higher expression in CO428, contained multiple amino acid substitutions, and localized to both the ER and PM in resistant and susceptible alleles. Collectively, these findings refine our understanding of candidate genes within the major tar spot resistance QTL *qRtsc8-1* and provide a foundation for future functional studies investigating their roles in maize immunity.

4.3. Genotypic Variations in MAMP-Triggered Responses

The results of this study indicate that CML495 and CO428 exhibit differences in selected MAMP-triggered responses. Specifically, CML495 displayed a stronger ROS burst and higher *PR5* expression following flg22 treatment than CO428. Since the ROS burst has been linked to salicylic acid accumulation and induction of defence-associated genes, including *PR5*, the elevated ROS production observed in CML495 may contribute to the increased *PR5* expression detected in this genotype (Herrera-Vásquez et al., 2015; Ding et al., 2022). However, not all inducible responses differed between genotypes. Although *An2* expression was induced by flg22 in CO428, no significant differences in *An2* transcript abundance were observed between CML495 and CO428.

Moreover, CML495 and CO428 originate from tropical and temperate germplasm, respectively, which differ in their adaptation to photoperiod and flowering time and possess distinct evolutionary histories and genetic backgrounds (Ding et al., 2015; Reid et al., 2019; Choquette et al., 2023; Muñoz-Zavala et al., 2024). Consequently, differences in MAMP-induced responses could reflect broader genetic variation rather than effects directly associated with tar spot resistance alleles. Since physiological and developmental traits were not characterized in this study, the extent to which such factors contributed to the observed responses remains unknown. Future studies should compare near isogenic lines segregating only in tar spot resistance alleles or genome-edited genotypes to determine the contribution of individual genes to resistance. Such approaches would help distinguish effects associated with resistance loci from those arising from broader genetic differences among maize genotypes.

5. Conclusion & Future Directions

Tar spot of maize has emerged as a major threat to maize production across North America. Understanding the molecular mechanisms underlying host resistance is therefore critical for informing durable management strategies aimed at minimizing losses for maize producers and protecting the broader agricultural economy. Here, we verified the gene expression of four candidate maize genes identified within the major QTL associated with tar spot resistance, *qRtsc8-1*. Of these, *ZmUXT2* and *ZmLRR-RLK* exhibited differential expression, whereas *GRMZM5G869967* and *GRMZM2G071228* did not. Although changes in gene expression can provide insight into potential involvement in downstream signalling of PTI, the absence of differential expression does not exclude the other genes as candidates for tar spot resistance, as they may function through alternative resistance mechanisms. Focusing on two promising

candidates, we further characterized *ZmUXT2* and *ZmLRR-RLK* across maize genotypes. *ZmUXT2* showed significantly higher expression in CML495 than in CO428 under both chitin and flg22 treatments, contained a unique amino acid substitution in CML495 compared to four susceptible maize genotypes, and consistently localized to the ER. In contrast, *ZmLRR-RLK* exhibited higher expression in CO428 under flg22 treatment, displayed multiple amino acid differences between genotypes, and localized to both the ER and PM in both alleles. This demonstrates that these genes have differences in both expression under MAMP induced treatment and sequences amongst different genotypes. Future work should aim to further validate the roles of *ZmUXT2* and *ZmLRR-RLK* in tar spot resistance. Sequencing upstream regulatory regions may reveal promoter variation associated with differential gene expression between genotypes. Additional functional analyses using transient expression systems in *N. benthamiana*, including assays for callose deposition and defence gene expression, could clarify their roles in immune signalling. Genome editing approaches such as CRISPR/Cas9 could provide direct functional validation by generating knockout genotypes for these candidate genes. The genetic diversity within maize may also be leveraged beyond the development of new genotypes. Finally, biochemical analyses of cell wall composition, including measurements of xylose, xylan, lignin, and other structural polysaccharides, may help determine whether differences in cell wall architecture contribute to the resistance phenotype observed in CML495. This study also demonstrates differences between the tar spot resistant genotype CML495 and the susceptible genotype CO428, as observed through ROS and gene expression assays. However, these differences may partially reflect inherent physiological variation and may not fully represent responses to pathogen invasion. Because *PR5* is commonly associated with salicylic acid (SA)-dependent defence and ROS can act upstream of SA accumulation, these findings suggest that resistance may be activated early within PTI

pathways. Future research could therefore evaluate whether salicylic acid analogues or other plant defence activators can enhance maize immunity, either alone or in combination with fungicide programs, to reduce tar spot severity.

One limitation of this study is that reproducible methods to induce *P. maydis* infection do not exist, limiting the approaches which can be used in studying resistance. In 2023, Solórzano et al. described a method for inducing *P. maydis* infection under controlled conditions using ascospores collected from infected field leaves. However, subsequent work by Jimenez-Beitia et al. (2026) highlighted difficulties in reproducing these results, demonstrating that disease development was strongly influenced by inoculum quality and environmental conditions. Although reproducibility was high in Ecuador, results were less consistent in the United States, suggesting that environmental variability and inoculum source contribute to the challenge of establishing a reliable inoculation system (Jimenez-Beitia et al., 2026). To date, no reproducible method has been established for inducing *P. maydis* infection in temperate maize, limiting the ability to directly challenge plants with the pathogen. Consequently, this study relied on MAMPs to induce defence responses rather than pathogen inoculation. Furthermore, the infection biology of tar spot remains incompletely understood, and the experimental time points used may not fully capture the dynamic host responses that occur during natural infection. These limitations highlight the broader challenges associated with studying obligate biotrophic pathogens and underscore the need for continued development of reproducible infection systems for *P. maydis*.

From an applied perspective, improving tar spot resistance is increasingly important as the disease continues to spread throughout North America. Identification of resistance-associated genes may support the development of resistant maize cultivars, helping to reduce yield losses and improve crop stability. However, continued pathogen evolution, expanding geographic

distribution, and climate variability are likely to sustain or intensify disease pressure in many maize-growing regions. Consequently, further investigation of plant defence mechanisms and their interactions with *P. maydis* will be critical for informing targeted management strategies. Functional studies aimed at understanding the molecular basis of tar spot resistance will provide insight into how resistance is established and maintained, while also contributing more broadly to our understanding of plant–pathogen interactions. Overall, this study advances our understanding of the molecular differences between tar spot resistant and susceptible maize genotypes. Continued investigation of host–pathogen interactions will be essential for developing effective strategies to manage tar spot and support sustainable maize production.

6. References

- Ahmad, S., Tsang, K. K., Sachar, K., Quentin, D., Tashin, T. M., Bullen, N. P., Raunser, S., McArthur, A. G., Prehna, G., & Whitney, J. C. (2020). Structural basis for effector transmembrane domain recognition by type VI secretion system chaperones. *eLife*, *9*, e62816. <https://doi.org/10.7554/eLife.62816>
- Alberts, B., Johnson, A., Lewis, J. et al. (2002). Transport from the ER through the Golgi Apparatus. *Molecular Biology of the Cell*. 4th edition. Available from: <https://www.ncbi.nlm.nih.gov/books/NBK26941/>
- Anelli, T., & Sitia, R. (2008). Protein quality control in the early secretory pathway. *The EMBO Journal*, *27*(2), 315–327. <https://doi.org/10.1038/sj.emboj.7601974>
- Aniento F, Sanchez de Medina Hernandez V, Dagdas Y, Rojas-Pierce M, Russinova E. (2022). Molecular mechanisms of endomembrane trafficking in plants. *The Plant Cell*, *34*(1), 146- 173.
- Armenteros, J. J. A., Salvatore, M., Emanuelsson, O., Winther, O., von Heijne, G., Elofsson, A., & Nielsen, H. (2019). Detecting sequence signals in targeting peptides using deep learning. *Nature Communications*, *10*, 535. <https://doi.org/10.1038/s41467-019-08344-7>

- Bacete, L., Mérida, H., Miedes, E., & Molina, A. (2018). Plant cell wall-mediated immunity: Cell wall changes trigger disease resistance responses. *The Plant Journal*, *93*(4), 614–636. <https://doi.org/10.1111/tpj.13807>
- Bajet, N. B., Renfro, B. L., & Carrasco, J. M. V. (1994). Control of tar spot of maize and its effect on yield. *International Journal of Pest Management*, *40*(2), 121–125. <https://doi.org/10.1080/09670879409371868>
- Balint-Kurti, P. J., & Carson, M. L. (2007). Analysis of quantitative trait loci for resistance to southern leaf blight in juvenile maize. *Phytopathology*, *96*(3), 221–225. <https://doi.org/10.1094/PHYTO-96-0221>
- Barros-Rios, J., Malvar, R. A., Jung, H.-J. G., & Santiago, R. (2011). Cell wall composition as a maize defense mechanism against corn borers. *Phytochemistry*, *72*(4–5), 365–371. <https://doi.org/10.1016/j.phytochem.2011.01.004>
- Bayer. (2020, December 21). Tar spot Q & A. *Bayer Crop Science*.
- Bellincampi, D., Cervone, F., & Lionetti, V. (2014). Plant cell wall dynamics and wall-related susceptibility in plant–pathogen interactions. *Frontiers in Plant Science*, *5*, 274. <https://doi.org/10.3389/fpls.2014.00274>
- Benson, J. M., Poland, J. A., Benson, B. M., Stromberg, E. L., & Nelson, R. J. (2015). Resistance to gray leaf spot of maize: Genetic architecture and mechanisms. *Plant Disease*, *99*(12), 1684–1690. <https://doi.org/10.1094/PDIS-02-15-0141-RE>
- Block, A. K., Tang, H. V., Hopkins, D., Mendoza, J., Solemslie, R. K., du Toit, L. J., & Christensen, S. A. (2021). A maize leucine-rich repeat receptor-like protein kinase mediates responses to fungal attack. *Planta*, *254*(4), 73. <https://doi.org/10.1007/s00425-021-03730-0>
- Boller, T., & Felix, G. (2009). A renaissance of elicitors: Perception of microbe-associated molecular patterns and danger signals by pattern-recognition receptors. *Annual Review of Plant Biology*, *60*, 379–406. <https://doi.org/10.1146/annurev.arplant.57.032905.105346>
- Boots, M., & Best, A. (2018). The evolution of constitutive and induced defences to infectious disease. *Proceedings of the Royal Society B: Biological Sciences*, *285*(1883), 20180658. <https://doi.org/10.1098/rspb.2018.0658>

Brauer, E. K., Ahsan, N., Dale, R., Kato, N., Coluccio, A. E., Piñeros, M. A., Kochian, L. V., Thelen, J. J., Popescu, S. C. (2016). The Raf-like Kinase *ILK1* and the High Affinity K⁺ Transporter *HAK5* Are Required for Innate Immunity and Abiotic Stress Response. *Plant Physiology*, Volume 171, Issue 2, June 2016, Pages 1470-1484, <https://doi.org/10.1104/pp.16.00035>

Brauer, E. K., Ahsan, N., Popescu, G. V., Thelen, J. J., & Popescu, S. C. (2022). Back from the dead: The atypical kinase activity of a pseudokinase regulator of cation fluxes during inducible immunity. *Frontiers in Plant Science*, 13, 931324. <https://doi.org/10.3389/fpls.2022.931324>

Brauer, E. K., Bosnich, W., Holy, K., Thapa, I., Krishnan, S., Moatter Syed, M., Bredow, M., Sproule, A., Power, M., Johnston, A., Cloutier, M., Haribabu, N., Khan, I. U. H., Diallo, J.-S., Monaghan, J., Chabot, D., Overy, D. P., Subramaniam, R., Piñeros, M., & Harris, L. J. (2024). A cyclic lipopeptide from *Fusarium graminearum* targets plant membranes to promote virulence. *Cell Reports*, 43(7), 114384. <https://doi.org/10.1016/j.celrep.2024.114384>

Brauer, E. K., Bosnich, W., Power, M., Luckert, D., Khanal, S., Liang, N., James, R., Syed, M., Charette, M., Wolfe, D., Pattang, A., Morrison, H., Poncos, S., Laniel, M., Tucker, J., Khanal, R., Parent, J.-S., & Samanfar, B. (2025). Transcriptional profiling and genetic mapping of barley responses to bacterial flagellin. *Molecular Plant-Microbe Interactions*, 38(2), 344–352. <https://doi.org/10.1094/MPMI-12-24-0159-FI>

Broders, K., Iriarte-Broders, G., Bergstrom, G. C., Byamukama, E., Chilvers, M., Cruz, C., Dalla-Lana, F., Duray, Z., Malvick, D., Mueller, D., Paul, P., Plewa, D., Raid, R., Robertson, A. E., Salgado-Salazar, C., Smith, D., Telenko, D., VanEtten, K., Kleczewski, N. M. (2022). *Phyllachora* species infecting maize and other grass species in the Americas represents a complex of closely related species. *Ecology and Evolution*, 12(4): e8832. doi:10.1002/ece3.8832.

Brown, D. M., Zeef, L. A. H., Ellis, J., Goodacre, R., & Turner, S. R. (2005). Identification of novel genes in *Arabidopsis* involved in secondary cell wall formation using expression profiling and reverse genetics. *The Plant Cell*, 17(8), 2281–2295. <https://doi.org/10.1105/tpc.105.031542>

Caldwell, D. L., Chilvers, M. I., Byrne, A. M., Smith, D. L., Ross, T. J., Kleczewski, N. M., & Telenko, D. E. (2024). Uncovering the infection strategy of *Phyllachora maydis* during maize colonization. *Phytopathology*, *114*(5):1075-1087. <https://doi.org/10.1094/PHTO-08-23-0298-KC>

Camiletti, B. (2025). Tar Spot on the Move: Tracking and Managing an Established Corn Threat in Illinois. *Farmdoc daily* (15):127, Department of Agricultural and Consumer Economics, University of Illinois at Urbana-Champaign. [Permalink](#)

Cannon, P. F. (1991). A revision of *Phyllachora* and related genera on the Poaceae. *Mycological Papers*, *163*, 1–302.

Cao, D. V., Pamplona, R. S., Kim, J., Oh, Y. K., Cho, S. K., Ahn, J., Yang, S. W., Riu, K. Z., & Boo, K. H. (2017). Optimization of *Agrobacterium*-mediated transient expression of heterologous genes in spinach. *Plant Biotechnology Reports*, *11*(6), 397–405. <https://doi.org/10.1007/s11816-017-0457-4>

Cao, S., Loladze, A., Yuan, Y., Wu, Y., Zhang, A., Chen, J., Huestis, G., Cao, J., Chaikam, V., Olsen, M., Prasanna, B. M., San Vicente, F., & Zhang, X. (2017). Genome-wide analysis of tar spot complex resistance in maize using genotyping-by-sequencing SNPs and whole-genome prediction. *The Plant Genome*, *10*(2). <https://doi.org/10.3835/plantgenome2016.10.0099>

Carpita, N. C., & Gibeaut, D. M. (1993). Structural models of primary cell walls in flowering plants: Consistency of molecular structure with the physical properties of the walls during growth. *The Plant Journal*, *3*, 1–30. <https://doi.org/10.1046/j.1365-313X.1993.00999.x>

Ceballos, H., & Deutsch, J. A. (1992). Inheritance of resistance to tar spot of maize caused by *Phyllachora maydis*. *Plant Disease*, *76*, 825–827.

Chaudhari, P., Ahmed, B., Joly, D. L., & Germain, H. (2014). Effector biology during biotrophic invasion of plant cells. *Plant Signaling & Behavior*, *9*(9), e973507. <https://doi.org/10.4161/15592324.2014.973507>

Chen, T. (2021). Identification and characterization of the LRR repeats in plant LRR-RLKs. *BMC Molecular and Cell Biology*, *22*, 9. <https://doi.org/10.1186/s12860-021-00344-y>

Cheng, W., Wang, Z., Xu, F., Ahmad, W., Lu, G., Su, Y., Xu, L. (2021). Genome-Wide Identification of LRR-RLK Family in *Saccharum* and Expression Analysis in Response to Biotic and Abiotic Stress. *Current Issues in Molecular Biology*, 43(3):1632-1651. doi: 10.3390/cimb43030116.

Chilvers, M. (2025). Managing tar spot in corn. *Michigan State University, MSU Extension, Corn*. <https://www.canr.msu.edu/news/managing-tar-spot-in-corn>

Chinchilla, D., Bauer, Z., Regenass, M., Boller, T., & Felix, G. (2006). The *Arabidopsis* receptor kinase FLS2 binds flg22 and determines the specificity of flagellin perception. *The Plant Cell*, 18(2), 465–476. <https://doi.org/10.1105/tpc.105.036574>

Chinchilla, D., Zipfel, C., Robatzek, S., Kemmerling, B., Nürnberger, T., Jones, J. D. G., Felix, G., & Boller, T. (2007). A flagellin-induced complex of the receptor FLS2 and BAK1 initiates plant defence. *Nature*, 448(7152), 497–500.

Choquette, N.E., Weldekidan, T., Brewer, J., Davis, S.B., Wisser, R.J., Holland, J.B. (2023). Enhancing adaptation of tropical maize to temperate environments using genomic selection. *G3 (Bethesda)*. 13(9):jkad141. doi: 10.1093/g3journal/jkad141.

Chung, C. L., Jamann, T., Longfellow, J., & Nelson, R. (2011). Characterization and fine mapping of a resistance locus for northern leaf blight in maize. *Theoretical and Applied Genetics*, 123, 131–140.

CIMMYT. (2005). Maize Inbred Lines Released by CIMMYT, a compilation of 497 CIMMYT maize lines (CMLs). *Repository: CIMMYT Organization*. <https://repository.cimmyt.org/server/api/core/bitstreams/419e7873-3427-40a0-bd09-3a49bbd6f552/content#:~:text=MAIZE%20INBRED%20LINES-,IRELEASED%20BY%20CIMM:YT,%2D%2D%2D%2D%2D%2D%2D>

Cline, E. (2019). *Phyllachora maydis*. U.S. National Fungus Collections, ARS, USDA. Retrieved March 16, 2026, from <https://nt.ars-grin.gov/sbmlweb/fungi/nomenSheets.cfm>

Coffey, M. D., Palevitz, B. A., & Allen, P. J. (1972). The fine structure of two rust fungi, *Puccinia helianthi* and *Melampsora lini*. *Canadian Journal of Botany*, 50, 231–240.

<https://doi.org/10.1139/b72-031>

Cosgrove, D. J. (1997). Relaxation in a high-stress environment: The molecular bases of extensible cell walls and cell enlargement. *The Plant Cell*, 9(7), 1031–1041.

<https://doi.org/10.1105/tpc.9.7.1031>

Cosgrove, D. J. (2005). Growth of the plant cell wall. *Nature Reviews Molecular Cell Biology*, 6(11), 850–861. <https://doi.org/10.1038/nrm1746>

Cosgrove, D. J., & Jarvis, M. C. (2012). Comparative structure and biomechanics of plant primary and secondary cell walls. *Frontiers in Plant Science*, 3, 204.

<https://doi.org/10.3389/fpls.2012.00204>

Cui, H., Tsuda, K., & Parker, J. E. (2015). Effector-triggered immunity: From pathogen perception to robust defense. *Annual Review of Plant Biology*, 66, 487–511.

<https://doi.org/10.1146/annurev-arplant-050213-040012>

Cunnac, S., Lindeberg, M., & Collmer, A. (2009). *Pseudomonas syringae* type III secretion system effectors: Repertoires in search of functions. *Current Opinion in Microbiology*, 12(1), 53–60.

<https://doi.org/10.1016/j.mib.2008.12.003>

Curry, T. M., Peña, M. J., & Urbanowicz, B. R. (2023). An update on xylan structure, biosynthesis, and potential commercial applications. *Cell Surface*, 9, 100101.

<https://doi.org/10.1016/j.tcs.2023.100101>

Daudi, A., Cheng, Z., O'Brien, J.A., Mammarella, N., Khan, S., Ausubel, F.M., Bolwell, G.P. The apoplastic oxidative burst peroxidase in Arabidopsis is a major component of pattern-triggered immunity. (2012). *The Plant Cell*. 24(1):275-87. [doi: 10.1105/tpc.111.093039](https://doi.org/10.1105/tpc.111.093039)

Dardick, C., & Ronald, P. (2006). Plant and animal pathogen recognition receptors signal through non-RD kinases. *PLoS Pathogens*, 2(1), e2.

<https://doi.org/10.1371/journal.ppat.0020002>

de Jesús-Pires, C., Ferreira-Neto, J. R. C., Pacifico Bezerra-Neto, J., Kido, E. A., de Oliveira Silva, R. L., Pandolfi, V., & Benko-Iseppon, A. M. (2020). Plant thaumatin-like proteins: Function, evolution, and biotechnological applications. *Current Protein & Peptide Science*, *21*(1), 36–51.

Delgado-Cerezo, M., Sánchez-Rodríguez, C., Escudero, V., Miedes, E., Fernández, P. V., Jordá, L., Hernández-Blanco, C., Sánchez-Vallet, A., Bednarek, P., Schulze-Lefert, P., Somerville, S., Estevez, J. M., Persson, S., & Molina, A. (2012). *Arabidopsis* heterotrimeric G-protein regulates cell wall defense and resistance to necrotrophic fungi. *Molecular Plant*, *5*(1), 98–114. <https://doi.org/10.1093/mp/ssu064>

Delmer, D., Dixon, A. R., Keegstra, K., & Mohnen, D. (2024). The plant cell wall—dynamic, strong, and adaptable—is a key player in plant biology. *Frontiers in Plant Science*, *15*, 11062476. <https://doi.org/10.3389/fpls.2024.11062476>

Dievart, A., Gottin, C., Périn, C., Ranwez, V., & Chantret, N. (2020). Origin and diversity of plant receptor-like kinases. *Annual Review of Plant Biology*, *71*, 131–156. <https://doi.org/10.1146/annurev-arplant-073019-025927>

Di Renzo, M. A., Bonamico, N. C., Díaz, D. G., Ibañez, M. A., Faricelli, M. E., Balzarini, M. G., & Salerno, J. C. (2004). Microsatellite markers linked to QTL for resistance to mal de Río Cuarto disease in *Zea mays* L. *The Journal of Agricultural Science*, *142*, 289–295. <https://doi.org/10.1017/S0021859604004307>

Ding, J. Q., Wang, X. M., Chander, S., & Li, J. S. (2008). Identification of QTL for maize resistance to common smut by using recombinant inbred lines developed from the Chinese hybrid Yuyu22. *Journal of Applied Genetics*, *49*, 147–154. <https://doi.org/10.1007/BF03195608>

Ding, J., Ali, F., Chen, G., Li H, Mahuku, G., Yang, N., Narro, L., Magorokosho, C., Makumbi, & D., Yan, J. (2015). Genome-wide association mapping reveals novel sources of resistance to northern corn leaf blight in maize. *BMC Plant Biology*, *15*:206. <https://doi.org/10.1186/s12870-015-0589-z>

Ding, L.N., Li, Y.T., Wu, Y.Z., Li, T., Geng, R., Cao, J., Zhang, W., Tan, X.L. (2022). Plant Disease Resistance-Related Signaling Pathways: Recent Progress and Future Prospects. *International Journal of Molecular Sciences*, 23(24):16200. doi: 10.3390/ijms232416200.

Dodds, P. N., Chen, J., & Outram, M. A. (2024). Pathogen perception and signaling in plant immunity. *The Plant Cell*, 36(5), 1465–1481. <https://doi.org/10.1093/plcell/koae020>

Du, X., Li, Y., Xia, Y.L., Ai, S.M., Liang, J., Sang, P., Ji, X.L., Liu, S.Q. (2016). Insights into Protein-Ligand Interactions: Mechanisms, Models, and Methods. *International Journal of Molecular Sciences*, 17(2):144. doi:10.3390/ijms17020144.

Ebert, B., Rautengarten, C., Guo, X., Xiong, G., Stonebloom, S., Smith-Moritz, A. M., Herter, T., Chan, L. J. G., Adams, P. D., Petzold, C. J., Pauly, M., Willats, W. G. T., Heazlewood, J. L., & Scheller, H. V. (2015). Identification and characterization of a Golgi-localized UDP-xylose transporter family from *Arabidopsis*. *The Plant Cell*, 27(4), 1218–1227. <https://doi.org/10.1105/tpc.114.133827>

Ebringerová, A., & Heinze, T. (2000). Xylan and xylan derivatives—Biopolymers with valuable properties: 1. Naturally occurring xylans, structures, isolation procedures and properties. *Macromolecular Rapid Communications*, 21(9), 542–556. [https://doi.org/10.1002/1521-3927\(20000601\)21:9<542::AID-MARC542>3.0.CO;2-7](https://doi.org/10.1002/1521-3927(20000601)21:9<542::AID-MARC542>3.0.CO;2-7)

Earley, K. W., Haag, J. R., Pontes, O., Opper, K., Juehne, T., Song, K., & Pikaard, C. S. (2006). Gateway-compatible vectors for plant functional genomics and proteomics. *The Plant Journal*, 45(4), 616–629. <https://doi.org/10.1111/j.1365-313X.2005.02617.x>

Egelund, J., Peterson, B. L., Motawia, M. S., Damager, I., Faik, A., Olsen, C. E., Ishii, T., Clausen, H., Ulvskov, P., & Geshi, N. (2006). *Arabidopsis thaliana* RGXT1 and RGXT2 encode Golgi-localized (1,3)-alpha-D-xylosyltransferases involved in the synthesis of pectic rhamnogalacturonan-II. *Plant Cell*, 18: 2593-2607.

Fedoreyeva, L. I. (2024). ROS as signaling molecules to initiate the process of plant acclimatization to abiotic stress. *International Journal of Molecular Sciences*, 25(21), 11820. <https://doi.org/10.3390/ijms252111820>

Felix, G., Duran, J. D., Volko, S., & Boller, T. (1999). Plants have a sensitive perception system for the most conserved domain of bacterial flagellin. *The Plant Journal*, *18*(3), 265–276.

<https://doi.org/10.1046/j.1365-313X.1999.00265.x>

Ferreira, L. C., de Moura, V. A. S., Resende, M. F. R., Jr., & Xavier, K. V. (2025). Pathobiome analyses reveal structural changes in maize microbiomes associated with *Phyllachora maydis* and the tar spot disease. *Phytobiomes Journal*, *9*. <https://doi.org/10.1094/PBIOMES-12-24-0118-R>

Fitchette-laine, A. C., Gomord, V., Chekkafi, A., & Faye, L. (1994). Distribution of xylosylation and fucosylation in the plant Golgi-apparatus. *Plant J*. *5*: 673-682.

Flor, H. H. (1971). Current status of the gene-for-gene concept. *Annual Review of Phytopathology*, *9*, 275–296. <https://doi.org/10.1146/annurev.py.09.090171.001423>

Franco, O. L., Rigden, D. J., Melo, F. R., & Grossi-de-Sá, M. F. (2002). Plant α -amylase inhibitors and their interaction with insect α -amylases: Structure, function and potential for crop protection. *European Journal of Biochemistry*, *269*(2), 397–412.

Freeman, B. C., & Beattie, G. A. (2008). An overview of plant defenses against pathogens and herbivores. *The Plant Health Instructor*. <https://doi.org/10.1094/PHI-I-2008-0226-01>

Gao, Y., He, C., Zhang, D., Liu, X., Xu, Z., Tian, Y., Liu, X. H., Zang, S., Pauly, M., Zhou, Y., & Zhang, B. (2017). Two trichome birefringence-like proteins mediate xylan acetylation, which is essential for leaf blight resistance in rice. *Plant Physiology*, *173*(1), 470–481.

<https://doi.org/10.1104/pp.16.01618>

Gao, Y., Qu, Q., Liu, N., Sun, M., Liu, X., Cao, Z., & Dong, J. (2025). Genome identification of the LRR-RLK gene family in maize (*Zea mays*) and expression analysis in response to *Fusarium verticillioides* infection. *BMC Plant Biology*, *25*, 524. <https://doi.org/10.1186/s12870-025-06495-w>

Giraldo, M. C., & Valent, B. (2013). Filamentous plant pathogen effectors in action. *Nature Reviews Microbiology*, *11*, 800–814. <https://doi.org/10.1038/nrmicro3119>

Goodstein, D. M., Shu, S., Howson, R., Neupane, R., Hayes, R. D., Fazo, J., Mitros, T., Dirks, W., Hellsten, U., Putnam, N., & Rokhsar, D. S. (2012). Phytozome: A comparative platform for green plant genomics. *Nucleic Acids Research*, *40*(D1), D1178–D1186.

<https://doi.org/10.1093/nar/gkr944>

Gómez-Gómez, L., & Boller, T. (1999). A single locus determines sensitivity to bacterial flagellin in *Arabidopsis thaliana*. *The Plant Journal*, *18*(3), 277–284.

Gómez-Gómez, L., & Boller, T. (2000). FLS2: An LRR receptor–like kinase involved in the perception of the bacterial elicitor flagellin in *Arabidopsis*. *Molecular Cell*, *5*(6), 1003–1011.

[https://doi.org/10.1016/S1097-2765\(00\)80265-8](https://doi.org/10.1016/S1097-2765(00)80265-8)

Gomord, V., Denmat, L. A., Fichette-Lainé, A. C., Satiat-Jeunemaitre, B., Hawes, C., & Faye, L. (1997). The C-terminal HDEL sequence is sufficient for retention of secretory proteins in the endoplasmic reticulum (ER) but promotes vacuolar targeting of proteins that escape the ER. *The Plant Journal*, *11*(2), 313–325.

Hadley, B., Maggioni, A., Ashikov, A., Day, C.J., Haselhorst, T. (2014). Structure and function of nucleotide sugar transporters: current progress. *Computational and Structural Biotechnology Journal*, *10*:23–32. doi: 10.1016/j.csbj.2014.05.003.

Hadley, B., Litfin, T., Day, C.J., Haselhorst, T., Zhou, Y., Tiralongo, J. (2019). Nucleotide Sugar Transporter SLC35 Family Structure and Function. *Computational and Structural Biotechnology Journal*, *17*:1123-1134. doi: 10.1016/j.csbj.2019.08.002.

Harris, L.J., Saparno, A., Johnston, A. *et al.* The Maize *An2* Gene is Induced by *Fusarium* Attack and Encodes an *ent*-Copalyl Diphosphate Synthase. *Plant Mol Biol* **59**, 881–894 (2005).

<https://doi.org/10.1007/s11103-005-1674-8>

Hatfield, R. D., Rancour, D. M., & Marita, J. M. (2017). Grass cell walls: A story of cross-linking. *Frontiers in Plant Science*, *7*, 2056. <https://doi.org/10.3389/fpls.2016.02056>

Han Z, & Schneiter R. (2024). Dual functionality of pathogenesis-related proteins: defensive role in plants versus immunosuppressive role in pathogens. *Frontiers Plant Science*, *15*:1368467. doi: [10.3389/fpls.2024.1368467](https://doi.org/10.3389/fpls.2024.1368467).

He, S. Y., Nomura, K., & Whittam, T. S. (2004). Type III protein secretion mechanism in mammalian and plant pathogens. *Biochimica et Biophysica Acta (BBA) - Molecular Cell Research*, 1694(1–3), 181–206. <https://doi.org/10.1016/j.bbamcr.2004.03.011>

Heese, A., Hann, D. R., Gimenez-Ibanez, S., Jones, A. M. E., He, K., Li, J., Schroeder, J. I., Peck, S. C., & Rathjen, J. P. (2007). The receptor-like kinase SERK3/BAK1 is a central regulator of innate immunity in plants. *Proceedings of the National Academy of Sciences*, 104(29), 12217–12222.

Helm, M., Singh, R., Hiles, R., Jaiswal, N., Myers, A., Iyer-Pascuzzi, A. S., & Goodwin, S. B. (2022). Candidate effector proteins from the maize tar spot pathogen *Phyllachora maydis* localize to diverse plant cell compartments. *Phytopathology*, 112(12), 2538–2548.

<https://doi.org/10.1094/PHYTO-05-22-0181-R>

Helm, M., Singh, R., Goodwin, S. B., Caldwell, D., & Iyer-Pascuzzi, A. (2022). Tar spot of maize: Tar Spot of Maize: Current knowledge of genetic interactions and future research prospects to improve disease resistance. *Authorea*.

<https://doi.org/10.22541/au.164642664.47870546/v2>

Hernández-Blanco, C., Feng, D. X., Hu, J., Sánchez-Vallet, A., Deslandes, L., Llorente, F., Berrocal-Lobo, M., Keller, H., Barlet, X., Sánchez-Rodríguez, C., Anderson, L. K., Somerville, S., Marco, Y., & Molina, A. (2007). Impairment of cellulose synthases required for *Arabidopsis* secondary cell wall formation enhances disease resistance. *The Plant Cell*, 19(3), 890–903.

<https://doi.org/10.1105/tpc.106.048058>

Herrera-Vásquez, A., Salinas, P., & Holuigue, L. (2015). Salicylic acid and reactive oxygen species interplay in the transcriptional control of defense genes expression. *Frontiers in Plant Science*, 6, 171.

Hock, J., Kranz, J., & Renfro, B. L. (1989). El complejo “mancha de asfalto” de maíz: Su distribución geográfica, requisitos ambientales e importancia económica en México. *Revista Mexicana de Fitopatología*, 7, 129–135.

Hock, J., Dittrich, U., Renfro, B. L., & Kranz, J. (1992). Sequential development of pathogens in the maize tar spot disease complex. *Mycopathologia*, *117*, 157–161.

<https://doi.org/10.1007/BF00442777>

Hock, J., Kranz, J., & Renfro, B. L. (1995). Studies on the epidemiology of the tar spot disease complex of maize in Mexico. *Plant Pathology*, *44*(3), 490–502. <https://doi.org/10.1111/j.1365-3059.1995.tb01671.x>

Hoffmann, N. (2024). Integrating Cell Wall Synthesis, Secretion, and Signaling with the Plant Endomembrane System. (PhD Thesis). *University of Toronto*.

Hoopes, G. M., Hamilton, J. P., Wood, J. C., Esteban, E., Pasha, A., Vaillancourt, B., Provart, N. J., & Buell, C. R. (2019). An updated gene atlas for maize reveals organ-specific and stress-induced genes. *The Plant Journal*, *97*(6), 1154–1167. <https://doi.org/10.1111/tpj.14184>

Hu, X., Cui, Y., Lu, X., Song, W., Lei, L., Zhu, J., Lai, J., E, L., & Zhao, H. (2020). Maize WI5 encodes an endo-1,4- β -xylanase required for secondary cell wall synthesis and water transport in xylem. *Journal of Integrative Plant Biology*, *62*(10), 1607–1624.

<https://doi.org/10.1111/jipb.12923>

Hufford, M. B., Xu, X., van Heerwaarden, J., Pyhäjärvi, T., Chia, J. M., Cartwright, R. A., Elshire, R. J., Glaubitz, J. C., Guill, K. E., Kaeppeler, S. M., Lai, J., Morrell, P. L., Shannon, L. M., Song, C., Springer, N. M., Swanson-Wagner, R. A., Tiffin, P., Wang, J., Zhang, G., ... Ross-Ibarra, J. (2012). Comparative population genomics of maize domestication and improvement. *Nature Genetics*, *44*(7), 808–811. <https://doi.org/10.1038/ng.2309>

Huang, Y., Yuan, Y., Yang, R., Gou, X., Dai, S., Zhou, J., Guo, J., Shen, J., Lu, Y., Liu, Y., & Cai, Y. (2024). A large-scale screening identifies receptor-like kinases with common features in kinase domains that are potentially related to disease resistance in planta. *Frontiers in Plant Science*, *15*, 1503773. <https://doi.org/10.3389/fpls.2024.1503773>

Hubbard, S. R., & Miller, W. T. (2007). Receptor tyrosine kinases: Mechanisms of activation and signalling. *Current Opinion in Cell Biology*, *19*(2), 117–123.

- Islam, M. M., El-Sappah, A. H., Ali, H. M., Zandi, P., Huang, Q., Soaud, S. A., et al. (2023). Pathogenesis-related proteins (PRs) countering environmental stress in plants: a review. *South African Journal of Botany*, 160: 414–427. doi: [10.1016/j.sajb.2023.07.003](https://doi.org/10.1016/j.sajb.2023.07.003)
- Jayamani, E., & Mylonakis, E. (2014). Effector triggered manipulation of host immune response elicited by different pathotypes of *Escherichia coli*. *Virulence*, 5(7), 733–739. <https://doi.org/10.4161/viru.29948>
- Johnson, E. T., Dowd, P. F., Ramirez, J. L., & Behle, R. W. (2023). Potential biocontrol agents of corn tar spot disease isolated from overwintered *Phyllachora maydis* stromata. *Microorganisms*, 11(6), 1550. <https://doi.org/10.3390/microorganisms11061550>
- Jones, J. D. G., & Dangl, J. L. (2006). The plant immune system. *Nature*, 444(7117), 323–329. <https://doi.org/10.1038/nature05286>
- Kadota, Y., Shirasu, K., & Zipfel, C. (2015). Regulation of the NADPH oxidase RBOHD during plant immunity. *Plant and Cell Physiology*, 56(8), 1472–1480. <https://doi.org/10.1093/pcp/pcv063>
- Kang, X., Kirui, A., Dickwella Widanage, M. C., et al. (2019). Lignin-polysaccharide interactions in plant secondary cell walls revealed by solid-state NMR. *Nature Communications*, 10, 347. <https://doi.org/10.1038/s41467-018-08252-0>
- Kileeg, Z., Haldar, A., Khan, H., Qamar, A., & Mott, G. A. (2023). Differential expansion and retention patterns of LRR-RLK genes across plant evolution. *Plant Direct*, 7(12), e556. <https://doi.org/10.1002/pld3.556>
- Kileeg, Z., & Mott, G. A. (2025). A species-wide inventory of receptor-like kinases in *Arabidopsis thaliana*. *BMC Biology*, 23, 360. <https://doi.org/10.1186/s12915-025-02364-y>
- Kirino, H., Yoshimoto, K., Shinya, R. (2020). Thaumatin-like proteins and a cysteine protease inhibitor secreted by the pine wood nematode *Bursaphelenchus xylophilus* induce cell death in *Nicotiana benthamiana*. *PloS One* 15, e0241613. doi: 10.1371/journal.pone.0241613

Kleczewski, N. M., Donnelly, J., & Higgins, R. (2019). *Phyllachora maydis*, causal agent of tar spot on corn, can overwinter in northern Illinois. *Plant Health Progress*, 20(3), 178–178.

<https://doi.org/10.1094/PHP-04-19-0030-BR>

Kleczewski, N. (2020). Managing corn tar spot in 2020. *Farmdoc Daily*, 10, 101.

Knappe, S., Flügge, U.-I., & Fischer, K. (2003). Analysis of the plastidic phosphate translocator gene family in *Arabidopsis* and identification of new phosphate translocator-related proteins.

Plant Physiology, 131(3), 1178–1190. <https://doi.org/10.1104/pp.102.016519>

Kobe, B., & Deisenhofer, J. (1994). The leucine-rich repeat: A versatile binding motif. *Trends in Biochemical Sciences*, 19(10), 415–421.

Köhler, U., Liaud, M.-F., Mendel, R. R., Cerff, R., & Hehl, R. (1995). The maize GapC4 promoter confers anaerobic reporter gene expression and shows homology to the maize anthocyanin regulatory locus C1. *Plant Molecular Biology*, 29(6), 1293–1298.

<https://doi.org/10.1007/BF00020469>

Koiwa H., Kato H., Nakatsu T., Oda J., Yamada Y., Sato F. (1999). Crystal structure of tobacco PR-5d protein at 1.8 Å resolution reveals a conserved acidic cleft structure in antifungal thaumatin-like proteins. *Journal of Molecular Biology*. 286, 1137–1145.

doi: 10.1006/jmbi.1998.2540

Kombrink, A., Sánchez-Vallet, A., & Thomma, B. P. H. J. (2011). The role of chitin detection in plant–pathogen interactions. *Microbes and Infection*, 13(14–15), 1168–1176.

<https://doi.org/10.1016/j.micinf.2011.07.010>

Kozlova, L. V., Nazipova, A. R., Gorshkov, O. V., Petrova, A. A., & Gorshkova, T. A. (2020). Elongating maize root: Zone-specific combinations of polysaccharides from type I and type II primary cell walls. *Scientific Reports*, 10, 10956. <https://doi.org/10.1038/s41598-020-67782-0>

Kundu, T., Smith, C. J., & Gupta, M. (2025). Effect of acetylation patterns of xylan on interactions with cellulose. *Biomacromolecules*, 26(3), 1659–1671.

<https://doi.org/10.1021/acs.biomac.4c01469>

Kunze, G., Zipfel, C., Robatzek, S., Niehaus, K., Boller, T., & Felix, G. (2004). The N-terminus of bacterial elongation factor Tu elicits innate immunity in *Arabidopsis* plants. *The Plant Cell*, *16*(12), 3496–3507. <https://doi.org/10.1105/tpc.104.026765>

Kumar, M., Campbell, L., & Turner, S. (2016). Secondary cell walls: Biosynthesis and manipulation. *Journal of Experimental Botany*, *67*, 515–531. <https://doi.org/10.1093/jxb/erv533>

Kumar S, Stecher G, Suleski M, Sanderford M, Sharma S, and Tamura K. (2024). MEGA12: Molecular Evolutionary Genetics Analysis version 12 for adaptive and green computing. *Molecular Biology and Evolution*, *41*: 1-9.

Kushalappa, A. C., Yogendra, K. N., & Karre, S. (2016). Plant innate immune response: Qualitative and quantitative resistance. *Critical Reviews in Plant Sciences*, *35*(1), 38–55. <https://doi.org/10.1080/07352689.2016.1148980>

Leiva-Mora, M., Capdesuñer, Y., Villalobos-Olivera, A., Moya-Jiménez, R., Saa, L. R., & Martínez-Montero, M. E. (2024). Uncovering the mechanisms: The role of biotrophic fungi in activating or suppressing plant defense responses. *Journal of Fungi*, *10*(9), 635. <https://doi.org/10.3390/jof10090635>

Lemmon, M. A., & Schlessinger, J. (2000). Cell signalling by receptor tyrosine kinases. *Cell*, *103*(2), 211–225.

Li, C., Ma, S., Tian, Y., & Zheng, X. (2025). Genome-wide identification and expression analyses of the LRR-RLK gene family in *Actinidia chinensis*. *Frontiers in Plant Science*, *16*, 1577679. <https://doi.org/10.3389/fpls.2025.1577679>

Li, J., Chu, Z.-H., Batoux, M., Nekrasov, V., Roux, M., Chinchilla, D., Zipfel, C., & Jones, J.D.G. (2009). *Specific ER quality control components required for biogenesis of the plant innate immune receptor EFR*. Proceedings of the National Academy of Sciences USA, *106*(37), 15973–15978

Liepmann, A. H., Wightman, R., Geshi, N., Turner, S. R., & Scheller, H. V. (2010). *Arabidopsis*—A powerful model system for plant cell wall research. *The Plant Journal*, *61*(6), 1107–1121. <https://doi.org/10.1111/j.1365-313X.2009.04161.x>

Lin, F., Jiang, L., Liu, Y., Lv, Y., Dai, H., & Zhao, H. (2014). Genome-wide identification of housekeeping genes in maize. *Plant Molecular Biology*, 86(4–5), 543–554.

<https://doi.org/10.1007/s11103-014-0246-1>

Lin, Y., Lai, Z., Liu, X., & Chen, Y. (2014). Validation of potential reference genes for qPCR in maize across abiotic stresses, hormone treatments, and tissue types. *PLoS ONE*, 9(5), e95445.

<https://doi.org/10.1371/journal.pone.0095445>

Lipps, S., Smith, D., Telenko, D., Paul, P., Kleczewski, N., & Jamann, T. (2022). Identification of resistance for *Phyllachora maydis* of maize in exotic-derived germplasm. *Crop Science*, 62(2), 859–866. <https://doi.org/10.1002/csc2.20709>

Liu, C., Weng, J., Zhang, D., Zhang, X., Yang, X., Shi, L., Meng, Q., Yuan, J., Guo, X., Hao, Z., Xie, C., Li, M., Ci, X., Bai, L., Li, X., & Zhang, S. (2014). Genome-wide association study of resistance to rough dwarf disease in maize. *European Journal of Plant Pathology*, 139, 205–216.

<https://doi.org/10.1007/s10658-014-0383-z>

Liu, T. (1973). *The genus Phyllachora and its allies on grasses*. *Mycologia Memoirs*, 3, 1–88.

Loladze, A., Mottaleb, K. A., Sonder, K., Kruseman, G., & San Vicente, F. (2019). Threats of tar spot complex disease of maize in the United States and its global consequences. *Frontiers in Plant Science*, 10, 552. <https://doi.org/10.3389/fpls.2019.00552>

Lorrain, C., Petre, B., & Duplessis, S. (2018). Show me the way: Rust effector targets in heterologous plant systems. *Current Opinion in Microbiology*, 46, 19–25.

<https://doi.org/10.1016/j.mib.2018.01.016>

Luis, M. J., Mehl, H. L., Plewa, D., & Kleczewski, N. M. (2023). Is *Microdochium maydis* associated with necrotic lesions in the tar spot disease complex? A culture-based survey of maize in Mexico and the Midwest United States. *Phytopathology*. <https://doi.org/10.1094/PHYTO-04-23-0109-R>

MacCready, J. S., Roggenkamp, E. M., Gdanetz, K., & Chilvers, M. I. (2023). Elucidating the obligate nature and biological capacity of an invasive fungal corn pathogen. *Molecular Plant-Microbe Interactions*, 36(7), 411–424. <https://doi.org/10.1094/MPMI-10-22-0213-R>

Madeira, F., Park, Y. M., Lee, J., Buso, N., Gur, T., Madhusoodanan, N., Basutkar, P., Tivey, A. R. N., Potter, S. C., Finn, R. D., & Lopez, R. (2019). The EMBL-EBI search and sequence analysis tools APIs in 2019. *Nucleic Acids Research*, *47*(W1), W636–W641.

<https://doi.org/10.1093/nar/gkz268>

Mahuku, G., Chen, J., Shrestha, R., Narro, L. A., Guerrero, K. V. O., Arcos, A. L., & Xu, Y. (2016). Combined linkage and association mapping identifies a major QTL (*qRtsc8-1*), conferring tar spot complex resistance in maize. *Theoretical and Applied Genetics*, *129*(6), 1217–1229. <https://doi.org/10.1007/s00122-016-2698-y>

Malinovsky, F. G., Fangel, J. U., & Willats, W. G. T. (2014). The role of the cell wall in plant immunity. *Frontiers in Plant Science*, *5*, 178. <https://doi.org/10.3389/fpls.2014.00178>

Mammadov, J., Sun, X., Gao, Y., Ochsenfeld, C., Bakker, E., Ren, R., Flora, J., Wang, X., Kumpatla, S., Meyer, D., & Thompson, S. (2015). Combining powers of linkage and association mapping for precise dissection of QTL controlling resistance to gray leaf spot disease in maize (*Zea mays* L.). *BMC Genomics*, *16*, 916. <https://doi.org/10.1186/s12864-015-2171-3>

Maublanc, A. (1904). Espèces nouvelles de champignons inférieurs. *Bulletin Trimestriel de la Société Mycologique de France*, *20*, 72.

McCoy, A. G., Roth, M. G., Shay, R., Noel, Z. A., Jayawardana, M. A., Longley, R. W., Bonito, G., & Chilvers, M. I. (2019). Identification of fungal communities within the tar spot complex of corn in Michigan via next-generation sequencing. *Phytobiomes Journal*, *3*, 235–243.

<https://doi.org/10.1094/PBIOMES-03-19-0017-R>

Meng, F., Li, Y., Wang, X., Feng, Y., Liu, Z., Zhang, W., et al. (2019). Thaumatin-like protein-1 gene (Bx-tlp-1) is associated with the pathogenicity of *Bursaphelenchus xylophilus*. *Phytopathology*. 109, 1949–1956. doi: [10.1094/PHYTO-03-19-0082-R](https://doi.org/10.1094/PHYTO-03-19-0082-R)

Meng, F., Li, Y., Liu, Z., Feng, Y., Wang, X., Zhang, X. (2022). Expression of the thaumatin-like protein-1 gene (Bx-tlp-1) from pine wood nematode *Bursaphelenchus xylophilus* affects terpene metabolism in pine trees. *Phytopathology*. 112, 888–897. doi: [10.1094/PHYTO-07-21-0289-R](https://doi.org/10.1094/PHYTO-07-21-0289-R)

- Menu-Bouaouiche L., Vriet C., Peumans W. J., Barre A., Van Damme E. J., Rougé P. (2003). A molecular basis for the endo-beta 1,3-glucanase activity of the thaumatin-like proteins from edible fruits. *Biochimie* 85, 123–131. [doi: 10.1016/s0300-9084\(03\)00058-0](https://doi.org/10.1016/s0300-9084(03)00058-0).
- Mideros, S., Warburton, M., Jamann, T., & Nelson, R. (2014). Quantitative trait loci associated with resistance to *Aspergillus flavus* infection in maize. *Crop Science*, 54, 114–125.
- Monaghan, J., & Zipfel, C. (2012). Plant pattern recognition receptor complexes at the plasma membrane. *Current Opinion in Plant Biology*, 15(4), 349–357.
- Mitsumasu, K., Seto, Y., & Yoshida, S. (2015). Apoplastic interactions between plants and plant root intruders. *Frontiers in Plant Science*, 6, 617. <https://doi.org/10.3389/fpls.2015.00617>
- Mishra, S., Roychowdhury, R., Ray, S., Hada, A., Kumar, A., Sarker, U., Aftab, A., Das, R. (2024). Salicylic acid (SA)-mediated plant immunity against biotic stresses: An insight on molecular components and signaling mechanism. *Plant Stress*. 11:100427. <https://doi.org/10.1016/j.stress.2024.100427>
- Molina, A., Miedes, E., Bacete, L., Rodríguez, T., Mélida, H., Denancé, N., Sánchez-Vallet, A., Rivière, M.-P., López, G., Freydier, A., & Rivas, S. (2021). *Arabidopsis* cell wall composition determines disease resistance specificity and fitness. *Proceedings of the National Academy of Sciences*, 118(5), e2010243118. <https://doi.org/10.1073/pnas.2010243118>
- Mottaleb, K. A., Loladze, A., Sonder, K., Kruseman, G., & San Vicente, F. (2019). Threats of tar spot complex disease of maize in the United States of America and its global consequences. *Mitigation and Adaptation Strategies for Global Change*, 24(2), 281–300. <https://doi.org/10.1007/s11027-018-9812-1>
- Mueller, D. S., Wise, K. A., Sisson, A. J., Allen, T. W., Bergstrom, G. C., Bissonnette, K. M., Bradley, C. A., Byamukama, E., Chilvers, M. I., Collins, A. A., Esker, P. D., Faske, T. R., Friskop, A. J., Hagan, A. K., Heiniger, R. W., Hollier, C. A., Isakeit, T., Jackson-Ziems, T. A., Jardine, D. J., ... Wiebold, W. J. (2020). Corn yield loss estimates due to diseases in the United States and Ontario, Canada, from 2016 to 2019. *Plant Health Progress*, 21, 238–247. <https://doi.org/10.1094/PHP-05-20-0038-RS>

Mueller, D., Wise, K., Sisson, A. (2023). Corn Disease Loss Estimates From the United States and Ontario, Canada — 2022. *Crop Protection Network*. CPN-2007-22. doi.org/10.31274/cpn-20230207-0.

Mueller, D., Wise, K., Sisson, A., Sikora, E., Faske, T., Meyer, R., Koehler, A., Kemerait, B., Mideros, S., Telenko, D., Robertson, A., Onofre, R., Price, T., Chilvers, M., Malvick, D., Allen, T., Bish, M., Jackson-Ziems, T., Broderick, K., Bergstrom, G., Heiniger, R., Ahumada, D., Friskop, A., Paul, P., Rodrigues Duffeck, M., Tenuta, A., Roth, G., Collins, A., Esker, P., Mueller, J., Plumblee, M., Shires, M., Kelly, H., Isakeit, T., Anderson, N., Langston, D., Zeng, Y., Smith, D. (2024). Corn Disease Loss Estimates from the United States and Ontario, Canada — 2023. *Crop Protection Network*. CPN-2007-23. doi.org/10.31274/cpn-20240315-0.

Müller, E., & Samuels, J. G. (1984). *Monographella maydis*: sp. nov. and its connection to the tar-spot disease of *Zea mays*. *Nova Hedwigia*, 40, 113–121.

Mukhtar, M. S., Carvunis, A.-R., Dreze, M., Epple, P., Steinbrenner, J., Moore, J., Tasan, M., Galli, M., Hao, T., Nishimura, M. T., Pevzner, S. J., Donovan, S. E., Ghamsari, L., Santhanam, B., Romero, V., Poulin, M. M., Gebreab, F., Gutierrez, B. J., Tam, S., ... Dangl, J. L. (2011). Independently evolved virulence effectors converge onto hubs in a plant immune system network. *Science*, 333(6042), 596–601. <https://doi.org/10.1126/science.1203659>

Muñoz-Zavala, C., Goodwin, P. H., Leyva-Mir, S. G., Loladze, A., Vargas-Hernández, M., García-León, E., Tovar-Pedraza, J. M., San Vicente-García, F. M., & Alakonya, A. (2024). Maize insensitivity to culture filtrates from *Exserohilum turcicum* is related to quantitative resistance. *Journal of Phytopathology*, 172, e13350. <https://doi.org/10.1111/jph.13350>

Narváez-Barragán, D. A., Tovar-Herrera, O. E., Guevara-García, A., Serrano, M., & Martínez-Anaya, C. (2022). Mechanisms of plant cell wall surveillance in response to pathogens, cell wall-derived ligands and the effect of expansins to infection resistance or susceptibility. *Frontiers in Plant Science*, 13, 969343. <https://doi.org/10.3389/fpls.2022.969343>

Nekrasov, V., Li, J., Batoux, M., Roux, M., Chu, Z.-H., Lacombe, S., Rougon, A., Bittel, P., Kiss-Papp, M., Chinchilla, D., van Esse, H. P., Jorda, L., Schwessinger, B., Nicaise, V., Thomma, B. P. H. J., Molina, A., Jones, J. D. G., & Zipfel, C. (2009). Control of the pattern-

recognition receptor EFR by an ER protein complex in plant immunity. *The EMBO Journal*, 28(21), 3428–3438. <https://doi.org/10.1038/emboj.2009.262>

Newman, M.-A., Sundelin, T., Nielsen, J. T., & Erbs, G. (2013). MAMP (microbe-associated molecular pattern) triggered immunity in plants. *Frontiers in Plant Science*, 4, 139. <https://doi.org/10.3389/fpls.2013.00139>

Ng, A., & Xavier, R. J. (2011). Leucine-rich repeat (LRR) proteins. *Autophagy*, 7(9), 1082–1084. <https://doi.org/10.4161/auto.7.9.16464>

Nie Z, Li W, Deng L, Gao K, Liu Q, Zhou Z. (2022). Comprehensive analysis of LRR-RLKs and key gene identification in *Pinus massoniana* resistant to pine wood nematode. *Frontiers Plant Science*, 13:1043261. doi: 10.3389/fpls.2022.1043261.

Noman, A., Aqeel, M., & Lou, Y. (2019). PRRs and NB-LRRs: From signal perception to activation of plant innate immunity. *International Journal of Molecular Sciences*, 20(8), 1882. <https://doi.org/10.3390/ijms20081882>

O'Brien, J. A., Daudi, A., Finch, P., Butt, V. S., Whitelegge, J. P., Souda, P., Ausubel, F. M., & Bolwell, G. P. (2012). A peroxidase-dependent apoplastic oxidative burst in cultured *Arabidopsis* cells functions in MAMP-elicited defense. *Plant Physiology*, 158(4), 2013–2027. <https://doi.org/10.1104/pp.111.190140>

Okekeogbu, I. O., Pattathil, S., Fernández-Niño, S. M. G., Penning, B. W., Lao, J., Heazlewood, J. L., et al. (2019). Glycome and proteomic components of Golgi membranes are common between two angiosperms with distinct cell wall structures. *The Plant Cell*, 31, 1094–1112. <https://doi.org/10.1105/tpc.18.00755>

Olukolu, B. A., Tracy, W. F., Wissler, R., De Vries, B., & Balint-Kurti, P. J. (2016). A genome-wide association study for partial resistance to maize common rust. *Phytopathology*, 106, 745–751. <https://doi.org/10.1094/PHYTO-11-15-0305-R>

Papatheodorou, I., Moreno, P., Manning, J., Muñoz-Pomer Fuentes, A., George, N., Fexova, S., Fonseca, N. A., Füllgrabe, A., Green, M., Huang, N., Huerta, L., Iqbal, H., Jianu, M., Mohammed, S., Zhao, L., Jarnuczak, A. F., Jupp, S., Marioni, J., Meyer, K., Petryszak, R., Prada

Medina, C. A., Talavera-López, C., Teichmann, S., Vizcaino, J. A., & Brazma, A. (2020). Expression atlas update: From tissues to single cells. *Nucleic Acids Research*, 48(D1), D77–D83. <https://doi.org/10.1093/nar/gkz947>

Parbery, D. G. (1967). Studies on graminicolous species of *Phyllachora* Nke. in Fckl. V. A taxonomic monograph. *Australian Journal of Botany*, 15, 271–375. <https://doi.org/10.1071/BT9670271>

Parbery, D. G. (1971). Studies on graminicolous species of *Phyllachora* Nke. in Fckl. VI. Additions and corrections to part V. *Australian Journal of Botany*, 19, 207–235.

Parker, J.L., Corey, R.A., Stansfeld, P.J. *et al.* (2019). Structural basis for substrate specificity and regulation of nucleotide sugar transporters in the lipid bilayer. *Nature Communication*, 10, 4657. <https://doi.org/10.1038/s41467-019-12673-w>

Pearce, R. (2021, February 4). Tracking tar spot in Ontario. *Corn Guide; Country Guide*. Glacier FarmMedia Limited Partnership.

Penning, B. W., Hunter, C. T., Tayengwa, R., Eveland, A. L., Dugard, C. K., Olek, A. T., Vermerris, W., Koch, K. E., McCarty, D. R., Davis, M. F., & Carpita, N. C. (2009). Genetic resources for maize cell wall biology: Expression profiling of cell wall genes in developing stems of maize B73. *Plant Physiology*, 149(2), 1068–1084. <https://doi.org/10.1104/pp.108.128827>

Pereyda-Hernandez, J., Hernandez-Morales, J., Sergio-Sandoval-Islas, J., Aranda-Ocampo, S., de León, C., & Gomez-Montiel, N. (2009). Etiology and management of tar spot (*Phyllachora maydis* Maubl.) of maize in Guerrero state of Mexico. *Agrociencia*, 43(4), 511–519.

Pfaffl M. W. (2001). A new mathematical model for relative quantification in real-time RT-PCR. *Nucleic Acids Research*, 29(9): e45. doi: 10.1093/nar/29.9.e45.

Portwood, J. L., II, Woodhouse, M. R., Cannon, E. K. S., Gardiner, J. M., Harper, L. C., Schaeffer, M. L., Walsh, J. R., Sen, T. Z., Cho, K. T., Schott, D. A., Braun, B. L., Dietze, M., Dunfee, B., Elsik, C. G., Manchanda, N., Coe, E. H., Sachs, M. M., Stinard, P. S., Tolbert, J., Zimmerman, S., & Andorf, C. M. (2019). MaizeGDB 2018: The maize multi-genome genetics

and genomics database. *Nucleic Acids Research*, 47(D1), D1146–D1154.

<https://doi.org/10.1093/nar/gky1046>

Popescu, S. C., Popescu, G. V., Bachan, S., Zhang, Z., Seay, M., Gerstein, M., Snyder, M., & Dinesh-Kumar, S. P. (2007). Differential binding of calmodulin-related proteins to their targets revealed through high-density *Arabidopsis* protein microarrays. *Proceedings of the National Academy of Sciences*, 104, 4730–4735.

Popescu SC, Brauer EK, Dimlioglu G and Popescu GV. (2017). Insights into the Structure, Function, and Ion-Mediated Signaling Pathways Transduced by Plant Integrin-Linked Kinases. *Frontiers. Plant Science*, 8:376. doi: [10.3389/fpls.2017.00376](https://doi.org/10.3389/fpls.2017.00376)

Quinn, D., & Telenko, D. (2022). Tar spot of corn: What to know and new research. *Purdue University Extension Entomology: Pest & Crop Newsletter*, 13.

Reid, L. M., Xiang, K., Zhu, X., & Morrison, M. J. (2019). CO468, CO469, CO470, CO471, CO472, and CO473 corn hybrids: Performance and resistance to pests and diseases. *Canadian Journal of Plant Science*, 99(6), 972–984. <https://doi.org/10.1139/cjps-2018-0298>

Ramírez-Zavaleta, C. Y., García-Barrera, L. J., Rodríguez-Verástegui, L. L., Arrieta-Flores, D., & Gregorio-Jorge, J. (2022). An overview of PRR- and NLR-mediated immunities: Conserved signaling components across the plant kingdom that communicate both pathways. *Plants*, 11(21), 2936. <https://doi.org/10.3390/plants11212936>

Remick, B. C., Gaidt, M. M., & Vance, R. E. (2023). Effector-triggered immunity. *Annual Review of Immunology*, 41(1), 453–481. <https://doi.org/10.1146/annurev-immunol-101721-031732>

Ren, J., Wu, P., Huestis, G. M., Zhang, A., Qu, J., Liu, Y., Zheng, H., Alakonya, A. E., Dhliwayo, T., Olsen, M., San Vicente, F., Prasanna, B. M., Chen, J., & Zhang, X. (2022). Identification and fine mapping of a major QTL (*qRtsc8-1*) conferring resistance to maize tar spot complex. *Theoretical and Applied Genetics*, 135(5), 1551–1563. <https://doi.org/10.1007/s00122-022-04053-8>

Rennie, E. A., & Scheller, H. V. (2014). Xylan biosynthesis. *Current Opinion in Biotechnology*, 26, 100–107. <https://doi.org/10.1016/j.copbio.2013.11.013>

Rivas, F. J. M., Fernie, A. R., & Aarabi, F. (2024). Roles and regulation of the RBOHD enzyme in initiating ROS-mediated systemic signaling during biotic and abiotic stress. *Plant Stress*, 11, 100327. <https://doi.org/10.1016/j.stress.2023.100327>

Riviere M. P., Marais A., Ponchet M., Willats W., Galiana E. (2008). Silencing of acidic pathogenesis-related PR-1 genes increases extracellular beta-(1-3)-glucanase activity at the onset of tobacco defence reactions. *Journal of Experimental Botany*, 59, 1225–1239.
doi: 10.1093/jxb/ern044

Roberts, W.K.; Selitrennikoff, C.P. Zeamatin, (1990). Zeamatin, an antifungal protein from maize with membrane-permeabilizing activity. *Journal of General Microbiology*, 136, 1771–1778.

Rocoo da Silva, C. R., Check, J., MacCready, J. S., Alakonya, A. E., Beiriger, R., Bissonnette, K. M., Collins, A., Cruz, C. D., Esker, P. D., Goodwin, S. B., Malvick, D., Mueller, D. S., Paul, P., Raid, R., Robertson, A. E., Roggenkamp, E., Ross, T. J., Singh, R., Smith, D. L., Tenuta, A. U., Chilvers, M. I., & Telenko, D. E. P. (2021). Recovery plan for tar spot of corn, caused by *Phyllachora maydis*. *Plant Health Progress*, 22(4), 596–616. <https://doi.org/10.1094/PHP-04-21-0074-RP>

Rogers, A., Jaiswal, N., Roggenkamp, E., Kim, H. S., MacCready, J. S., Chilvers, M. I., Scofield, S. R., Iyer-Pascuzzi, A. S., & Helm, M. (2024). Genome-informed trophic classification and functional characterization of virulence proteins from the maize tar spot pathogen *Phyllachora maydis*. *Phytopathology*, 114(8), 1940–1949.
<https://doi.org/10.1094/PHYTO-01-24-0037-R>

Rogers, A., Jaiswal, N., Caldwell, D. L., Roggenkamp, E. M., Scofield, S. R., Chilvers, M. I., Iyer-Pascuzzi, A. S., & Helm, M. (2026). Current understanding of the genetic and molecular interactions between the tar spot pathogen *Phyllachora maydis* and maize. *Molecular Plant-Microbe Interactions*. <https://doi.org/10.1094/MPMI-01-26-0009-IRW>

- Roggenkamp, E., Check, J., Smith, D. L., Chilvers, M. I., Da Silva, C. R., Byrne, A. M., Kleczewski, N. M., Ross, T. J., & Telenko, D. E. (2025). Survey of maize differential gene expression upon environmental exposure to the tar spot pathogen *Phyllachora maydis*. *PhytoFrontiers*, 5(4):571-581. <https://doi.org/10.1094/PHYTOFR-12-24-0136-R>
- Romay, M. C., Millard, M. J., Glaubitz, J. C., Peiffer, J. A., Swarts, K. L., Casstevens, T. M., Elshire, R. J., Acharya, C. B., Mitchell, S. E., Flint-Garcia, S. A., McMullen, M. D., Holland, J. B., Buckler, E. S., & Gardner, C. A. (2013). Comprehensive genotyping of the USA national maize inbred seed bank. *Genome Biology*, 14(6), Article R55. <https://doi.org/10.1186/gb-2013-14-6-r55>
- Ruhl, G., Romberg, M. K., Bissonnette, S., Plewa, D., Creswell, T., & Wise, K. A. (2016). First report of tar spot on corn caused by *Phyllachora maydis* in the United States. *Plant Disease*, 100, 1496.
- Saijo, Y., Tintor, N., Lu, X., Rauf, P., Pajerowska-Mukhtar, K., Häweker, H., Dong, X., Robatzek, S., & Schulze-Lefert, P. (2009). Receptor quality control in the endoplasmic reticulum for plant innate immunity. *The EMBO Journal*, 28(21), 3439–3449. <https://doi.org/10.1038/emboj.2009.263>
- Sánchez-Vallet, A., Mesters, J. R., & Thomma, B. P. H. J. (2015). The battle for chitin recognition in plant-microbe interactions. *FEMS Microbiology Reviews*, 39(2), 171–183. <https://doi.org/10.1093/femsre/fuu003>
- Santiago, R., Barros-Rios, J., & Malvar, R. A. (2013). Impact of cell wall composition on maize resistance to pests and diseases. *International Journal of Molecular Sciences*, 14, 6960–6980. <https://doi.org/10.3390/ijms14046960>
- Sapouna, I., Kärkönen, A., & McKee, L. S. (2023). The impact of xylan on the biosynthesis and structure of extracellular lignin produced by a Norway spruce tissue culture. *Plant Direct*, 7(6), e500. <https://doi.org/10.1002/pld3.500>
- Sayers, E. W., Beck, J., Bolton, E. E., Brister, J. R., Canese, K., Comeau, D. C., Funk, K., Kim, S., Klimke, W., Landrum, M. J., Lathrop, S., Lu, Z., Madden, T. L., Malheiro, A., Marchler-

Bauer, A., Murphy, T. D., Phan, L., Pujar, S., Rangwala, S. H., Schneider, V. A., Tse, T., Wang, J., Ye, J., Trawick, B. W., & Pruitt, K. D. (2023). Database resources of the National Center for Biotechnology Information. *Nucleic Acids Research*, *51*(D1), D29–D38.

<https://doi.org/10.1093/nar/gkac1032>

Scheible, W.-R., & Pauly, M. (2004). Glycosyltransferases and cell wall biosynthesis: Novel players and insights. *Current Opinion in Plant Biology*, *7*(3), 285–295.

<https://doi.org/10.1016/j.pbi.2004.03.006>

Scheller, H. V., & Ulvskov, P. (2010). Hemicelluloses. *Annual Review of Plant Biology*, *61*, 263–289. <https://doi.org/10.1146/annurev-arplant-042809-112315>

Schwessinger, B., & Zipfel, C. (2008). News from the frontline: Recent insights into PAMP-triggered immunity in plants. *Current Opinion in Plant Biology*, *11*, 389–395.

Semagn, K., Magorokosho, C., Vivek, B.S., Makumbi, D., Beyene, Y., Mugo, S., Prasanna, B.M., Warburton, M.L. (2012). Molecular characterization of diverse CIMMYT maize inbred lines from eastern and southern Africa using single nucleotide polymorphic markers. *BMC Genomics*, *13*:113

Serrano, M., Coluccia, F., Torres, M., L'Haridon, F., & Métraux, J.-P. (2014). The cuticle and plant defense to pathogens. *Frontiers in Plant Science*, *5*, 274.

<https://doi.org/10.3389/fpls.2014.00274>

Sharma, A., Sharma, H., Rajput, R., Pandey, A., Upadhyay, S. K. (2021). Molecular characterization revealed the role of thaumatin-like proteins of bread wheat in stress response. *Frontiers Plant Science*, *12*:807448. doi: [10.3389/fpls.2021.807448](https://doi.org/10.3389/fpls.2021.807448).

Sharpe, L., Henrickson, M., & Jeschke, M. (2021). Tar spot of corn in Canada. *Corteva Agriscience*, *13*(8), 1–2.

Shi, L., Lv, X., Weng, J., Zhu, H., Liu, C., Hao, Z., Zhou, Y., Zhang, D., Li, M., Ci, X., Li, X., & Zhang, S. (2014). Genetic characterization and linkage disequilibrium mapping of resistance to gray leaf spot in maize (*Zea mays* L.). *The Crop Journal*, *2*, 132–143.

<https://doi.org/10.1016/j.cj.2014.02.001>

Shi, Y., Bao, X., & Song, X. (2023). The leucine-rich repeat receptor-like kinase protein TaSERK1 positively regulates high-temperature seedling plant resistance to *Puccinia striiformis* f. sp. *tritici* by interacting with TaDJA7. *Phytopathology*, *113*(7), 1325–1334.

Sikora, E., Faske, T., Meyer, R., Betts, A., Kemerait, B., Camiletti, B., Telenko, D., Robertson, A., Mueller, D., Sisson, A., Onofre, R., Wise, K., Kerns, S., Padgett, B., Price, T., Chilvers, M., Malvick, D., Allen, T., Bish, M., ... Smith, D. (2025). Corn disease loss estimates from the United States and Ontario, Canada—2024. *Crop Protection Network*.

<https://cropprotectionnetwork.org/publications/corn-disease-loss-estimates-from-the-united-states-and-ontario-canada-2024>

Singh, R., Shim, S., Telenko, D. E. P., & Goodwin, S. B. (2023). Parental inbred lines of the nested association mapping population of corn show sources of resistance to tar spot. *Plant Disease*, *107*(2), 262–266. <https://doi.org/10.1094/PDIS-02-22-0314-SC>

Solórzano, J. E., Cruz, C. D., Arenz, B. E., Malvick, D. K., & Kleczewski, N. M. (2023). Tar spot of corn: A diagnostic and methods guide. *Plant Health Progress*, *24*(1), 117–122.

<https://doi.org/10.1094/PHP-04-22-0033-DG>

Solórzano, J. E., Issendorff, S. E., Drott, M. T., Check, J. C., Roggenkamp, E. M., Cruz, C. D., Kleczewski, N. M., Gongóra-Canul, C. C., & Malvick, D. K. (2023). A new and effective method to induce infection of *Phyllachora maydis* into corn for tar spot studies in controlled environments. *Plant Methods*, *19*(1), 83. <https://doi.org/10.1186/s13007-023-01052-8>

Sonah H, Deshmukh RK, Bélanger RR. (2016). Computational Prediction of Effector Proteins in Fungi: Opportunities and Challenges. *Frontier Plant Science*, *7*:126. [doi: 10.3389/fpls.2016.00126](https://doi.org/10.3389/fpls.2016.00126).

Song, W., Wang, B., Li, X., Wei, J., Chen, L., Zhang, D., Zhang, W., & Li, R. (2015). Identification of immune-related LRR-containing genes in maize (*Zea mays*) by genome-wide sequence analysis. *International Journal of Genomics*, *2015*, 231358.

<https://doi.org/10.1155/2015/231358>

- Spears, B. J., Howton, T. C., Gao, F., Garner, C. M., Mukhtar, M. S., & Gassmann, W. (2019). Direct regulation of the EFR-dependent immune response by *Arabidopsis* TCP transcription factors. *Molecular Plant-Microbe Interactions*, 32(1), 78–91. <https://doi.org/10.1094/MPMI-07-18-0201-FI>
- Sperschneider, J., Dodds, P. N., Gardiner, D. M., Manners, J. M., Singh, K. B., Taylor, J. M. (2015). Advances and Challenges in Computational Prediction of Effectors from Plant Pathogenic Fungi. *PLoS Pathogens*, 11(5): e1004806. <https://doi.org/10.1371/journal.ppat.1004806>
- Sperschneider, J., Catanzariti, A. M., DeBoer, K., Petre, B., Gardiner, D. M., Singh, K. B., Dodds, P. N., & Taylor, J. M. (2017). LOCALIZER: Subcellular localization prediction of both plant and effector proteins in the plant cell. *Scientific Reports*, 7, 44598. <https://doi.org/10.1038/srep44598>
- Sperschneider, J., & Dodds, P. N. (2022). EffectorP 3.0: Prediction of apoplasmic and cytoplasmic effectors in fungi and oomycetes. *Molecular Plant–Microbe Interactions*, 35(2), 146–156. <https://doi.org/10.1094/MPMI-08-21-0201-R>
- Sun, Y., Li, L., Macho, A. P., Han, Z., Hu, Z., Zipfel, C., Zhou, J.-M., & Chai, J. (2013). Structural basis for flg22-induced activation of the *Arabidopsis* FLS2–BAK1 immune complex. *Science*, 342(6158), 624–628.
- Sun, J., Li, L., Wang, P., Zhang, S., & Wu, J. (2017). Genome-wide characterization, evolution, and expression analysis of the leucine-rich repeat receptor-like protein kinase (LRR-RLK) gene family in Rosaceae genomes. *BMC Genomics*, 18(1), 763. <https://doi.org/10.1186/s12864-017-4155-y>
- Sun, Y., Wang, X., & Liu, F. (2023). A leucine-rich repeat receptor-like kinase TaBIR1 contributes to wheat resistance against *Puccinia striiformis* f. sp. *tritici*. *International Journal of Molecular Sciences*, 24(7), 6438.

Tan, L., Eberhard, S., Pattathil, S., Warder, C., Glushka, J., Yuan, C., ... Hahn, M. G. (2013). An *Arabidopsis* cell wall proteoglycan consists of pectin and arabinoxylan covalently linked to an arabinogalactan protein. *The Plant Cell*, 25(1), 270–287. <https://doi.org/10.1105/tpc.112.107334>

Tariq, F., Ma, C., & Zhao, S. (2025). Integrative dynamics of cell wall architecture and plant growth under salt stress. *Frontiers in Plant Science*, 16, 1644412. <https://doi.org/10.3389/fpls.2025.1644412>

Telenko, D. E., Ross, T. J., Smith, D. L., Byrne, A. M., Chilvers, M. I., Kleczewski, N. M., ... Wise, K. A. (2019). Tar spot of corn in the United States: Distribution, impact, and management. *Plant Health Progress*, 20(3), 178–179. <https://doi.org/10.1094/PHP-03-19-0018-BR>

Telenko, D., Chilvers, M., Kleczewski, N., Mueller, D., Plewa, D., Robertson, A., Smith, D., Sisson, A., Tenuta, A., & Wise, K. (2020). An overview of tar spot. *Crop Protection Network*. <https://doi.org/10.31274/cpn-20190620-008>

Telenko, D., Chilvers, M., Kleczewski, N., Mueller, D., Plewa, D., Robertson, A., Smith, D., Sisson, A., Tenuta, A., & Wise, K. (2021). Tar spot of corn web book: Tar spot disease cycle. *Crop Protection Network*. <https://cropprotectionnetwork.org/web-books/tar-spot-of-corn?section=tar-spot-disease-cycle>

Telenko, D. E., Chilvers, M. I., Byrne, A., Check, J., Da Silva, C. R., Kleczewski, N., Roggenkamp, E., Ross, T. J., & Smith, D. L. (2022). Fungicide efficacy on tar spot and yield of corn in the Midwestern United States. *Plant Health Progress*, 23:281-287. <https://doi.org/10.1094/PHP-10-21-0125-RS>

Todd, J. N. A., Carreón-Anguiano, K. G., Islas-Flores, I., & Canto-Canché, B. (2022). Fungal effectomics: A world in constant evolution. *International Journal of Molecular Sciences*, 23, 13433. <https://doi.org/10.3390/ijms232113433>

Trudel, J., Grenier, J., Potvin, C., & Asselin, A. (1998). Several thaumatin-like proteins bind to β -1,3-glucans. *Plant Physiology*, 118(4), 1431–1438.

Tryfona, T., Bourdon, M., Delgado Marques, R., Busse-Wicher, M., Vilaplana, F., Stott, K., & Dupree, P. (2023). Grass xylan structural variation suggests functional specialization and

distinctive interaction with cellulose and lignin. *The Plant Journal*, 113(5), 1004–1020.

<https://doi.org/10.1111/tpj.16096>

Trygestad, J. B. (2021). Genetic and genetic by environment effects on tar spot resistance and hybrid yield in maize. (Master's thesis). *Michigan State University*.

Valle-Torres, J., Ross, T. J., Plewa, D., Avellaneda, M. C., Check, J., Chilvers, M. I., Cruz, A. P., Dalla Lana, F., Groves, C., Gongora-Canul, C., Henriquez-Dole, L., Jamann, T., Kleczewski, N., Lipps, S., Malvick, D., McCoy, A. G., Mueller, D. S., Paul, P. A., Puerto, C., ... Cruz, C. D. (2020). Tar spot: An understudied disease threatening corn production in the Americas. *Plant Disease*, 104, 2541–2550. <https://doi.org/10.1094/PDIS-02-20-0449-FE>

Van Loon, L. C., Pierpoint, W. S., Boller, T., & Conejero, V. (1994). Recommendations for naming plant pathogenesis-related proteins. *Plant Molecular Biology Reporter*, 12(3), 245–264.

Van Loon, L. C., Rep, M., & Pieterse, C. M. J. (2006). Significance of inducible defense-related proteins in infected plants. *Annual Review of Phytopathology*, 44, 135–162.

Waese, J., Fan, J., Pasha, A., Yu, H., Fucile, G., Shi, R., Cumming, M., Kelley, L. A., Sternberg, M. J., Krishnakumar, V., Ferlanti, E., Miller, J., Town, C., Stuerzlinger, W., & Provar, N. J. (2017). ePlant: Visualizing and exploring multiple levels of data for hypothesis generation in plant biology. *The Plant Cell*, 29(8), 1806–1821. <https://doi.org/10.1105/tpc.17.00073>

Wan, J., He, M., Hou, Q., Zou, L., Yang, Y., Wei, Y., & Chen, X. (2021). Cell wall associated immunity in plants. *Stress Biology*, 1(1), 3. <https://doi.org/10.1007/s44154-021-00003-4>

Wang, M., Yan, J., Zhao, J., Song, W., Zhang, X., Xiao, Y., & Zheng, Y. (2012). Genome-wide association study (GWAS) of resistance to head smut in maize. *Plant Science*, 196, 125–131. <https://doi.org/10.1016/j.plantsci.2012.08.004>

Wang F, Yuan S, Wu W, Yang Y, Cui Z, Wang H, Liu D. (2020). TaTLP1 interacts with TaPR1 to contribute to wheat defense responses to leaf rust fungus. *PLoS Genetics*, 16(7): e1008713. [doi: 10.1371/journal.pgen.1008713](https://doi.org/10.1371/journal.pgen.1008713).

Wang F., Shen S., Zhao C., Cui Z., Meng L., Wu W., et al. (2022). TaPR1 interacts with TaTLP1 via the α IV helix to be involved in wheat defense to *Puccinia triticina* through the CAPE1 motif. *Frontiers Plant Science*, 13:874654. doi: [10.3389/fpls.2022.874654](https://doi.org/10.3389/fpls.2022.874654)

Wang, Q., Zhang, B., Zhang, L., Li, Y., Wang, Y., Li, X., Zhao, Y., & Li, J. (2023). Natural variation of ZmLNG1 alters organ shapes in maize. *New Phytologist*, 237, 215–230. <https://doi.org/10.1111/nph.18563>

Wang, C., Tang, X., Liu, W. et al. (2025). Identification and expression analysis of LRR-RLK genes reveal their roles in plant development and stress responses in Kiwifruit (*Actinidia chinensis*). *Sci Rep* 15, 26346. <https://doi.org/10.1038/s41598-025-12363-2>

Wen W, Araus JL, Trushar S, Cairns J, Mahuku G, Banziger M, Torres JL, Sanchez C, Yan J (2011). Molecular characterization of a diverse maize inbred line collection and its potential utilization for stress tolerance improvement. *Crop Science*, 51 (6): 2569–2581. <https://doi.org/10.2135/cropsci2010.08.0465>

Whisson, S. C., Boevink, P. C., Wang, S., & Birch, P. R. J. (2016). The cell biology of late blight disease. *Current Opinion in Microbiology*, 34, 127–135. <https://doi.org/10.1016/j.mib.2016.09.002>

Witte, J.S. (2014). Genome-wide association studies and beyond. *Annual Review of Public Health*, 2010;31:9-20. doi: [10.1146/annurev.publhealth.012809.103723](https://doi.org/10.1146/annurev.publhealth.012809.103723).

Xu, Y., Fan, Y., Liu, L., Cao, J., Zhou, J., Liu, E., Li, R., Ma, P., Yao, W., Wu, J., Li, T., & Zhang, H. (2025). Enhancing maize resistance to *Fusarium verticillioides* through modulation of cell wall structure and components by ZmXYXT2. *Journal of Advanced Research*, 78, 111–128. <https://doi.org/10.1016/j.jare.2025.02.023>

Yan, S., Loladze, A., Wang, N., Sun, S., Chilvers, M. I., Olsen, M., Burgueño, J., Petroli, C. D., Molnar, T., San Vicente, F., Zhang, X., & Prasanna, B. M. (2022). Association mapping of resistance to tar spot complex in maize. *Plant Breeding*, 141(6), 745–757. <https://doi.org/10.1111/pbr.13056>

Yang Q, Guo J, Zeng H, Xu L, Xue J, Xiao S, Li JF. (2021). The receptor-like cytoplasmic kinase CDG1 negatively regulates Arabidopsis pattern-triggered immunity and is involved in AvrRpm1-induced RIN4 phosphorylation. *Plant Cell*. 33(4):1341-1360. doi: [10.1093/plcell/koab033](https://doi.org/10.1093/plcell/koab033).

Yang, W., Cai, H., Zhang, Y., Hao, J., Ma, Y., He, Q., Zhao, K., Li, H., Fang, A., Hou, D., & Ren, X. (2025). Functional Analysis of the *ZmPR5* Gene Related to Resistance Against *Fusarium verticillioides* in Maize. *Plants*, 14(5), 737. <https://doi.org/10.3390/plants14050737>

Ye, J., Coulouris, G., Zaretskaya, I., Cutcutache, I., Rozen, S., & Madden, T. L. (2012). Primer-BLAST: A tool to design target-specific primers for polymerase chain reaction. *BMC Bioinformatics*, 13, 134.

Yin, Z., Wang, Y., Wu, F., Gu, X., Bian, Y., Wang, Y., & Deng, D. (2014). Quantitative trait locus mapping of resistance to *Aspergillus flavus* infection using a recombinant inbred line population in maize. *Molecular Breeding*, 33, 39–49. <https://doi.org/10.1007/s11032-013-9932-y>

Yu, X., Feng, B., He, P., & Shan, L. (2017). From chaos to harmony: Responses and signaling upon microbial pattern recognition. *Annual Review of Phytopathology*, 55(1), 109–137. <https://doi.org/10.1146/annurev-phyto-080516-035649>

Zhang X, Valdés-López O, Arellano C, Stacey G, Balint-Kurti P. (2017). Genetic dissection of the maize (*Zea mays L.*) MAMP response. *Theoretical and Applied Genetics*. 130(6):1155-1168. doi: [10.1007/s00122-017-2876-6](https://doi.org/10.1007/s00122-017-2876-6).

Zhang J, Wang F, Liang F, Zhang Y, Ma L, Wang H, Liu D. (2018). Functional analysis of a pathogenesis-related thaumatin-like protein gene TaLr35PR5 from wheat induced by leaf rust fungus. *BMC Plant Biology*. 18(1):76. doi: [10.1186/s12870-018-1297-2](https://doi.org/10.1186/s12870-018-1297-2).

Zhang, W., Qin, W., Li, H., & Wu, A. (2021). Biosynthesis and transport of nucleotide sugars for plant hemicellulose. *Frontiers in Plant Science*, 12:723128. <https://doi.org/10.3389/fpls.2021.723128>

Zhang, G., Liu, W., Wang, L., Cheng, X., Tian, X., Du, Z., Kang, Z., & Zhao, J. (2022). Evaluation of the potential risk of the emerging Yr5-virulent races of *Puccinia striiformis* f. sp. *tritici* to 165 Chinese wheat cultivars. *Plant Disease*, *106*, 1867–1874.

<https://doi.org/10.1094/PDIS-11-21-2622-RE>

Zhang, L., Gao, C., Gao, Y., Yang, H., Jia, M., Wang, X., Zhang, B., & Zhou, Y. (2025). New insights into plant cell wall functions. *Journal of Genetics and Genomics*, *52*, 1308–1324.

<https://doi.org/10.1016/j.jgg.2025.04.013>

Zhao, X., Liu, N., Shang, N., Zeng, W., Ebert, B., Rautengarten, C., Zeng, Q.-Y., Li, H., Chen, X., Beahan, C., Bacic, A., Heazlewood, J. L., & Wu, A.-M. (2018). Three UDP-xylose transporters participate in xylan biosynthesis by conveying cytosolic UDP-xylose into the Golgi lumen in *Arabidopsis*. *Journal of Experimental Botany*, *69*(5), 1125–1134.

<https://doi.org/10.1093/jxb/erx448>

Zheng, H., Chen, J., Mu, C., Makumbi, D., Xu, Y., & Mahuku, G. (2018). Combined linkage and association mapping reveal QTL for host plant resistance to common rust (*Puccinia sorghi*) in tropical maize. *BMC Plant Biology*, *18*, 310. <https://doi.org/10.1186/s12870-018-1520-1>

Zhong, R., & Ye, Z.-H. (2015). Secondary cell walls: Biosynthesis, patterned deposition and transcriptional regulation. *Plant and Cell Physiology*, *56*(2), 195–214.

<https://doi.org/10.1093/pcp/pcu140>

Zhong, R., Cui, D., & Ye, Z.-H. (2019). Secondary cell wall biosynthesis. *New Phytologist*, *221*, 1703–1723. <https://doi.org/10.1111/nph.15537>

Zhu, F., Zhao, Y., Wang, X., Zhang, Y., & Chen, J. (2024). Inducers of plant immunity in sustainable disease prevention and control. *Crop Protection*, *176*, 106586.

<https://doi.org/10.1016/j.cropro.2023.106586>

Zipfel, C., Robatzek, S., Navarro, L., Oakeley, E. J., Jones, J. D. G., Felix, G., & Boller, T. (2004). Bacterial disease resistance in *Arabidopsis* through flagellin perception. *Nature*, *428*(6984), 764–767.

Zipfel, C., Kunze, G., Chinchilla, D., Caniard, A., Jones, J. D. G., Boller, T., & Felix, G. (2006). Perception of the bacterial PAMP EF-Tu by the receptor EFR restricts *Agrobacterium*-mediated transformation. *Cell*, 125(4), 749–760. <https://doi.org/10.1016/j.cell.2006.03.037>

Zuch, D. T., Doyle, S. M., Majda, M., Smith, R. S., Robert, S., & Torii, K. U. (2022). Cell biology of the leaf epidermis: Fate specification, morphogenesis, and coordination. *The Plant Cell*, 34(1), 209–227. <https://doi.org/10.1093/plcell/koab250>

Supplemental Tables

Supplementary Table S1: List of primers used in this study to conduct qPCR analysis.

Gene	Gene ID	Forward (5' --> 3')	Reverse (3' -->5')
<i>ZmUXT2</i>	<i>GRMZM2G063511</i>	TGCTCCTTCTGGTGTTGGT	TGCCAGCAAGGAGAGTATGG
<i>ZmLRR-RLK</i>	<i>GRMZM2G073884</i>	CCCGAATGAGATAGGACGCC	TTCGGAAGATGCCCTAGGGA
	<i>GRMZM2G071228</i>	AGAGTGTGCAGGATCAAGCC	TGACCCATCGGAGTCCTCAT
	<i>GRMZM5G869967</i>	AGCAATTACGCCTGGAGGTC	AGATCCAGCTGACTCGTTGC
<i>DUF</i>	<i>Zm00001d039138</i>	GGGCCAACTACCTTCAACAAT	CAGCGCCACTTAGGTTACTAT C
<i>CYP</i>	<i>Zm00001d023192</i>	CGTCATCCCCGAGTTCATGT	GCTTGCACGAACTTCTC
<i>An2</i>	<i>Zm00001d029648</i>	GTCTTACCCATCTCCGTAAC A	GAACCATGATCCATCCGTTTC T
<i>PR5</i>	<i>Zm00001d024303</i>	GTCCTCCTGCTGCTCCT	AGTTGTTGGTGATGGTGAAGG

Supplementary Table S2: List of primers used in this study for sequencing.

Gene	Forward (5' --> 3')	Reverse (3' -->5')	Sequencing
<i>ZmUXT2</i> (<i>GRMZM2G063511</i>)	GTTTCGAGGGCAGCGAAGAT	TGAAAGAAACAAACTCGAACCAA	Nanospore
	CTCATCGACCCAAGTCTCT	TACACTCTGGGTTGGCTTCC	
	ACACTCTCGTCTCCCTCCTC	ATGGAGCACGCAGATCTACG	Sanger
	CGTAGATCTGCGTGCTCCAT	CAGCCAGAGCAGAACAGACA	
	TGTCTGTTCTGCTCTGGCTG	GTGCAGTAACAGACCCGTGA	
	GGCTTCAACTCTGTTGGGTT	AAGATGACAGTGCACGGGAT	
	CATCCCGTGCAGTGTCTCT	CCATCAAGGAAGGGGCCAAT	
	ATTGGCCCCTTCCTTGATGG	CTGCTGTGGGAGACTTCAG	
	GAACCGAACCACACTCTCGT	GCACCAGAACTACAACCCGA	
<i>ZmLRR-RLK</i> (<i>GRMZM2G073884</i>)	AGGATGCACGGGATGTGTTT	CGCTTCCCTGTGAGCATTTC	Nanospore
	CACACACGACCACTGCAAAA	CCTCACAGAGCCATCGAAAG	
	GCTGACCCGTTCCACACAAT	GCAGAGCACGAGATACCGAT	
	AGCTGGCCACACAGTTGTTT	CACGATGAGACAGTCTCCGG	
	TCTTTGTGGTTGGGCTGGTT	TATGCTTTGCGGTCGTCCTT	Sanger
	GTCCGCTGCGATTTCCATTC	TCCCTAGGGCATCTTCCGAA	
	AAGGACGACCGCAAAGCAT A	CTGTTCCGGCCTCGATCTAC	
	TTCGGAAGATGCCCTAGGGA	CAACCTCTCGGATCTACGCC	
	GTAGATCGAGGCCGGAACA G	GCTGGCGTTGATCATCCTCT	
AAACAGCGACTGGGGAATG A	GAATGGAAATCGCAGCGGAC		